

MODELING THE COOLING OF SWEET CORN

JOSEPH EDWIN BERINYUY

A DISSERTATION PRESENTED TO THE GRADUATE SCHOOL
OF THE UNIVERSITY OF FLORIDA IN
PARTIAL FULFILLMENT OF THE REQUIREMENTS
FOR THE DEGREE OF DOCTOR OF PHILOSOPHY

UNIVERSITY OF FLORIDA

1988

Dedicated to
my wife
Caroline
my Daughter
Dorala
and my sons
Yitony and Kpuudzeka

ACKNOWLEDGEMENTS

The author is very grateful to Dr. Khe Van Chau, his major professor, for his guidance and assistance throughout the course of this work.

The author is also grateful to Dr. Carl D. Baird, Mr. Jerome J. Gaffney, Dr. Jeffrey K. Brecht and Dr. Chung K. Hsieh for their suggestions which aided in the completion of this research.

The author is especially appreciative of the technical support and friendship given by Mr. Loren Miller.

Special thanks are extended to Mr. and Mrs. Fendick for their moral support and to Mike Schmidt for his valuable friendship.

The author is also grateful to the Univesity Centre of Dschang and U.S.A.I.D. for providing financial aid for this project.

TABLE OF CONTENTS

ACKNOWLEDGEMENTS	iii
LIST OF SYMBOLS	vi
LIST OF TABLES	viii
LIST OF FIGURES	ix
ABSTRACT	xii
INTRODUCTION	1
REVIEW OF LITERATURE	4
Precooling of Fruits and Vegetables	4
Quality Evaluation	9
Heat Transfer in Beds of Biological Products	10
Thermophysical Properties	17
Thermal Diffusivity	17
Thermal Conductivity	21
Specific Heat Capacity	23
Convection Heat Transfer Coefficient	24
Respiration	28
DEVELOPMENT OF NUMERICAL MODEL	33
Interior Node	36
Center Node	39
Interface Node	40
Surface Node	42
The Bed Model	45
EXPERIMENTAL PROCEDURE	53
Thermal Diffusivity	54
Methodology for Thermal Diffusivity	54
Experimental Procedure	54
Thermal diffusivity of cob	58

Thermal diffusivity of kernel	58
Thermal diffusivity of husk	59
Corn as a homogeneous material	59
Calculation of Thermal Diffusivity	60
Convection Heat Transfer Coefficient	61
Hydrocooling	63
Forced Air Cooling	67
Pressure Drops Across Crates of Sweet Corn	71
Moisture Content	74
RESULTS AND DISCUSSIONS	75
Thermal Diffusivity	75
Hydrocooling	81
Convection Heat Transfer Coefficient	100
Pressure Drops	105
Forced Air Cooling	112
Mathematical Modeling	121
CONCLUSIONS	139
APPENDIX A EVALUATION OF h FOR THERMAL DIFFUSIVITY EXPERIMENT	142
APPENDIX B EXPERIMENTAL DETERMINATION OF SAMPLE VOLUME AND DENSITY	145
APPENDIX C STEADY STATE HEAT TRANSFER RESISTANCE	147
APPENDIX D TRANSPIRATION FROM FRUITS AND VEGETABLES	148
APPENDIX E COMPUTER PROGRAM	150
LIST OF REFERENCES	191
BIOGRAPHICAL SKETCH	199

LIST OF SYMBOLS

A	-	cross sectional area of layer
a	-	surface area per unit bed volume
B_i	-	Biot number
C_p	-	specific heat capacity
d	-	diameter
F_o	-	Fourier number
h	-	forced convection heat transfer coefficient
J_o	-	Bessel function of zero order
J_1	-	Bessel function of first order
k	-	thermal conductivity
m	-	constant slope
Nu	-	Nusselt number
Pr	-	Prandtl number
Q	-	heat flow rate
Q_t	-	rate of transpiration
q	-	heat flow
Re	-	Reynolds number
r	-	radius to heat exchange surface
T	-	temperature
U	-	overall heat transfer coefficient
v_{max}	-	maximum velocity
v	-	velocity

α - thermal diffusivity
 ϵ - void fraction of bed
 ρ - density
 μ - fluid dynamic viscosity
 ν - fluid kinematic viscosity
 Δr - spatial increment along the radius
 Δt - time increment
 Δz - time increment along the length

Subscripts

a - air
 abs - absolute
 b - bulk
 c - composite
 f - fluid
 i - position in direction of radius
 j - position in direction of length
 o - initial
 p - product
 s - surface
 so - solids
 w - water
 z_i - representing z-direction
 ∞ - cooling medium

LIST OF TABLES

TABLE		PAGE
1	Inputs to the Numerical Model	49
2	Average Physical Properties of Ears with Thermocouples Per Crate of Sweet Corn Used in Hydrocooling Tests	66
3	Average Physical Properties of Ears with Thermocouples Per Crate of Sweet Corn Used in Forced Air Cooling Tests	70
4	Tests and Replicates Conducted During Hydrocooling of Sweet Corn	72
5	Tests and Replicates Conducted During Forced Air Cooling of Sweet Corn	73
6	Experimentally Determined Thermal Diffusivities of the Components of Sweet Corn	77
7	Calculated Thermophysical Properties of the Components of Sweet Corn	79
8	Experimental Determination of the Density and Calculated Diffusivities of the Components of Sweet Corn	80
9	Convection Heat Transfer Coefficients Measured During Hydrocooling	103
10	Convection Heat Transfer Coefficients Measured During Forced Air Cooling	104
11	Pressure Drops Measured Across Crates of Sweet Corn	107
12	Modified Pressure Drops Measured Across Crates of Sweet Corn	108

LIST OF FIGURES

FIGURE		PAGE
1	Heat of Respiration of Three Vegetables	30
2	Cross Section and Shape of an Ear of Sweet Corn Showing Nodes and Volumes Used in the Model	34
3	Division of the Crate into Layers	46
4	Flow Diagram for the Computer Program	50
5	A Wire Bound Crate Configuration with Thermocouple Locations	55
6	Apparatus Used to Experimentally Determine Thermal Diffusivities	56
7	An Apparatus Used in The Experimental Hydrocooling of Wire Bound Crates of Sweet Corn	64
8	An Apparatus Used in The Experimental Forced Air Cooling of Wire Bound Crates of Sweet Corn ..	68
9	Spacers Used in the Experimental Forced Air Cooling of Wire Bound Crates of Sweet Corn	69
10	Half cooling Times for Sweet Corn at Three Water Flow Rates	82
11	Seven-Eight cooling Times for Sweet Corn at Three Water Flow Rates	83
12	Half cooling Times for Reheated Sweet Corn at Three Water Flow Rates	85
13	Seven-Eight cooling Times for Reheated Sweet Corn at Three Water Flow Rates	86

14	Cob Temperature Variation at Three Locations in the First Crate During Hydrocooling at $2.0 \text{ l/(s.m}^2\text{)}$	87
15	Cob Temperature Variation at Three Locations in the First Crate During Hydrocooling at $4.8 \text{ l/(s.m}^2\text{)}$	88
16	Cob Temperature Variation at Three Locations in the First Crate During Hydrocooling at $6.8 \text{ l/(s.m}^2\text{)}$	89
17	Temperatures of Water Exiting Some Crates During Hydrocooling at $2.0 \text{ l/(s.m}^2\text{)}$	90
18	Temperatures of Water Exiting Some Crates During Hydrocooling at $4.8 \text{ l/(s.m}^2\text{)}$	91
19	Temperatures of Water Exiting Some Crates During Hydrocooling at $6.8 \text{ l/(s.m}^2\text{)}$	92
20	Experimental Cob Temperatures for Hydrocooling Six Crates of Sweet Corn at $2.0 \text{ l/(s.m}^2\text{)}$	94
21	Experimental Cob Temperatures for Hydrocooling Six Crates of Sweet Corn at $4.8 \text{ l/(s.m}^2\text{)}$	95
22	Experimental Cob Temperatures for Hydrocooling Six Crates of Sweet Corn at $6.8 \text{ l/(s.m}^2\text{)}$	96
23	Experimental Cob Temperatures for Hydrocooling Six Crates of Sweet Corn at $2.0 \text{ l/(s.m}^2\text{)}$ with Either End Facing the Direction of Water Flow	98
24	Experimental Cob Temperatures for Hydrocooling Six Crates of Sweet Corn at $6.8 \text{ l/(s.m}^2\text{)}$ with Either End Facing the Direction of Water Flow	99
25	Nusselt-Reynolds Relationship During Forced Air Cooling of Sweet Corn	101
26	Pressure Drops Across Six Crates of Corn During Forced Air Cooling	110
27	Pressure Drops Measured Across Individual Crates of Sweet Corn During Forced Air Cooling	111

28	Half Cooling Times for Sweet Corn at Two Air Flow Rates	112
29	Seven-Eight Cooling Times for Sweet Corn at Two Air Flow Rates	113
30	Experimental Cob Temperatures for Air Cooling of Six Crates of Sweet Corn at $5.2 \times 10^{-4} \text{ m}^3/(\text{s.kg})$	114
31	Experimental Cob Temperatures for Air Cooling of Six Crates of Sweet Corn at $1.3 \times 10^{-3} \text{ m}^3/(\text{s.kg})$	115
32	Experimental Air Temperatures Measured After Each Crate During Forced Air Cooling at $5.2 \times 10^{-4} \text{ m}^3/(\text{s.kg})$	117
33	Experimental Air Temperatures Measured After Each Crate During Forced Air Cooling at $1.04 \times 10^{-3} \text{ m}^3/(\text{s.kg})$	118
34	Experimental Air Temperatures Measured After Each Crate During Forced Air Cooling at $1.3 \times 10^{-3} \text{ m}^3/(\text{s.kg})$	119
35	Comparison of the Numerical Scheme with Analytical Solution for the Center of a Cylinder at h of $28 \text{ W}/(\text{m}^2.\text{C})$	124
36	Simulation and Experimental Result for the Composite Model for a Single Ear of Corn at h of $85 \text{ W}/(\text{m}^2.\text{C})$	125
37	Comparison of the Mass-average Temperature and the Kernel Temperature at h of $85 \text{ W}/(\text{m}^2.\text{C})$	126
38	Simulation and Experimental Result for the homogeneous Model for a Single Ear of Corn at h of $85 \text{ W}/(\text{m}^2.\text{C})$	128
39	Simulation and Experimental Cob Temperatures for the First Crate of a Bed of Sweet Corn at $5.2 \times 10^{-4} \text{ m}^3/(\text{s.kg})$	129
40	Simulation and Experimental Cob Temperatures for the Second Crate of a Bed of Sweet Corn at $5.2 \times 10^{-4} \text{ m}^3/(\text{s.kg})$	130

41	Simulation and Experimental Cob Temperatures for the Third Crate of a Bed of Sweet Corn at $5.2 \times 10^{-4} \text{ m}^3/(\text{s.kg})$	131
42	Simulation and Experimental Cob Temperatures for the First Crate of a Bed of Sweet Corn at $1.0 \times 10^{-3} \text{ m}^3/(\text{s.kg})$	132
43	Simulation and Experimental Cob Temperatures for the Second Crate of a Bed of Sweet Corn at $1.0 \times 10^{-3} \text{ m}^3/(\text{s.kg})$	133
44	Simulation and Experimental Cob Temperatures for the Third Crate of a Bed of Sweet Corn at $1.0 \times 10^{-3} \text{ m}^3/(\text{s.kg})$	134
45	Simulation and Experimental Cob Temperatures for the First Crate of a Bed of Sweet Corn at $1.3 \times 10^{-3} \text{ m}^3/(\text{s.kg})$	135
46	Simulation and Experimental Cob Temperatures for the Second Crate of a Bed of Sweet Corn at $1.3 \times 10^{-3} \text{ m}^3/(\text{s.kg})$	136
47	Simulation and Experimental Cob Temperatures for the Third Crate of a Bed of Sweet Corn at $1.3 \times 10^{-3} \text{ m}^3/(\text{s.kg})$	137

Abstract of Dissertation Presented to the Graduate School
of the University of Florida in Partial Fulfillment of the
Requirements for the Degree of Doctor of Philosophy

MODELING THE COOLING OF SWEET CORN

By

JOSEPH EDWIN BERINYUY

August 1988

Chairman: Khe Van Chau

Major Department: Agricultural Engineering

Fresh fruits and vegetables are living tissue subject to continuous change after harvest. The energy for this change comes from respiration. Respiration results in senescence, product deterioration and loss of salable weight. Precooling and refrigerated storage is essential to slow down respiration.

To accurately simulate product heat transfer during cooling, knowledge of its thermophysical properties is essential. This study presents experimental data for the thermal diffusivity of the cob, kernel and husks of an ear of sweet corn. It also attempts to determine the thermal diffusivity of the whole ear of corn by assuming that it is a homogeneous cylinder.

Convection heat transfer coefficients between an ear of corn and the cooling fluid were measured and presented for forced air cooling and hydrocooling of sweet corn in wire bound crates. A Nusselt-Reynolds relationship was obtained for forced air cooling.

The study also presents procedures for measuring pressure drops across wire bound crates of sweet corn. Correlations are presented between the pressure drops, the air velocity and the number of crates.

Cooling tests were conducted on wire bound crates of supersweet (sh₂) corn. Using water and then air, experimental data were collected for the cooling of single ears of corn and also for the cooling of wire bound crates of corn in stacks of six high. Experimental results show that forced air cooling of crates of sweet corn, while utilizing high air flow rates, produced cooling that was comparable to hydrocooling.

An explicit finite difference numerical model is presented which can accurately predict the heat and mass transfer within an ear of corn and within a bulk consisting of wire bound crates of sweet corn during cooling. The model accounts for the effects of respiration, evaporative cooling, convective heat and mass transfer, and radiation.

INTRODUCTION

Sweet corn production in the U.S. increased in value by two hundred and twenty percent over a ten-year period from 1970 to 1980 (U.S.D.A., 1982). Florida, the nation's leading producer of fresh market sweet corn, marketed 10.6 million crates in the 1985-86 crop year at a value of \$60.3 million (Florida Agric. Stat., 1986). Sweet corn is ranked fourth in value among vegetables produced in the state of Florida. It is exceeded only by tomatoes, potatoes and green peppers.

Sweet corn is highly perishable and is seldom stored except to protect an excess supply temporarily. Corn as it usually arrives in the market should not be expected to keep even in 0 C storage for more than four to eight days (Appleman, 1918). Corn is relished when it is sweet, fresh-looking and tender, attributes measured in terms of the amount of sugar and moisture retained. Sugar to starch conversion begins immediately after the corn is picked (Appleman, 1918). This conversion is slowed down by precooling and refrigerated transportation.

Usually, corn is hydrocooled, but vacuum cooling is also satisfactory if the sweet corn is prewet and top-iced

after cooling. Most Florida sweet corn is hydrocooled. In former practices, wire bound crates were handled individually. The large hydrocoolers use mechanical refrigeration and pump the water over cooling coils and partially submerged crates of corn. The crates are moved through a large tank on a conveyor belt beneath the shower of cold water. The smaller units use cracked ice for refrigeration and move the crates through a shower of cold water without partially submerging them (Showalter, 1958).

Currently, sweet corn is handled in pallets and field heat is removed by spraying cold water onto the pallet. Most of the water sprayed simply flows over instead of through the pallet and the interior of the pallet may have a temperature reduction of only a few degrees during the entire cooling operation. Slushed ice in waxed fiberboard is also being used to precool sweet corn. Batch cooling of pallet loads of sweet corn is not efficient. The hot spots left in the pallet may later accelerate heating throughout the pallet. Although palletization has improved handling and reduced labor, it has made hydrocooling of sweet corn inefficient.

Much research has been conducted to determine the efficiency of hydrocooling unit loads of sweet corn (Bennett et al., 1976, Bennett and Henry, 1978, Henry et al., 1976). Most of this work has involved indentifying

flow rates or cooling systems that will provide effective cooling at reasonable cost. Although the inadequacy of these methods to establish the cooling properties of sweet corn has been known for some time, little use has been made of mathematical modeling to study the heat and mass transfer during the cooling of sweet corn.

This research has the following objectives:

- (a) measure the thermal diffusivity of the cob, kernel and husk of sweet corn,
- (b) develop a simulation model for the cooling of sweet corn in bulk, and
- (c) validate the model by comparison with experimental values.

REVIEW OF LITERATURE

Precooling of Fruits and Vegetables

Vegetables are living organisms carrying on many life sustaining processes. The energy for these processes comes from the food reserves that accumulated while the product was still attached to the parent plant. This energy conversion occurs during respiration: a process whereby a tissue uses simple sugars like glucose and combines them with oxygen to release chemical heat and energy. Water is a by-product of this process and is sent to the atmosphere through transpiration. Respiration continues even after the vegetable or fruit has been harvested.

Some of the energy that is produced through respiratory activity is utilized in maintaining life processes. Excess energy is released in the form of heat called vital heat, the amount varying with the type and maturity of the fruit or vegetable. Product temperature is a major determinant of the process of respiration. It has been estimated that some fresh fruits and vegetables deteriorate as much in one hour at 32 C as in a day at 10 C (Guillou, 1958).

Respiration results in senescence, the aging of the product and product deterioration. Precooling is essential to remove the field heat from the commodity and to slow down the respiratory activity. Field heat can be rapidly removed from a commodity by hydrocooling, forced air cooling or vacuum cooling. Package ice and top ice can also be used in the absence of precooling facilities (Mitchell, 1985, Ryall and Pentzer, 1982, Bennett, 1964 and Stewart and Couey 1963). The choice of a particular method depends on the commodity's tolerance to the cooling fluid, the risk of contamination by microorganisms born in the medium and the cost of the cooling method.

Sweet corn is generally hydrocooled with water at about 1.0 C. Vacuum cooling also produces satisfactory results if the corn is wetted before vacuum cooling (Showalter, 1957, Winter et al., 1951).

Appleman and Arthur (1919) first studied the effect of temperature on sugar loss from sweet corn. Their research showed that the rate of total sugar loss in green sweet corn was doubled for every 10 C rise in temperature for the first 30 C. At 30 C, fifty percent of the total sugar loss occurred during the first twenty four hours. The depletion rate was reduced more than three times for the same period at 10 C (Appleman and Arthur, 1918). This depletion did not proceed at a uniform rate but became

slower with time, stopping when the initial sugar content was decreased by sixty-two percent.

Quality of sweet corn is affected by the maturity at harvest, duration of marketing period and the handling in stores (Showalter, 1955). Quality is improved by harvesting at optimum maturity, shortening the marketing period and providing more adequate refrigeration during storage.

Showalter (1957) compared hydrocooling and vacuum cooling of sweet corn in Florida. Vacuum cooling was capable of reducing cob temperatures of sweet corn an average of 24 C in thirty-two minutes while hydrocooling could only reduce it by 14 C in twenty-nine minutes. Vacuum cooling, without prewetting the ears with water, reduced their weight and succulence, and resulted in dented kernels and wilted husks after cold storage for five or eight days (Showalter, 1957).

In another study, Showalter (1958) found that succulence of sweet corn changed very little during marketing but noted a marked increase in toughness (pericarp). The pericarp increased by sixty-two percent during the first five days and by eighty-four percent at the end of ten days in a retail store. The retail temperature averaged 13.9 C (Showalter, 1958).

The effect of vacuum cooling on the quality of sweet corn was also the subject of a study by Stewart and Barger

(1959). They reported that prewetting with water did not improve the cooling but helped to retain quality. Top icing was required in addition to prewetting to maintain quality after cooling (Stewart and Barger, 1960). Denting became visible for uncooled corn after holding for a day at 21 C.

The amount of sugar lost by sweet corn depends on the variety. Garwood et al. (1976) found that high sugar varieties lost sugar during storage but the initial sugar content was so high that even after four days at 27 C the level was equal to freshly harvested standard sweet corn.

Sugar depletion after harvest may be reduced by the use of cultivars with genetic modifications of carbohydrate metabolism (Evensen and Boyer, 1986). Standard sweet corn is homozygous for the recessive allele sugary (su), which results in greatly increased levels of water soluble polysaccharides (WSP) compared to field corn. Mutants affecting carbohydrate metabolism include Shrunken-2 (sh2), Amylase Extender (ae) and Sugary Enhancer (se). These genes have been incorporated into commercial cultivars in various ways to improve the sensory quality of sweet corn. Evensen and Boyer (1986) compared some of these with standard cultivars and found that higher levels of water soluble polysaccharides were maintained in the enhanced varieties during fourteen days storage at 10 C. There was an increase in pericarp also (Boyer and Evensen, 1986).

Sims et al. (1971) and Showalter (1967, 1963) independently investigated the effect of different cultural practices on the shelf life of sweet corn. Not trimming the shanks and husks increased senescence and reduced shelf life. Quality was maintained if sweet corn was top-iced during refrigerated shipping (Stewart and Barger, 1960). Maturity at harvest and the duration on the shelf also affected the quality.

Controlled atmosphere maintains the quality of sweet corn stored at 1.7 C. Spalding et al. (1978) investigated the effect of controlled atmosphere on the quality of sweet corn. Their research showed sugar levels of corn that was stored at 1.7 C for three weeks at greater than ninety percent relative humidity and two percent oxygen were comparable to those of corn stored at close to 0 C. The cost of producing and maintaining the controlled atmosphere, however, makes this method unattractive for commercial use.

Sweet corn is currently cooled in pallet loads to facilitate handling. Henry et al. (1976) found this method inefficient as hot spots were left in the pallet. They presented 'hydraircooling' as a method to reduce this problem. This is a method where air is circulated around the base of the pallet while cold water is being sprayed from the top. This method results in faster cooling at the

bottom of the pallet and more uniform product temperature than hydrocooling alone because of improved water contact produced by the forced air (Henry and Bennett, 1976, Henry et al., 1976).

Quality Evaluation

Quality of vegetable products is a combination of characteristics, attributes and properties that give the commodity value to humans for food. It is a combination of components that collectively determine the acceptability of the commodity. These components are appearance, texture, flavor, nutritive value and safety (Kader, 1985). The consumer can only make a cursory assessment at the time of purchase and so the relative importance of each quality characteristic available for his/her assessment is distinct from the relative importance of all known qualities of the product.

Grade standards (U.S. Fancy, U.S. No I, U.S. No II, etc.) identify the degrees of quality in any given commodity that provide the basis for its usability and value (Anon, 1973). Grade standards are issued by regulation bodies like the USDA or Food Safety Quality Service.

Rigorous quality evaluation requires techniques such as impact testing and yield strength (Artheny, 1975) which require complicated equipment and a high level of skill.

These are very elaborate, complex and time consuming and are not satisfactory for quick assessment of quality.

Stewart and Barger (1960) used an arbitrary scale of 1 to 9 to rate the quality of sweet corn and peas. They used husk and kernel appearance as their criteria for grading the corn. One on their scale represented an inedible fruit while nine represented an excellent fruit. Corn graded four or less was unacceptable for consumption. Showalter (1957) used kernel denting and husk appearance to measure quality in Florida sweet corn.

Heat Transfer In Beds of Biological Products

Predicting temperature within a bed of biological product involves the mathematical description of the transfer of heat and, in some cases, mass, from the product to the medium, as well as the quantification of the heat generated by respiration within the bulk. The review of literature here will be mainly for the cases involving heat transfer, heat generation and mass transfer. Literature outside this area will be mentioned only to put the subject into historical perspective.

Early work on heat transfer in porous beds involved mainly non-agricultural products. One of the early contributions was due to Shuman (1929). He obtained an analytical solution for the cooling or heating rates of solids by a fluid flowing uniformly past them. His

equations simplified to the following:

$$\frac{\partial T}{\partial t} = -V_a \frac{\partial T}{\partial x} - \frac{ha}{\rho_a \epsilon C_a} (T - T_{so}) \quad (1)$$

$$\frac{\partial T_s}{\partial t} = \frac{ha}{\rho_s C_s (1 - \epsilon)} (T - T_{so}) \quad (2)$$

where

T = temperature of the gas,

T_{so} = temperature of the solids,

V_a = interstitial air velocity,

h = Convective heat transfer coefficient,

a = Surface area per unit bed volume,

ϵ = Void fraction of the bed,

ρ = density,

C = heat capacity, and the subscripts

a = air,

Shuman (1929) expressed the solution to these equations as modified Bessel functions of the first kind. He also proposed charts for their solution.

Furnas (1930) solved the Shuman equations (1) and (2) by graphical integration for a wide range of bed depths. His solutions extended the usability of the Shuman charts to times greater than one hundred seconds. These solutions are exact for systems where the thermal conductivity of the

solid particle is large and their size small. It is also assumed that air and solid particle properties are constant. These stipulations limit the use of these charts; biological products are generally large and do not satisfy the stipulations mentioned above.

Hougen and Marshall (1947) developed differential equations relating time, position, temperature and concentrations in gas and solid during the adsorption of dilute gases flowing through granular beds. Modified Shuman-Furnas charts were developed for the special cases where linear equilibrium relations exist between adsorbate contents of the gas and solid. Graphical techniques were also applied to situations with non-linear equilibrium. The isothermal requirements preclude the use of this analysis for predicting moisture loss from agricultural products.

Barker (1965) reviewed the research on heat transfer in packed beds and published summarized results from various sources. During the period reviewed, several researchers proposed or obtained solutions to simplified models for the cooling of particles in bulk. These models were mostly for nonagricultural products.

Bakker-Arkema (1970) proposed a simplified model for the cooling of agricultural products. Deep bed cooling models were developed and solved numerically for simultaneous heat and mass transfer during cooling with

varying inlet air conditions. The simplified model did not include the heat generation by respiration.

Baird and Gaffney (1976) developed a model for heat transfer in spherical objects surrounded by a fluid with arbitrarily varying temperature. Their model was extended to predict the temperature variation in a bed of spheres. By performing an energy balance on a control volume the following equation was obtained.

$$(\nu \rho C_p)_a \frac{\partial T_a}{\partial x} = -(\rho C_p)_p \frac{\partial T_p}{\partial t} \quad (3)$$

where

ν = velocity,

ρ = density,

C = specific heat,

T = temperature,

t = time,

x = distance in the direction of fluid flow, and

subscripts

a = air,

p = product.

Finite difference representations of equations (3) and the governing equations for the heat transfer from a single sphere constituted their model. Their model did not include heat generation by respiration and moisture loss by transpiration from the product.

Bellagha and Chau (1985) proposed a model for the cooling of spherical objects singly and in bulk. Their model was basically similar to that proposed by Baird and Gaffney (1976) but differed in that it included heat generation by respiration and evaporative cooling due to transpiration. Another feature of this model was the use of the noncapacitance surface node. This improvement reduced the dependence of the time step on the surface heat transfer coefficient thereby improving the stability and the speed of the numerical solution.

Snyder (1986) developed a mathematical model for the heat transfer in thermally processed shrimp. In his study, he approximated the shrimp by a short cylinder followed by a right circular cone.

Some experimental work has been done on the cooling of sweet corn (Bennett et al., 1976, Henry and Bennett, 1973, Perry and Perkins 1968, Grizzell and Bennett 1966). These researchers based their studies on the assumption that heat transfer from a single corn obeys Newtonian cooling expressed in the form:

$$\frac{dq}{dt} = -hA(T_p - T_f) \quad (4)$$

where

$\frac{dq}{dt}$ = the rate of heat flow from the corn across

area A, and the subscripts p and f represent product and fluid respectively. The solution to equation (4) with the appropriate boundary and initial conditions takes the form

$$T = T_1 \exp(-\lambda t) \quad (5)$$

where

$T = T_t - T_\infty$, the temperature difference,

$T_1 = T_o - T_\infty$, the temperature difference at $t=0$,

$\lambda =$ a constant called the cooling coefficient, and

$T_t =$ product temperature at any time, t .

Henry and Bennett (1973) used this relationship to propose an equation for predicting the product final temperature after one hour. Newtonian cooling assumes that heat transfer from a commodity is limited only by the rate of convection by the cooling or heating medium. This stipulation precludes the use of equation (5) to accurately predict temperature changes during hydrocooling of biological products. Biological products generally have low conductivities.

Sweet corn is made of three distinct components, the cob, kernels and husk. Assuming Newtonian cooling for sweet corn is inappropriate, because it implies a high thermal conductivity within the corn and a low heat transfer

coefficient between the corn and the medium. In most rapid precooling situations, the conditions of Newton's law are seldom satisfied. A considerable temperature gradient generally develops within the product depending on the properties and the rate of surface heat transfer. This suggests that heat transfer from the corn may be limited by how fast it is conducted to the surface and not by how fast it is convected away from the surface, which is the inherent assumption of Newtonian cooling.

Pflug et al. (1965) discussed a transient method which can be used to correlate experimental data, predict heating and cooling times and predict heat transfer and physical property data for biological products of infinite geometries. Plotting the natural logarithm of the difference in temperature between the product and the medium on the vertical axis and the time on the horizontal axis, they defined two parameters: f , the direction function and j , the intercept function. The direction function is the time for the temperature-time curve to traverse one log cycle. The direction function relates the geometry and the thermal diffusivity of the object while the intercept function relates the initial temperature difference of the object.

Solutions for other regular shapes may be obtained from those of the infinite shapes for prescribed surface

temperature or film coefficient if the thermal conductivity is isotropic (Pflug et al., 1965). Composite solutions are the product of the respective individual direction solutions and for a solid with heat transfer in three directions, the direction function can be calculated from

$$\frac{1}{f_c} = \frac{1}{f_1} + \frac{1}{f_2} + \frac{1}{f_3} \quad (6)$$

The subscript c represents the composite object and 1, 2 and 3 represent the three directions of heat transfer in the object.

Thermophysical Properties

Thermal Diffusivity

Thermal diffusivity is a measure of the rate of heat diffusion through a body. This may be determined from

$$\alpha = \frac{k}{\rho C_p} \quad (7)$$

where

α = thermal diffusivity,

k = thermal conductivity,

ρ = density, and

C_p = specific heat capacity.

Experimental determination of thermal diffusivity is also possible.

Dickerson (1965) described an apparatus that can be used in the determination of thermal diffusivity of food products. This apparatus is a cylinder with both ends insulated to restrict heat transfer only in the radial direction. It requires the measurement of the temperature of the food product as it is heated or cooled. This apparatus in a modified form has been used by Bhowmik and Hayakawa (1979). They used the temperatures monitored at the geometric center of the cylinder together with an analytical formula for heat conduction in an infinite cylinder.

Reidel (1969) measured the thermal diffusivity of fourteen food products with high water and proposed the following correlation for α :

$$\alpha = 0.833 \times 10^{-7} + (\alpha_w - 0.833 \times 10^{-7}) \times M_w \quad (8)$$

where M_w is the percent moisture content, wet basis, of the food product and α_w is the thermal diffusivity of water. The correlation is valid for a temperature range of 5 to 55 C and a moisture content of greater than thirty-eight percent.

Nix et al. (1967) used a line heat source technique to measure thermal conductivity and diffusivity simultaneously. They measured temperatures on both sides of

the line source and proposed a forty-term series for calculating the thermal diffusivity. McCurry (1968) presented a numerical procedure for implementing the forty-term series and proposed a relation for maximizing the computation.

Mohsenin (1980) suggested that the definition of thermal diffusivity may be used to determine the thermal diffusivity of one object by comparing it to another object of known thermal diffusivity. If the times to cool the two materials of the same thickness and under identical conditions are known, the thermal diffusivity may be determined from

$$\frac{\alpha_1}{\alpha_2} = \frac{\Delta t_2}{\Delta t_1}$$

where Δt_1 and Δt_2 are the times to cool materials 1 and 2 to the same final temperature, respectively. This method is simple but it appears that it may work only for cases with materials whose thermal diffusivities were close.

Computational methods, based on the series solution of the heat diffusion equation, have been found satisfactory in determining the thermal diffusivity (Murakami et al., 1985, Uno and Hayakawa, 1980, Hayakawa and Bakal, 1973, and Beck, 1966).

The theoretical basis for the experimental determinations of thermal diffusivity is the analytical

solution to the heat diffusion equation. This solution is in the form of an infinite series. If the body is transferring heat by convection to a surrounding medium at constant temperature, the solution to the diffusion equation is

$$\theta = \sum_{n=1}^{\infty} A_n(r) \exp[-\beta_n^2 F_o] \quad (9)$$

(Dzizik, 1980; Ekert and Drake 1972)

where

$$\theta = \frac{T - T_{\infty}}{T_o - T_{\infty}}, \text{ the temperature ratio,}$$

$$F_o = \frac{\alpha t}{r_o^2}, \text{ the Fourier number.}$$

r_o = the characteristic dimension in the direction of heat flow for the geometry being considered,

β_n = the nth root of the transcendental equation particular to the geometry,

$A_n(r)$ = function of β_n , geometry and position in the object, and

$$t = \text{time.}$$

The subscripts represent

$$\infty = \text{medium, and}$$

$$o = \text{initial condition.}$$

For an infinite cylinder the transcendental equation is

$$J_0(\beta_n)B_i = \beta_n J_1(\beta_n) \quad (10)$$

J_0 and J_1 are the Bessel functions of zero and first order respectively, and

$$B_i = \frac{h r_o}{k} \text{ is the Biot number.}$$

For a slab, the transcendental equation is

$$B_i = \beta_n \tan(\beta_n) \quad (11)$$

The series decays very rapidly so that after sufficient time has elapsed ($F_o > 0.2$), only the first term is effective. A semi-logarithmic plot of the temperature ratio versus the time is a straight line and the slope of this line can be used to determine the thermal diffusivity. Gaffney et al. (1980) presented procedures for determining the thermal diffusivity for a sphere, a finite cylinder and a slab. The procedures for the finite geometries utilised the product properties of the series solution of the heat diffusion equation.'

Thermal Conductivity

Thermal conductivities may be determined from equation 7 if the other parameters are available.

Researchers have mostly used experimental methods because of the lack of these parameters. Methods of determining thermal conductivity of food products can be grouped into two categories, steady state methods and transient methods (Reidy and Rippen, 1971). Steady state methods are generally an application of a mathematical solution which is only true for a homogeneous sample (Bennett et al., 1964). Because steady state methods require the measurement of the heat flowing through a sample, these methods are time consuming and generally less accurate.

Transient methods do not require heat flow measurements and rapid results are possible (Reidy and Rippen, 1969). Numerical methods are also becoming acceptable. Murakami et al. (1985) developed an interactive computer program for determining thermal conductivity of food materials based on their composition and temperature. Most numerical methods utilize the solution of the heat diffusion equation.

Sweat (1974) developed an equation for calculating the conductivity of food products that are denser than water and have a moisture content greater than sixty percent. His equation takes the form

$$k = 0.148 + 0.00493 \times M_w \quad (12)$$

where M_w is the percent moisture content, wet basis, of the food product and k is the thermal conductivity in $W/(m.C)$. This equation produces acceptably accurate values of thermal conductivity for high moisture food products. Similar correlations have been published relating moisture content and temperature for high moisture food products (Harper, 1976, Kazarian and Hall, 1965, Lentz, 1961). Choi (1985) correlated thermal conductivity and temperature for food product components of protein, fats, carbohydrates, ash and water. Murakami et al. (1985) developed an interactive computer program for determining thermal properties of foods using Choi's (1985) correlations.

Specific Heat Capacity

The most publicized correlation for specific heat determination is that due to Seibel (1892):

$$C_p = 0.837 + 0.034 \times M_w \quad (13)$$

The specific heat C_p is measured in $kJ/(kg.C)$ and M_w is the percent moisture content, wet basis. Equation (13) is only true for values of specific heat above freezing. Mohsenin (1980) stated that Seibel's equation produced acceptably accurate results for high moisture content materials. Staph (1949) published the only departure from Seibel's equation for temperatures below freezing.

The only values for effective thermal properties of sweet corn were published by Grizzell and Bennett (1966). They published a value of $0.98 \times 10^{-7} \text{ m}^2/\text{s}$ for the effective thermal diffusivity, 815.4 kg/m^3 for the density and 0.273 W/(m.C) for the conductivity. They approximated the corn as a finite cylinder and restricted heat flow to the radial direction only. Cooling data for the corn was then used to determine the effective thermal diffusivity and effective thermal conductivity of sweet corn. Perry and Perkins (1968) used a value of 0.07 W/(m.C) for the thermal conductivity of corn but did not mention the source.

No reference was found in the literature for the thermal properties of the cob, kernel and husk of corn.

Convection Heat Transfer Coefficient

A considerable amount of research has been carried out on the prediction of the convection heat transfer coefficient for flow over single bodies of various geometrical shapes. Using the boundary layer theory analytical solutions have been obtained for a limited number of cases. Convection heat transfer coefficients are generally obtained using experimental methods. Correlations are then made based on these results.

Semi-empirical equations for estimating the heat transfer coefficient between a single cylinder and a fluid flowing perpendicularly to the axis of the cylinder are

expressed in the form

$$\text{Nu} = C_r \text{Re}^m \text{Pr}^n \quad (14)$$

$\text{Nu} = \frac{hd}{k}$, the Nusselt number,

$\text{Re} = \frac{dv\rho}{\mu}$, the Reynolds number,

d = diameter of the cylinder,

k = conductivity of fluid,

v = average velocity in the duct ahead of the cylinder,

ρ = density of the fluid,

μ = dynamic viscosity of the fluid,

$\text{Pr} = \frac{\nu}{\alpha}$, the Prandtl number,

ν = kinematic viscosity, and

α = thermal diffusivity.

C_r , m and n are constants. Heldman and Singh (1981) used 0.683, 0.466 and 0.33, respectively for C_r , m and n for Reynolds numbers between 40 and 4000. Geankoplis (1972) used 0.281, 0.5 and 0.44 respectively for C_r , m and n for the same range of Reynolds number.

Relations also exist for the heat transfer coefficient from a bed of cylinders to a fluid flowing perpendicular to the cylinders. For flow of water normal to banks of tubes staggered ten rows deep, McAdams (1954) proposed the following equation for determining the heat transfer coefficient:

$$h = 986(1.214 + 0.0121T_f) \frac{v_{\max}^{0.6}}{d^{0.4}} \quad (15)$$

where v_{\max} is the maximum velocity, T_f the fluid temperature and d is the diameter of the tube. An equation for air flowing past lines of tubes staggered ten deep has been published by Perry et al. (1984). This is in the form

$$h = \frac{0.47 C_p^{\frac{1}{3}} k^{\frac{2}{3}} \rho^{0.6} v_{\max}^{0.6}}{\mu^{0.267} d^{0.4}} \quad (16)$$

where

C_p is the specific heat capacity,

k is the thermal conductivity,

ρ is the density of the air,

v_{\max} is the maximum velocity,

μ is the dynamic viscosity, and

d is the average diameter of the tube.

Bird et al. (1966) used the Colburn J factor to determine h from the equation

$$J_H = 0.89 \text{ Re}^{-0.51} \quad (\text{Re} < 50)$$

and

$$J_H = 0.56 \text{ Re}^{0.41} \quad (\text{Re} > 50) \quad (17)$$

The Colburn factor J_H is defined by the following equation:

$$J_H = \frac{h}{C_{pb}v} \left(\frac{C_p \mu}{k} \right)_f^{\frac{2}{3}}$$

The subscripts b and f indicate that the properties are calculated at the bulk and fluid temperatures, respectively.

Gaffney et al. (1980) presented an experimental method for approximating h during the processing of fruits and vegetables. The method involves measuring temperature versus time data on a sample of known specific heat capacity, physical properties and a high thermal conductivity like copper. The lumped heat capacity solution (equation 5) can then be employed. The constant λ in equation (5) is then identical to

$$\lambda = \frac{hA}{\rho C_p V} \quad (18)$$

where A is the total surface area and V is the volume. The convection heat transfer coefficient, h, is the only unknown in this equation and can be calculated from the slope of the semilog plot of temperature ratio versus time (Gaffney et al., 1980).

Sastry (1984) used this method to determine convective heat transfer coefficient for canned whole mushrooms processed in still retort. He used mushroom-shaped aluminum castings and found that the results were within acceptable range of empirical equations for forced convection over a body with a characteristic dimension equivalent to the major diameter of the mushroom cap. This technique was also used successfully by Snyder (1986) to determine the heat transfer coefficient during the thermal processing of shrimp.

Respiration

Respiration is the overall process by which stored organic materials are oxidised and broken down into simple end products with a release of chemical and heat energy. Carbon dioxide is a by-product of this process. The released internal energy is commonly referred to as respiratory heat evolution, or vital heat. The energy produced is generally calculated based on the amount of carbon dioxide released. Although the rate of substrate depletion can also be used, the carbon dioxide method gives values that are satisfactory (Green et al., 1941). The loss of stored energy reserves from the product during senescence inevitably results in loss of food value and salable weight.

The respiration rate of perishable commodities is affected by the temperature of the product. Respiration increases significantly with increasing product temperature and lowering the product temperature is one way of slowing the biological activity of perishable commodities (Fig. 1). Technologies for quickly lowering the temperature of the perishable commodity include hydrocooling, top-icing, slushed or package ice, forced-air cooling and vacuum cooling (Ryall and Pentzer, 1982).

Green et al. (1941) described a calorimeter for measuring the heat of respiration and an apparatus for determining the carbon dioxide produced by fresh fruits and vegetables. The research showed that the values of the heat

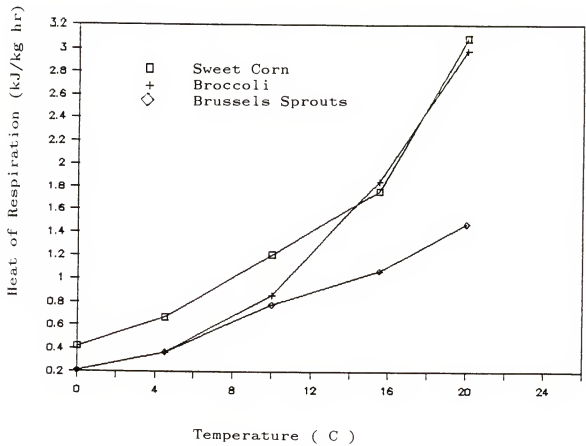


Figure 1 Heat of Respiration of Three Vegetables.
(Source: Hardenburg et al., 1986)

produced which were obtained by calculations based on the rate of production of carbon dioxide were within 10 percent of those obtained by means of the calorimeter.

The rate of respiration determines the relative rate at which a commodity will ripen, age and perish. Awbery (1927) showed that the temperature excess at the center of an apple caused by its heat of respiration after two hours of cooling was only 0.023 C. Data available in Hardenburg et al. (1986), shows that at 5 C apples produce less than one joule of heat per kilogram in one hour. Kader (1985) and Scholz et al. (1963) rated the respiration rate of sweet corn as extremely high. Sweet corn releases greater than 1.54 kJ/(kg.hr) at 5 C (Scholz et al., 1963). Respiration therefore contributes significantly to the cooling load of sweet corn.

Haile and Sorenson (1968) found a significant interaction between temperature and moisture content on the respiration rate of sorghum grain. The rate of heat evolution increased with time for higher moisture content grain.

Evenson and Boyer (1986) presented data for the respiration of the Silver Queen variety of sweet corn stored at 0 and at 10 C. Reducing sugars depleted rapidly after harvest, decreasing faster at 10 C than at 0 C. While the sucrose levels remained fairly constant at 10 C for

seven days, at 0 C the sucrose content increased up to seven days (Evenson and Boyer, 1986). This suggests a storage life of about eight days for sweet corn at 0 C.

No reference was found for heat generation in the Super Sweet (sh₂) variety of sweet corn used in this study. Data from Scholz et al. (1963) was used to obtain a correlation for the heat generation in sweet corn. A correlation

$$Q = 1.17 T^{0.17} \quad (19)$$

was obtained. Q is the heat evolution rate measured in kJ/(kg.hr) and T is the temperature in C. The correlation coefficient for the data was 0.68.

DEVELOPMENT OF NUMERICAL MODEL

For this work the single ear of corn was represented by the shape shown in Figure 2 with three layers in the radial direction. The three layers were the cob, the kernels and the husk. These components were assumed to be discrete layers in thermal contact with each other. The layer referred to as the husk actually is a composite layer consisting of the husks, the silk and air spaces. It was necessary to approximate these to a single discrete layer to simplify the computations. The heat diffusion equation is

$$\frac{1}{r} \frac{\partial}{\partial r} \left(k_u r \frac{\partial T}{\partial r} \right) + \frac{\partial}{\partial z} \left(k_z \frac{\partial T}{\partial z} \right) + Q_u = (\rho C_p)_u \frac{\partial T}{\partial t} \quad (20)$$

where the subscript u has the values 1, 2 and 3 for the cob, kernels and husk, z represents the direction along the length of the cylinder, and Q_u is the rate of heat generation in each layer. The initial and boundary conditions for this case are stated below.

$$T(r, z, 0) = F_u(r, z); \text{ for } t = 0. \quad (21)$$

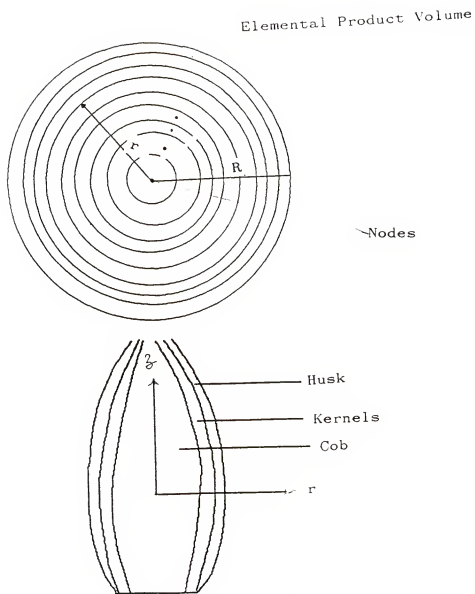


Figure 2 Cross Section and the Shape of an Ear of Sweet Corn Showing Nodes and Volumes Used in the Mathematical Model.

$$k_u \frac{\partial T_u}{\partial r} = k_{u+1} \frac{\partial T_{u+1}}{\partial r}; \quad t > 0, \quad u=1,2 \quad (22)$$

$$T_u = T_{u+1} \quad t > 0, \quad u=1,2 \quad (23)$$

$$k_s \frac{\partial T}{\partial x} = h(T - T_\infty) = 0; \quad t > 0 \quad (24)$$

where

$T(r,z,t)$ = temperature,

$F_u(r,z)$ = initial temperature field,

k_u = thermal conductivity of layer u ,

and subscript s represents the surface layer.

Equations (22) and (23) are the boundary conditions at the interfaces between the layers and (24) is the boundary condition on the surface of the cylinder both around the curved surface and at the top and the bottom where convection is taking place between the cylinder and the cooling medium.

Before developing the model some simplifying assumptions were made;

- (i) Each layer is homogeneous, isotropic and has thermal properties that are constant within the layer but different from those of the adjacent layer;
- (ii) the convective heat transfer coefficient is the same all round the surface and on the bottom and on the top.

The lateral cross-section of sweet corn is not exactly a circle. However, to simplify the model to a two-

dimensional problem, the corn was assumed to have a circular cross-section whose diameter was equal to the average of the major and minor diameters. The domain for the cooling problem was discretized in volume elements and nodes in order to apply the finite difference method. The finite difference equations were developed by performing an energy balance at each node. There are four types of nodes; the center node, the internal node, the interface node and the surface node.

Performing an energy balance for each node means summing the heat energy flowing into and out of each volume element and equating it to the change in internal energy of the volume element. This energy comprises the rate of conduction into and out of the node and the heat generated by respiration. For the surface node, the heat energy includes exchange with the cooling medium and transpiration.

Interior Node

The heat flowing into node i, j is given by

$$q_{i-1,j} + q_{i+1,j} + q_{i,j-1} + q_{i,j+1} + q_i^* = \text{rate of heat stored} \quad (25)$$

$q_{i-1,j}$ = heat flow rate into node (i, j) from node $(i-1, j)$,

q_i^* = heat of respiration.

Using Fourier's law in equation (25) will give

$$\begin{aligned}
& k_{i-1} \frac{A_{i-1,j}}{\Delta r_{u,j}} (T_{i-1,j} - T_{i,j}) + k_i \frac{A_{i,j}}{\Delta r_{u,j}} (T_{i+1,j} - T_{i,j}) \\
& + \frac{k_j A_{z_{i,j-1}}}{\Delta z} (T_{i,j-1} - T_{i,j}) \\
& + \frac{k_j A_{z_{i,j}}}{\Delta z} (T_{i,j+1} - T_{i,j}) \\
& + \rho_i V_i Q_i = \text{Heat stored.} \quad (26)
\end{aligned}$$

the heat stored is defined by

$$\text{heat stored} = \frac{\rho_i C_{p_i} V_{i,j}}{\Delta t} (T_{i,j}^{n+1} + T_{i,j}^n) \quad (27)$$

The subscript u denotes each of cob, kernel or husk, the components of the ear of corn. The areas are defined as follows:

$$\begin{aligned}
A_{i,j} &= 2 \pi r_{i,j} \Delta z \\
A_{z_{i,j}} &= \pi (r_{i,j}^2 - r_{i-1,j}^2) \\
V_{i,j} &= A_{z_{i,j}} \Delta z
\end{aligned}$$

The radius, r_i is the radius of the volume element at whose center the node is located (Fig 2). It is measured from the center to the heat transfer surface.

Rearranging the above equations

$$\begin{aligned}
T_{i,j}^{n+1} = & T_{i,j}^n + \frac{\Delta t}{\rho_i C_{p_i} V_{i,j}} \left\{ \frac{k_{i-1} A_{i-1,j}}{\Delta r_{u,j}} (T_{i-1,j}^n \right. \\
& - T_{i,j}^n) + \frac{k_i A_{i,j}}{\Delta r_{u,j}} (T_{i+1,j}^n - T_{i,j}^n) + \\
& \frac{k_j A_{i,j-1}}{\Delta r_{u,j}} (T_{i,j-1} - T_{i,j}) + \\
& \left. \frac{k_j A_{i,j}}{\Delta r_{u,j}} (T_{i,j} + T_{i,j+1}) + \rho_i V_i Q_i \right\} \quad (28)
\end{aligned}$$

The assumption that each layer is homogeneous and isotropic means that

$$k_i = k_j$$

For an interior node

$$\begin{aligned}
T_{i,j}^{n+1} = & T_{i,j}^n + \frac{\alpha_u \Delta t}{V_{i,j}} \left\{ \frac{A_{i,j}}{\Delta r_{u,j}} (T_{i+1,j}^n - T_{i,j}^n) + \right. \\
& + \frac{A_{i-1,j}}{\Delta r_{u,j}} (T_{i-1,j}^n - T_{i,j}^n) \\
& + \frac{A_{i,j-1}}{\Delta z} (T_{i,j-1}^n - T_{i,j}) +
\end{aligned}$$

$$\frac{A_{i,j}}{\Delta z} (T_{i,j} + T_{i,j+1}^n) + \frac{\rho_i V_i Q_i}{k} \} \quad (29)$$

Equation (29) may be further rearranged as follows:

$$\begin{aligned} T_{i,j}^{n+1} &= \frac{\alpha_u \Delta t}{V_{i,j}} \left\{ \frac{A_{i,j}}{\Delta r_{u,j}} T_{i+1,j}^n + \frac{A_{i-1,j}}{\Delta r_{u,j}} T_{i-1,j}^n \right. \\ &+ \frac{A_{z_{i,j-1}}}{\Delta z} T_{i,j-1}^n + \frac{A_{z_{i,j}}}{\Delta z} T_{i,j+1}^n + \frac{\rho_i V_i Q_i}{k} \} \\ &+ \left[1 + \frac{\alpha_u \Delta t}{V_{i,j}} \left(-\frac{A_{i,j}}{\Delta r_{u,j}} - \frac{A_{i-1,j}}{\Delta r_{u,j}} \right. \right. \\ &\quad \left. \left. - \frac{A_{z_{i,j-1}}}{\Delta z} - \frac{A_{z_{i,j}}}{\Delta z} \right) \right] T_{i,j}^n \end{aligned} \quad (30)$$

where $\alpha_u = \frac{k_u}{\rho_u C_{pu}}$, is the diffusivity of each component of the ear of corn. Respiration data from Schol et al (1963) was curve fitted and the following relation obtained

$$Q_i = 1.17 T_i^{0.17}$$

Center Node

The center node is different from the general node in that it has only three other nodes surrounding it. Heat

thus flows from it in the radial direction but none flows into it during the cooling process. The simplified equation is

$$\begin{aligned}
 T_{i,j}^{n+1} = & T_{1,j}^n + \frac{\alpha_1 \Delta t}{V_{1,j}} \left\{ \frac{A_{1,j}}{\Delta r_{1,j}} (T_{2,j}^n - T_{1,j}^n) \right. \\
 & + \frac{Az_{i,j-1}}{\Delta z} (T_{1,j-1}^n - T_{1,j}^n) + \\
 & \left. \frac{Az_{i,j-1}}{\Delta z} (T_{1,j} + T_{1,j+1}^n) + \frac{\rho_1 V_1 Q_1}{k} \right\}
 \end{aligned}$$

or

$$\begin{aligned}
 T_{i,j}^{n+1} = & \left(1 - \frac{\alpha_1 \Delta t}{V_{1,j}} \left(\frac{A_{1,j}}{\Delta r_{1,j}} + \frac{Az_{i,j-1}}{\Delta z} + \frac{Az_{i,j}}{\Delta z} \right) \right) \\
 & + \frac{\alpha_1 \Delta t}{V_{1,j}} \left\{ \frac{A_{1,j}}{\Delta r_{1,j}} T_{2,j}^n + \frac{Az_{i,j-1}}{\Delta z} T_{1,j-1}^n \right. \\
 & \left. + \frac{Az_{i,j-1}}{\Delta z} T_{1,j+1}^n + \frac{\rho_1 V_1 Q_1}{k} \right\} \quad (31)
 \end{aligned}$$

Interface Node

An interface node is a node at the interface of two different materials. There is an interface node between the cob and the kernels and another interface node between the

kernels and the husk. The volume element is made up of one half of the volume elements of the components on each side of the node. For this case $k_{i+1} \neq k_i$ and k_j was assumed to be equal to the weighted average of the two conductivities of the components surrounding the node. The energy stored in the volume element was weighted accordingly.

$$T_{i,j}^{n+1} = T_{i,j}^n + \frac{2\Delta t}{\rho_{i-1}C_{P_{i-1}}V_{i-1,j} + \rho_i C_{P_i}V_{i,j}}$$

$$\left\{ \frac{k_{i-1}A_{i-1,j}}{\Delta r_{i-1,j}} (T_{i-1,j}^n - T_{i,j}^n) \right.$$

$$+ \frac{k_i A_{i,j}}{\Delta r_{i,j}} (T_{i+1,j}^n - T_{i,j}^n) +$$

$$\frac{k_j A_{z_{i,j-1}}}{\Delta z} (T_{i,j-1}^n - T_{i,j}^n) +$$

$$\left. \frac{k_j A_{z_{i,j}}}{\Delta z} (T_{i,j}^n - T_{i,j+1}^n) + \rho_i^* V_i^* Q_i \right\}$$

Rearranging the equation gives

$$T_{i,j}^n = \left(1 - \frac{2\Delta t}{\rho_{i-1}C_{P_{i-1}}V_{i-1,j} + \rho_i C_{P_i}V_{i,j}} \left(\frac{k_{i-1}A_{i-1,j}}{\Delta r_{i-1,j}} \right. \right.$$

$$\begin{aligned}
& + \frac{k_i A_{i,j}}{\Delta r_{i,j}} + \frac{k_j A_{z_{i,j-1}}}{\Delta z} + \frac{k_j A_{z_{i,j}}}{\Delta z}) \Big) T_{i,j}^n + \\
& \frac{2\Delta t}{\rho_{i-1} C_{p_{i-1}} V_{i-1,j} + \rho_i C_{p_i} V_{i,j}} \left\{ \frac{k_{i-1} A_{i-1}}{\Delta r_{i-1,j}} T_{i-1,j}^n \right. \\
& + \frac{k_i A_{i,j}}{\Delta r_{i,j}} T_{i+1,j}^n + \frac{k_j A_{z_{i,j-1}}}{\Delta z} T_{i,j-1}^n \\
& \left. + \frac{k_j A_{z_{i,j}}}{\Delta z} T_{i+1,j}^n \right) + \rho_i^* V_i^* Q_i \Big\} \quad (32)
\end{aligned}$$

where

$$k_j = \frac{A_{i-1} k_{i-1} + A_i k_i}{A_{i-1} + A_i},$$

$$V_{i,j}^* \rho^* = V_{i-1,j} \rho_{i-1} + V_{i,j} \rho_i$$

Surface Node

The surface node exchanges heat with the surrounding nodes and also with the cooling medium. In this study the surface node was treated as a non-capacitance node as described by Chau et al. (1984) and has no volume element associated with it. Because there is no volume element attached to this node, the energy storage term disappears from the energy balance equation. The net energy flow by conduction, convection, radiation and evaporative cooling is given as follows:

$$\frac{kA_{s-1,j}}{\frac{\Delta r_{s-1,j}}{2}} (T_{s-1,j}^n - T_{s,j}^n) = hA_{s,j} (T_{s,j}^n - T_{\infty}^n) \\ + A_{s,j} F \sigma \epsilon [(T_{abs,s,j}^n)^4 - (T_{abs,\infty}^n)^4] + A_{s,j} L Q_t^n$$

where L = latent heat of vaporization

Q_t = transpiration rate per unit area

F = radiation shape factor

σ = Stefan-Boltzman constant

ϵ = surface emissivity

A = area, and

the subscripts

s = surface node,

abs = absolute.

The transpiration rate Q_t is calculated from moisture loss measurements of the product and is a function of the water vapor pressure of the surrounding air and the evaporating surface, the skin and air mass transfer coefficients (Romero, 1987, Chau and Gaffney, 1985, Gaffney et al., 1985).

Chau et al. (1984) have shown that the radiation and convection terms can be combined to yield a term

$$h_o A_s (T_{s,j}^n - T_{\infty}^n)$$

where $h_o = h_c + h_r$, is the combined heat transfer coefficient. The subscripts c and r represent convection and radiation respectively.

$$h_r = F\sigma\epsilon \left(T_{abs,s,j}^{n+1} + T_{\infty}^n \right) \left\{ (T_{abs,s,j}^n)^2 + (T_{\infty}^n)^2 \right\}$$

The surface temperature and the radiation heat transfer coefficient are unknowns at any time step and may be determined by iterating the equation until a preset condition between two successive values of either the surface temperature or the heat transfer coefficient is satisfied. For this problem radiation was assumed to be negligible and the surface temperature at the preceeding time step was used in the computation. Rearranging the equation for the surface temperature

$$T_{s,j}^n = \frac{B_{ir} A_{s,j} T_{\infty}^n + A_{s-1,j} T_{s-1,j}^n - \frac{\Delta r A_{s,j} L Q_t^n}{k}}{B_{ir} A_{s,j} + A_{s-1,j}} \quad (33)$$

where the term B_{ir} is defined as

$$B_{ir} = \frac{h_o \Delta r}{2k}$$

Equation (33) was used at the surface for $r = r_o$, the radius of the cylinder and at the top and bottom of the cylinder where $z = L, 0$ respectively. At the top and bottom of the cylinder the term B_{ir} was redefined as

$$B_{iz} = \frac{h_o \Delta z}{2k}$$

The area was also replaced by $Az_{i,j}$.

Equations 30, 31, 32 and 33 are the finite difference equations used in the numerical scheme.

The Bed Model

In developing the bed model, the following assumptions were made:

- (i) flow rates of the medium were constant in all interstices of the bulk load,
- (ii) heat transfer between the corn and the cooling medium was by convection only.
- (iii) thermal properties of the medium and corn were constant.

A heat balance was performed for a control volume $A dx$ as shown in Figure 3. The fluid flowing through the product picks up heat energy and the change in energy of the fluid is equal to the change in energy of the product in the control volume.

$$v_f \rho_f C_{p,f} A \frac{\partial T_f}{\partial x} dx dt = - \rho_p C_{p,p} \frac{\partial T_p}{\partial t} A dx dt$$

where

T_f = temperature of air,

T_p = temperature of product,

A = cross-sectional area of bed,

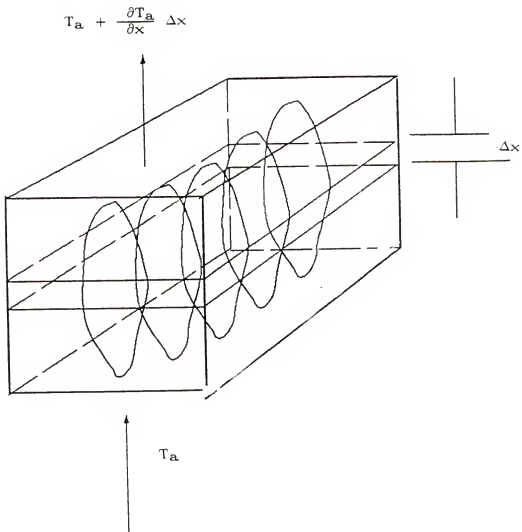


Figure 3 Division of the Crate into Layers.

- v_f = superficial velocity of air,
 ρ_p = bulk density of product,
 ρ_f = density of fluid,
 $C_{p,f}$ = specific heat capacity of fluid,
 $C_{p,p}$ = specific heat capacity of product,
 x = distance from air inlet,
 t = time.

$$\text{i.e} \quad \frac{\partial T_f}{\partial x} = - \frac{(\rho C_p)_p}{(\nu \rho C_p)_f} \frac{\partial T_p}{\partial t} \quad (34)$$

In finite difference form, the equation becomes

$$\frac{\Delta T_f}{\Delta x} = - \frac{(\rho C_p)_p}{(\nu \rho C_p)_f} \frac{\Delta T_p}{\Delta t} \quad (35)$$

Rearranging the equation gives

$$T_{p,i}^{n+1} = T_{p,i}^n + \frac{\Delta t (\rho C_p \nu)_f}{(\rho C_p)_p} \left\{ \frac{T_{f,i-1}^n - T_{f,i}^n}{\Delta x} \right\} \quad (36)$$

The box used in the forced air cooling tests was placed in a room controlled at 1.7 C and it was assumed that heat transfer occurred between the box and the room. This was calculated from

$$Q = UA\Delta T \quad (37)$$

where U is the overall heat transfer coefficient between

the box and the room, A the total surface area for heat transfer and ΔT the temperature difference between the air in the box and the air in the controlled room.

The solution to equations (36), (37) together with equations (30), (31), (32) and (33) constitute the numerical model for the heat transfer during the cooling of ears of corn in a bed. A computer program was written to implement these equations using the inputs in Table 1. The flow diagram is shown in Figure 4.

To solve this set of equations, it is necessary to compute the mass-average temperature of the individual ears of corn in each layer of the bulk load after each time period. Mass-average temperature denotes a single value from the temperature profile of a product that would become the uniform product temperature upon reaching equilibrium under adiabatic conditions.

The mass-average temperature was determined by computing the mass-average temperature of each cylindrical shell and computing a weighted average temperature based on the mass of each cylindrical shell. This temperature was then assigned to the layer and used in subsequent computations.

Ames (1977) and Carnahan et al. (1969) discussed the criteria for the stability of explicit numerical schemes in the solution of heat transfer problems. For a parabolic equation of the form

Table 1

Inputs to the Numerical Model

Initial fluid temperature	Initial product temperature
Product diameter	Product length
Number of layers	Number of products per layer
Number of nodes in radius	Number of nodes in length
Product respiration rate	Time increment
Specific heat of cob	Conductivity of cob
Density of cob	Density of kernel
Conductivity of Kernel	Specific heat of kernel
Conductivity of husk	Density of husk
Fluid flow rate	Simulation time
Bulk density	Specific heat of husk

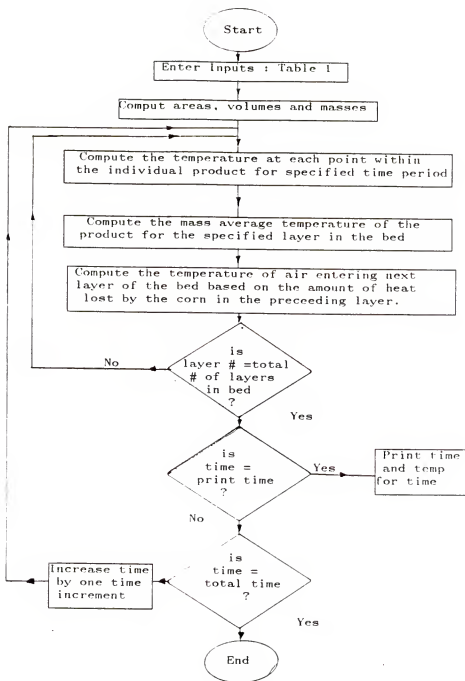


Fig 4 Flow Chart for the Computer Program

$$U_t = aU_{xx} + bU_{xy} + cU_{yy} \quad (38)$$

where a , b and c can be functions of both x and y . The classical explicit recurrence relation can be written in the form

$$U_{i,j+1} = a_o U_{i-1,j} + b_o U_{i,j} + c_o U_{i+1,j} \\ + dU_{i,j-1} + eU_{i,j+1} \quad (39)$$

The subscript o is used to indicate that the values of the coefficients in equation (38) are not necessarily the same in equation (39). The stability criterion for equation (39) is that b_o be positive. Ames (1977) stated that satisfying this condition also assured convergence for a well derived set of equations. This requires that from equation (30)

$$1 - \frac{\alpha_i \Delta t}{V_{i,j}} \left\{ \frac{A_{i,j}}{\Delta r_{i,j}} + \frac{A_{i-1,j}}{\Delta r_{i,j}} + \frac{Az_{i,j}}{\Delta z} + \frac{Az_{i,j-1}}{\Delta z} \right\} \geq 0 \quad (40)$$

Applying the same procedure for the center and interface nodes respectively, the following criteria for stability are obtained.

$$1 - \frac{\alpha_1 \Delta t}{V_{i,j}} \left\{ \frac{A_1}{\Delta r_{1,j}} + \frac{Az_{1,j-1}}{\Delta z} + \frac{Az_{i,j}}{\Delta z} \right\} \geq 0 \quad (41)$$

$$1 - \frac{2\Delta t}{\rho_{i-1} C_{pi-1} V_{i-1,j} + \rho_i C_{pi} V_i} \left\{ \frac{k_{i-1} A_{i-1,j}}{\Delta r_{i-1,j}} + \right.$$

$$\frac{k_i A_{i,j}}{\Delta r_{i,j}} - \frac{k_z A_{z_{i,j-1}}}{\Delta z} - \frac{k_z A_{z_{i,j}}}{\Delta z} \geq 0 \quad (42)$$

Solving for Δt in the above equations yields

$$\Delta t \leq \frac{V_{i,j}}{\alpha_i \left\{ \frac{A_{i,j}}{\Delta r_{i,j}} + \frac{A_{i-1,j}}{\Delta r_{i-1,j}} + \frac{A_{z_{i,j}}}{\Delta z} + \frac{A_{z_{i,j}}}{\Delta z} \right\}} \quad (43)$$

$$\Delta t \leq \frac{V_{1,j}}{\alpha_1 \left\{ \frac{A_{1,j}}{\Delta r_{1,j}} + \frac{A_{z_{1,j-1}}}{\Delta z} + \frac{A_{z_{1,j}}}{\Delta z} \right\}} \quad (44)$$

$$\Delta t \leq \frac{\rho_{i-1} C_{p_{i-1}} V_{i-1,j} + \rho_i C_{p_i} V_i}{2 \left\{ \frac{k_{i-1} A_{i-1,j}}{\Delta r_{i-1,j}} + \frac{k_i A_{i,j}}{\Delta r_{i,j}} + \frac{k_z A_{z_{i,j-1}}}{\Delta z} + \frac{k_z A_{z_{i,j}}}{\Delta z} \right\}} \quad (45)$$

Eight nodes were chosen to simulate the interior of the corn in either direction since a large temperature gradient was expected. The number of nodes will affect the spatial increments and the time step requirement. The time step must satisfy all the conditions above for stability to be achieved. For the sizes and the thermal properties of the corn used, the time step was found to be 7.2 seconds.

EXPERIMENTAL PROCEDURE

The sweet corn used for this study was the Supersweet (sh₂) and purchased from a local grocery store. The corn had been previously precooled and top-iced before shipping to the store.

The experiments were conducted in three phases; thermophysical property determination, hydrocooling and forced air cooling.

Sample preparation was identical in both cooling tests. Three 36-gauge copper-constantan thermocouples were used to monitor temperatures in the cob, kernel and husk of an ear of corn. The thermocouples were located at one third of the length from the base of the ear of corn and placed radially. To monitor the temperature of the cob, kernels and husks, the thermocouples were placed at the center of the cob, the base of the kernels and inside the husks respectively. Sampled ears had approximately the same weight and diameter.

A typical wire bound crate of sweet corn measures 0.23 m wide, 0.61 m long and 0.28 m deep. The crates are filled with corn so that the corn is parallel to the 0.28 m side. The crates are stacked in the pallet with this side

vertical. Temperature sampling per crate was achieved with six ears of corn, two at each location on a diagonal as shown in Figure 5. At each location, one ear of corn had the silk end directed towards the direction of fluid flow and the other had the silk end pointed in the opposite direction. The thermocouples were connected to a Campbell Scientific data logger model 21X.

Thermal Diffusivity

Methodology For Thermal Diffusivity

Thermal diffusivities of the cob, kernels and husks were determined using the method described by Gaffney et al. (1980). This method utilizes the series solution of the heat diffusion equation. Temperatures are measured at the center of the sample and a graph is plotted of the natural logarithm of the temperature ratio on the vertical axis and the time on the horizontal axis. The thermal diffusivity is determined from the slope of the linear section of the graph.

Experimental Procedure

The equipment used to determine the diffusivities of the cob, the kernels and the husks comprised a heat exchanger, a constant temperature bath and a data logger for recording temperatures (Fig 6). Compressed air was used to agitate the ice bath and the heat exchanger used to lower

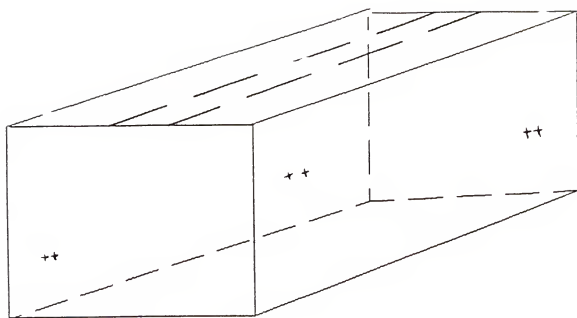


Figure 5 A Wire Bound Crate Configuration with Thermocouple Locations

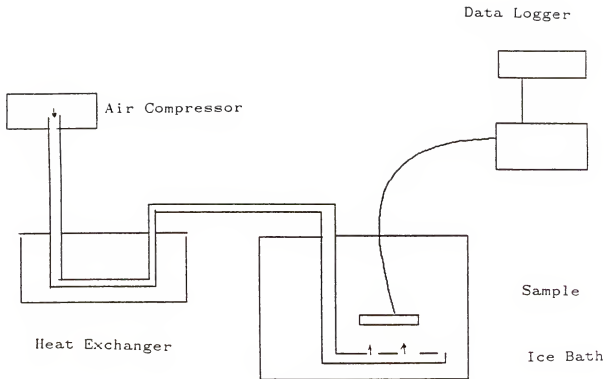


Figure 6 Apparatus Used to Experimentally Determine Thermal Diffusivity

the temperature of the air before it entered the ice bath. Compressed air was passed through the bath to provide enough agitation to produce a very high convection heat transfer coefficient. Six replicates were made on each sample.

Sample preparation was different for each component and for the whole ear of corn. Thermocouples were located at the geometric centers of the samples and temperatures were monitored on a Campbell Scientific model 10X data logger until a temperature difference of 1 C was attained between the sample and the bath. The prepared samples were brought to thermal equilibrium with tap water at 26.6 C and then transferred to an agitated ice bath. Researchers (Cowell et al., 1959, Gaffney et al., 1980) have shown that conduction errors along the thermocouple within the solid will primarily affect the lag factor and will have little effect on the slope of the temperature curve. Thus, if conduction errors occur within the product, very little error is introduced into the calculated value of the thermal diffusivity as determined from the slope of the cooling curve. These researchers (Cowell et al., 1959, Gaffney et al., 1980) also noted that the presence of fluid within the sample would cause more serious conduction errors, but these errors could be reduced by using small gauge thermocouples.

Thermal diffusivity of the cob

A hollow cylinder was constructed from copper with an internal diameter of 2.55 cm, an external diameter of 2.70 cm and a length of 5.13 cm. Two copper plates 4.0 cm square were also made to fit onto the ends of the hollow copper cylinder. A 0.05 mm hole was drilled halfway down the side of the cylinder to hold a 36-gauge copper-constantan thermocouple. A cob sample, with the cob intact, was placed in the cylinder and a thermocouple inserted along the radius of the cylinder to the center of the cob. The copper plates were clamped to the ends of the cylinder and silicone glue smeared around the edges and around the thermocouple to stop water from getting into the sample. The prepared sample was allowed to equilibrate to room temperature.

Thermal diffusivity of the kernels

A hollow copper cylinder with an internal diameter of 2.59 cm and a length of 10.15 cm was constructed for the experiment. One end of the cylinder was welded to a copper plate and another plate made to fit across the other end. The kernel sample was ground into a slurry and put in the copper cylinder. A thermocouple was introduced along the radius of the cylinder to the center of the specimen through a 0.05 mm hole drilled on the side of the cylinder. A 36-gauge thermocouple was used to reduce the

errors that may be caused by conduction of the high moisture slurry. The plate was clamped to the other end of the cylinder and silicone glued used to seal the cylinder.

Thermal diffusivity of the husk

Corn husks were removed from four ears of corn (thirty leaves) placed between two copper plates, 6.7 mm thick, measuring 10.8 cm by 5.7 cm and 1.06 cm thick. this thickness of the plate would introduce little resistance to heat transfer across the plates to the sample (Appendix C). The husks were trimmed to the size of the plates. The copper plates were then removed and a 36-gage copper-constantan thermocouple was placed at the geometric center of the sample. The sample was then wrapped in plastic wrap, secured tightly and sandwiched between the two copper plates.

Corn as a homogeneous material

The effective thermal diffusivity of the ear of corn was needed for use in the homogeneous model to investigate if heat transfer from an ear of corn could be modeled as heat transfer from a homogeneous material. An ear of corn was trimmed to represent a solid cylinder of length to diameter ratio of 2. A 36-gauge thermocouple was inserted along the axis to the geometric center of the sample and the ends sealed.

The samples were brought to a uniform initial temperature by placing them in water at 26.6 C. They were then introduced into the agitated bath maintained at 0 C.

Calculation of Thermal Diffusivity

Knowledge of the roots of the transcendental equation 10 for a cylinder or equation 11 for a slab is required before the thermal diffusivity can be calculated from experimental data. The solutions for the finite geometries used were obtained from the concept of product solutions as discussed by Gaffney et al. (1980). The thermal diffusivity of the sample in the form of a finite cylinder can be determined from the slope (m) of the straight line portion of the semi-log plot of temperature ratio versus time for any position within the object as

$$\alpha = \frac{-m}{\left(\left(\frac{\beta_1}{l} \right)^2_{\text{cyl}} + \left(\frac{\beta_1}{l} \right)^2_{\text{slab}} \right)} \quad (46)$$

The subscript cyl represents the cylinder while the subscript slab represents a slab of thickness equal to the length of the cylinder. A similar equation is obtained for a finite slab as

$$\alpha = \frac{-m}{\left(\left(\frac{\beta_1}{l} \right)^2_{\text{slab}_1} + \left(\frac{\beta_1}{l} \right)^2_{\text{slab}_2} + \left(\frac{\beta_1}{l} \right)^2_{\text{slab}_3} \right)} \quad (47)$$

(Gaffney et al. 1980)

Slab₁, slab₂ and slab₃ are the three slabs of thicknesses equal to the three dimensions of the solid. The symbol β_1 represents the first root of equation 10 or equation 11. For an infinite geometry, when the Biot number tends to infinity, β_1 has the values 2.4048 and $\pi/2$ for a cylinder and slab. The root β_1 for a finite geometry can be obtained from

$$(\beta_1)^2 = \frac{(\beta_1)_\infty^2}{(1 + \frac{I}{BiS})} \quad (48)$$

(Luikov, 1968);

where the subscript ∞ represents the root for an infinite cylinder or slab. $I = 2.45$ and $S = 1.04$ for an infinite cylinder; and $I = 2.24$, $S = 1.02$ for an infinite slab. Gaffney et al. (1980) have observed that this relationship will predict β_1 to an accuracy of better than 0.1% when $8 < Bi < \infty$.

Convection Heat Transfer Coefficient

The convection heat transfer coefficient, h , in the Biot number was measured experimentally. The convection heat transfer coefficient between the corn and the fluid is also needed in the model and was measured experimentally during forced air cooling and hydrocooling of wire bound crates of sweet corn.

The method for determining the heat transfer coefficient is based on the lumped heat capacity analysis. The analysis assumes that the temperature distribution at any instant within a solid exchanging heat with a fluid is sufficiently uniform such that the temperature of the solid can be considered a function of time only. A plot of the natural logarithm of the temperature ratio of a high conductivity material on the vertical axis and the time on the horizontal axis will produce a linear section whose slope can be used to determine the convection heat transfer coefficient.

A copper cylinder measuring 2.9 cm in diameter by 10.6 cm long was used for the experiment. A hole was drilled along the axis of the cylinder to the geometric center and a 36-gauge thermocouple inserted into it. The apparatus and the procedures used to collect data for the thermal diffusivity tests were used to collect the data used in the calculation of the convection heat transfer coefficient. The analysis of the data involved taking the slope of the linear section of the semi-log plot of the temperature ratio versus time and computing the convection heat transfer coefficient from equations 5 and 18.

To determine the convection heat transfer coefficient between the corn and cooling medium, a solid copper cylinder was also placed inside the crate of sweet

corn during cooling. The temperature-time data collected from this was used in the computation of the heat transfer coefficient between the cooling fluid and the sweet corn.

Hydrocooling

The apparatus used for hydrocooling sweet corn during the research is shown in Figure 7. A box measuring 0.46 m by 0.76 m by 1.83 m was constructed from plywood to contain six crates of sweet corn stacked one on the other. The upper 0.61 m of the box was detachable. This was to facilitate loading and unloading. At the top of the box was a shower pan used to provide uniform water distribution over the area of the crates. The box was mounted on an insulated mixing tank with a capacity of 208 liters. The purpose of the mixing tank was to provide cooling water at a constant temperature.

Control of the water temperature was achieved by placing a YSI series 600 temperature controller probe inline from the mixing tank. The temperature probe was connected to a YSI model 63RC thermistor controller which powered a solenoid valve located inline from the cold water tank. When the solenoid valve was opened, 3.3 C water was pumped from the cold water tank into the mixing tank. A constant temperature of $4.4\text{ C} \pm 0.1\text{ C}$ was maintained in the mixing tank.

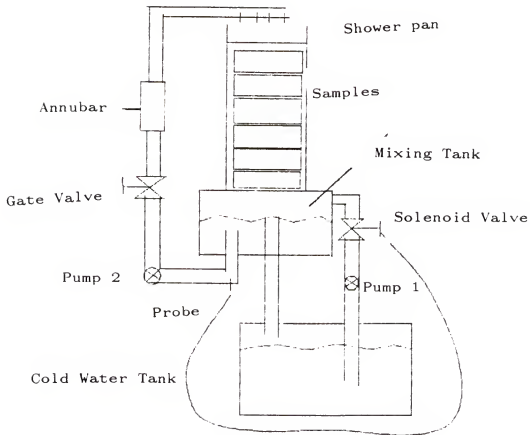


Figure 7 An Apparatus Used in the Experimental Hydrocooling of Wire Bound Crates of Sweet Corn

The hydrocooling unit served a dual function. It was used to run the cooling tests and also to reheat the corn to a uniform initial temperature before each test.

The weights and dimensions of the ears of corn into which the thermocouples were placed were measured. Although the sizes of the ears of corn may vary by as much as 10 mm in each crate, the ears that contained thermocouples were comparable in size. The physical dimensions of the ears used in the hydrocooling tests which contained thermocouples are shown in Table 2. The diameter is the average of the major and minor diameters.

At the beginning of the tests, the crates of corn were loaded into the cooling unit and the thermocouples were connected to the data logger. The annubar was connected to the flow meter and the flow rate adjusted with the gate valve located from the pump. A uniform initial temperature was achieved by running tap water at 26.6 C through the corn. Tap water was then turned off, the discharge closed and the return valve opened to let cooling water back into the mixing tank. Three water flowrates of 2.0 l/(s.m²), 4.8 l/(s.m²) and 6.8 l/(s.m²) were used and two replicates were made for each flow rate and for each load of sweet corn. Water flow rate was controlled through a gate valve placed in the line from the pump. An Annubar provided measurements for the water flow rates.

Table 2

Average Physical Properties of Ears with Thermocouples Per
Crate of Sweet Corn Used in the Hydrocooling Tests

<u>Weight</u>	<u>Diameter</u>	<u>Length</u>	<u>Crate #</u>
(gm)	(mm)	(m)	
293.28	49.23	0.18	1
235.44	45.51	0.17	2
272.47	48.32	0.17	3
312.83	50.79	0.17	4
231.23	45.83	0.16	5
286.75	48.75	0.18	6

Forced Air Cooling

A box measuring 0.23 m by 0.61 m by 2.4 m was constructed from plywood to contain six crates of sweet corn (Fig 8). Spacers were made from foam rubber reinforced with plywood to separate the crates and to prevent air leakage to the sides of the crates during cooling (Figure 9).

The slit at the center of the spacer coincided with that on the wire bound crate of corn. The foam rubber overlapped by 10 mm over the edges of the plywood. This provided a tighter fit when the crates were loaded into the box. Table 3 shows properties of the corn used in the tests.

The box was placed in the research facility described by Baird et al. (1972) controlled at 1.7 °C. Air was forced through the sweet corn with a high pressure, high volume Dayton blower model 7C447 mounted on a 0.3 kW Dayton motor. A diaphragm attached to the intake of the blower provided precise air flow control.

Air flow rates were measured with a 0.1 m diameter Ellison annubar connected through a Datametrics Barocel pressure sensor, rated at 133 kPa to a Datametrics electronic manometer.

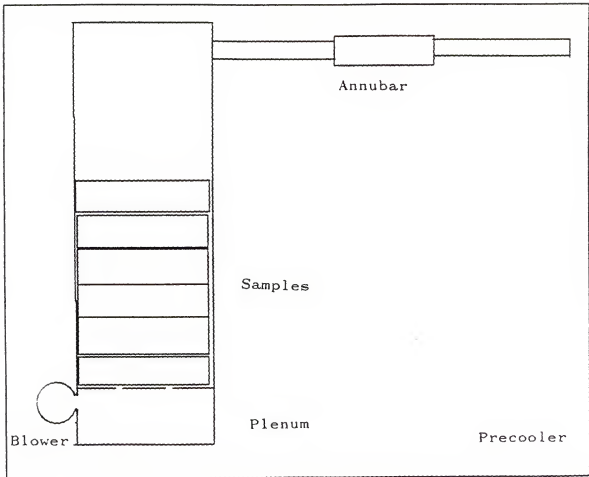


Figure 8 An Apparatus Used in the Experimental Forced Air Cooling of Wire Bound Crates of Sweet Corn

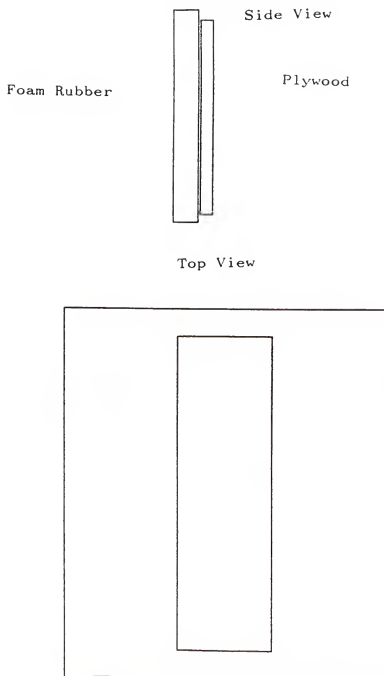


Figure 9 Spacers Used in the Experimental Forced Air Cooling of Wire Bound Crates of Sweet Corn

Table 3

Average Physical Properties of Ears with Thermocouples Per
Crate of Sweet Corn Used in the Forced Air Cooling Tests

<u>Wt of Corn</u>	<u>Diameter</u>	<u>Length</u>	<u>Wt of Crate</u>	<u>Crate #</u>
(gm)	(mm)	(m)	(kg)	
315.82	52.50	0.18	16.4	1
282.20	51.14	0.17	16.8	2
279.29	50.19	0.16	15.9	3
330.75	51.79	0.17	16.9	4
323.67	52.16	0.19	16.7	5
289.79	52.13	0.16	16.8	6

The precooler was cooled down to 1 C before the test was begun. The crates of corn were then loaded into the box with the spacers placed in between the crates. During the loading, all the crates were taken into the precooler to maintain as close to the same initial temperature as possible at the start of the test. When the box was tightly closed and the thermocouples plugged in, the blower was turned on and the desired flow rate set. Three flow rates were used during the test; $5.2 \times 10^{-4} \text{ m}^3/(\text{s.kg})$, $1.04 \times 10^{-3} \text{ m}^3/(\text{s.kg})$ and $1.25 \times 10^{-3} \text{ m}^3/(\text{s.kg})$ and two replicates were made for each flow rate. The test was stopped when all the temperatures read 5 C or lower.

Data from these tests were transferred to a computer, sorted and stored on disks for later analysis. The number of tests conducted at each flow rate for water and air cooling are shown in Tables 4 and 5.

Pressure Drops Across Crates of Sweet Corn

The box for the forced air tests (Fig 8) was also used for the determination of pressure drops across wire bound crates of sweet corn. Holes were drilled into the sides of the box so that pressure drops could be measured across one, two or up to six crates. The pressure drops were measured on a Datameterics electronic manometer. Air was forced through the crate or crates with a high pressure, high volume blower. Flow rates were varied by a

Table 4
 Tests and Replicates Conducted During Hydrocooling of
 Sweet Corn

<u>No of Crates</u>	<u>Flow Rate</u> (L/s m ²)	<u>Replicates</u>
6	6.8	4
6	4.8	4
6	2.0	4
3	6.8	4
3	4.8	4
3	2.0	4

Table 5

Tests and Replicates Conducted during Forced Air cooling
of Sweet Corn

<u>No of Crates</u>	<u>Flow Rate</u> (m ³ /s kg × 10 ³)	<u>Replicates</u>
6	1.0	4
6	0.5	4
3	1.3	4
3	1.0	4
3	0.5	4

diaphragm attached to the blower intake. An Annubar flow meter measured the air flow rates through the system.

The pressure drops were measured for individual crates and for six crates. The crate or crates were placed in the air cooling unit, the lid tightly placed in place and the blower turned on. Air flow rates were varied with the diaphragm on the blower and several pressure drop readings taken at each flow rate. A regression was performed on the data from these tests to establish a relationship between the number of crates, air flow rates and pressure drops.

At the beginning of each test the corn was graded for visual appearance on an arbitrary scale of 1 to 9. Grading was also done at the end of each test to evaluate the effect on the quality of the cooling rate. The crates were also weighed to assist in setting the air flow rates.

Moisture Content

Knowledge of the moisture content is required to determine the thermal properties from equation 12 and equation 13. The moisture contents of the cob, kernel and husks were measured. The cob was ground into small pieces, weighed and placed in a 103 C convection oven for forty eight hours. The samples were weighed again at the end of the forty eight hours and the loss in weight computed.

RESULTS AND DISCUSSIONS

Thermal Diffusivity

The technique for measuring thermal diffusivity as used here produces satisfactory results only if the surface heat transfer coefficient is known accurately or if it is so high that it can be assumed infinite. (Gaffney et al., 1980). The vigorous agitation of the ice bath by the use of compressed air during the cooling, as described earlier resulted in very high values of heat transfer coefficient. A value of 3907.62 W/m^2 was obtained for the heat transfer coefficient over a copper cylinder 28.72 mm in diameter during the determination of the diffusivity. For the sample size used in this test, the Biot number is 107.9 and this, according to Gaffney et al. (1980) would produce an error in the measured value of less than two percent. This value of the Biot number yields a root of $\beta_1 = 2.382$, less than one tenth of a percent of the root for an infinite cylinder. The convection heat transfer coefficients were also measured during the determination of the diffusivity of the husk and the effective diffusivity of an ear of corn.

The thermal diffusivities of the cob, kernel and husk were measured using the method described earlier. The

measured values are tabulated in Table 6. The effective diffusivity of a whole corn was also measured by treating the corn as a homogeneous cylinder and using the procedure outlined earlier. Because of the high moisture content of the specimens it was expected that the values should be less than and close to that of water at the same temperature which is $1.35 \times 10^{-7} \text{ W/m}^2$. This was the case with the diffusivities of the cob and kernels. The diffusivity of the husk was twelve percent higher than that of water.

The effective diffusivity of an ear of corn was found to be less than the diffusivities of the components measured (Table 6). This lower value for effective diffusivity was in agreement with the findings of other researchers (Bennett, 1970, Gaffney et al., 1980) who found that the measured effective thermal diffusivities of whole citrus fruits were as much as twenty to thirty percent lower than those of individual components. This difference in diffusivity between the whole fruit and its components is due to the assumption of a homogeneous material during the experimental determination. This assumption is not valid for whole products. Thermal conductivities of the cob, kernels and husks were obtained from the moisture contents of these components and equation (13).

Table 6

Experimentally Determined Thermal Diffusivities of The
Components of Sweet Corn.

<u>Material</u>	<u>Thermal Diffusivity</u> ($\text{m}^2/\text{s} \times 10^7$)	<u>Standard Deviation</u> ($\times 10^8$)
Cob	1.25	1.99
Kernel	1.33	1.08
Husk	1.57	0.61
Corn (as a whole)	0.82	0.66

The moisture contents were determined using oven-drying techniques as described earlier. Moisture contents obtained during this study were 76.3, 80.2 and 74.9 for the cob, kernels and husks respectively. The specific heat capacity was also determined from moisture contents and Seibel's equation (equation 14). The use of these equations to calculate thermal properties produces acceptably accurate results for higher moisture materials. The values are tabulated in Table 7.

The densities of the cob and kernels were determined by using the ratio of the mass to the volume for the cob, kernels and husks. These values were used to compute the thermal diffusivities from equation 7 shown in Table 8.

The values of the diffusivities obtained using the two methods differ significantly (Table 6 and Table 8). These differences may have arisen from the techniques used in their determination. The procedure for measuring density is simple and may be assumed accurate. These density values were used together with equations 13 and 14 to determine the diffusivities of the respective components. These values are greater than and not closer to the diffusivity of water ($1.35 \times 10^{-7} \text{ W/m}^2$) at the same temperature. Equations 13 and 14 were derived under different conditions that may not be applicable in this situation. Their use in determining the diffusivity may have introduced errors.

Table 7

Calculated Thermophysical Properties of The Components of
Sweet Corn.

<u>Material</u>	<u>Conductivity</u>	<u>Specific Heat</u>
	(W/(m.C))	(kJ/kg.C)
cob	0.52	3.42
Kernels	0.54	3.56
Husks	0.52	3.38

Table 8

Experimentally Determined Values of the Density and
Calculated Diffusivities of The Components of Sweet Corn.

<u>Material</u>	<u>Density</u> (kg/m ³)	<u>Standard Dev.</u>	<u>Diffusivity</u> (m ² /s X 10 ⁷)
Cob	895.41	34.23	1.54
Kernel	963.37	32.03	1.47
Husk	534.89	27.87	2.90

The diffusivity values measured directly were used in the model development. These values were within expected level of accuracy. Valid comparison between the two methods for determining the thermal diffusivity can only be made if the thermal conductivity and the specific heats are also determined experimentally. This was not done during this research.

Hydrocooling

Temperature-time data collected from each hydrocooling test were plotted. Half cooling times and seven-eight cooling times were calculated. Figures 10 and 11 show that at 2.04 l/s m^2 it took less than three hours to cool six wire bound crates of sweet corn from 27°C down to 5°C when using water at 0.6°C . This time was reduced by only twenty percent when the flow rate was more than tripled to 6.84 l/s m^2 . Higher flow rates also improved uniformity of cooling of individual crates and whole loads.

Bennett and Henry (1978) reported that repeated heating and cooling reduced the cooling time in subsequent runs of sweet corn cooled in corrugated containers. This phenomenon was also observed in this study during the cooling of sweet corn in wire bound crates at the half cooling time. Some difference in cooling rates were

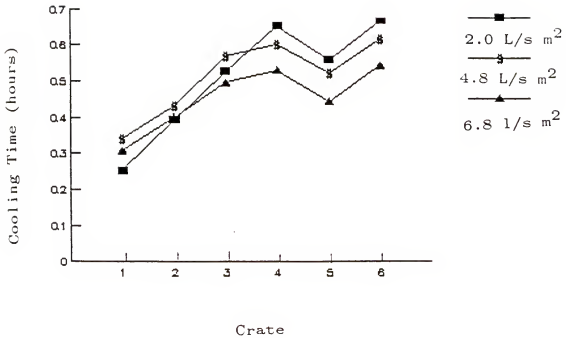


Figure 10 Half Cooling Times for Sweet Corn at Three Water Flow Rates

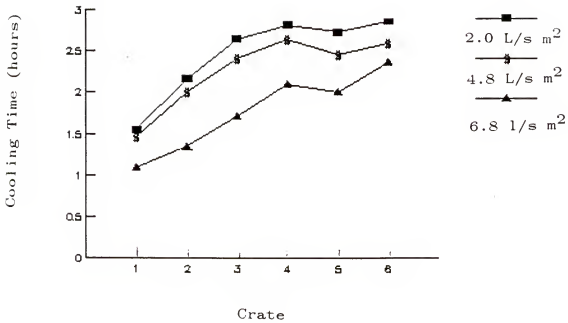


Figure 11 Seven-Eight Cooling Times for Sweet Corn at Three Water Flow Rates

observed at the seven-eight cooling time but this was small and could be attributed to experimental variation (Figures 12 and 13).

The rate of cooling also depended on the location of the ear of corn in the crate. Corn directly under the slit in the wire bound crate cooled faster than corn in other locations in the crate (figures 14, 15 and 16). By the half cooling time corn at the center of the first crate had cooled twenty percent faster, compared to corn at the sides, at $2.0 \text{ l}/(\text{s.m}^2)$ and forty percent at $6.8 \text{ l}/(\text{s.m}^2)$. The same pattern was repeated in crates two through six although the magnitude differed at each level. The faster cooling at this location can be attributed to more water available for the cooling because of the slit in the crate. Other areas received cooling water but this may have been flowing slower and at a smaller amount thereby reducing the effective cooling.

Figures 17 to 19 show temperatures measured at the bottom of the crates on a plate 2.0 cm square and indicate that higher flow rates reduced the fluctuations in temperatures at these points. Higher flow rates would therefore improve the availability of water in the crates resulting in faster cooling of the corn. The temperature measured after the third crate did not show the same fluctuation even at the lowest flow rate.

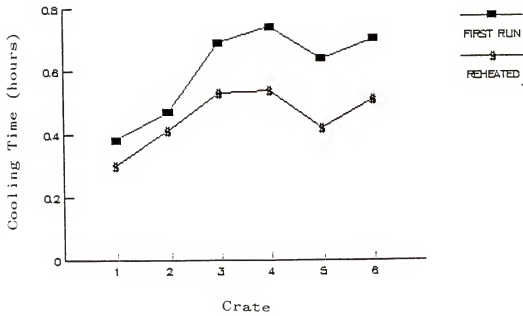


Figure 12 Half Cooling Times for Reheated Sweet Corn

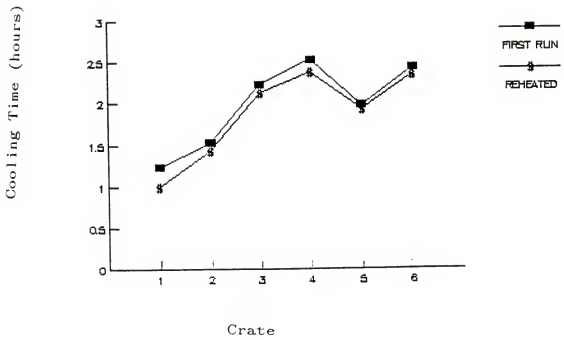


Figure 13 Seven-Eight Cooling Time for Reheated Sweet Corn

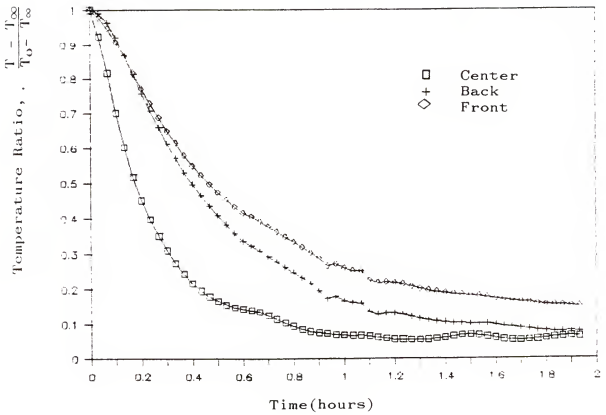


Figure 14 Cob Temperature Variation at Three Locations in the First Crate During Hydrocooling at $2.0 \text{ l/(s.m}^2\text{)}$

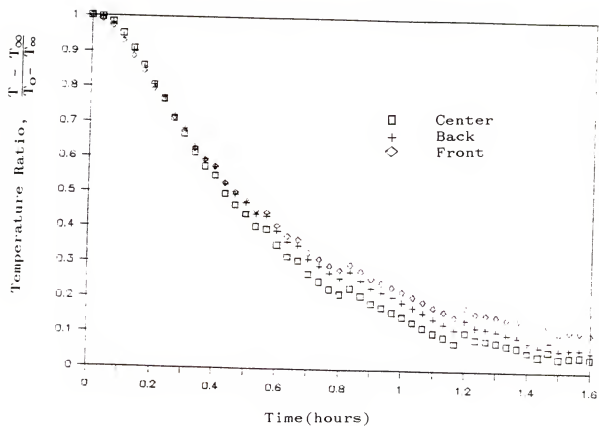


Figure 15 Cob Temperature Variation at Three Locations in the First Grate During Hydrocooling at $4.8 \text{ L/(s.m}^2\text{)}$

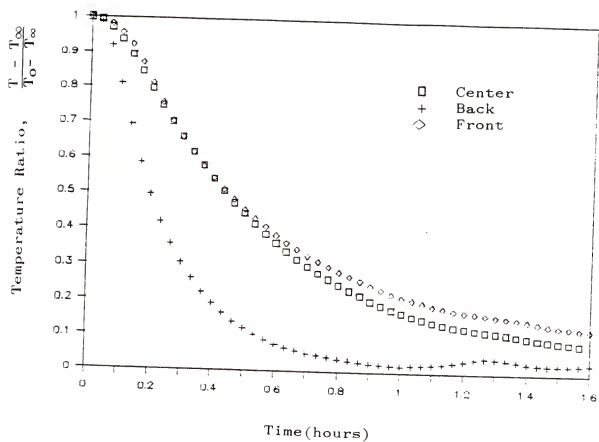


Figure 16 Cob Temperature Variation at Three Locations in the First Crate During Hydrocooling at $6.8 \text{ l/(s.m}^2\text{)}$

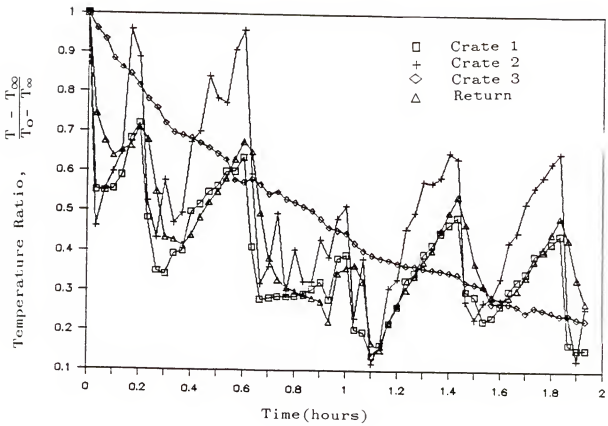


Figure 17 Temperatures of Water Exiting Some Crates During Hydrocooling at $2.0 \text{ l/(s.m}^2\text{)}$

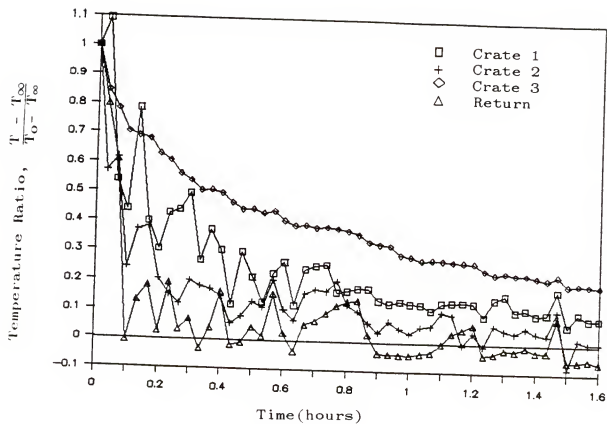


Figure 18 Temperatures of Water Exiting Some Crates During Hydrocooling at $4.8 \text{ l}/(\text{s} \cdot \text{m}^2)$

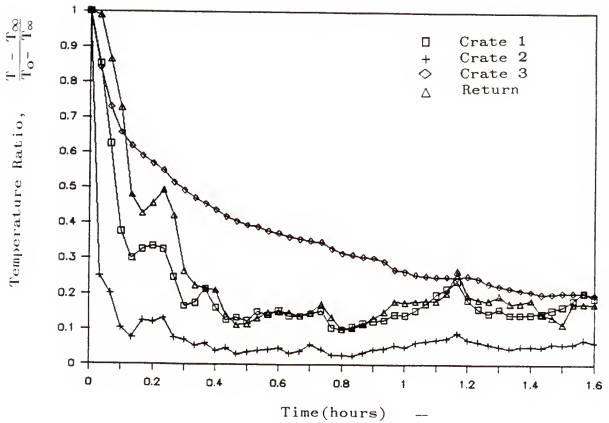


Figure 19 Temperatures of Water Exiting Some Crates During Hydrocooling at $6.8 \text{ L}/(\text{s} \cdot \text{m}^2)$

There are a few explanations that may contribute to this, one being that the water flowing out of the third crate may have already picked up heat and did not lower the temperature rapidly. The other explanation is that the temperature measuring device did not get in contact with water and the temperature measured was therefore that of the surrounding air in the box. This appears to be a better explanation because it would also explain why the fourth crate did not cool down as fast as was expected.

These observations suggest that although higher flow rates make more water available, most of the water flowed over the crates and only a small portion was utilized in the cooling. In addition, water exiting the crates slowed down considerably and the effective convection coefficient was reduced.

Figures 20 to 22 show the experimental data obtained for the cob temperatures during hydrocooling. These also show that the fifth crate, numbered in the direction of water flow, cooled consistently faster than the fourth crate during all the tests, a phenomenon observed in tests conducted over a large interval of time. This behavior was also observed by Henry and Bennett, (1978). They postulated that it was due to improved air circulation at the bottom caused by the cooling water and used this as the argument for investigating hydraircooling.

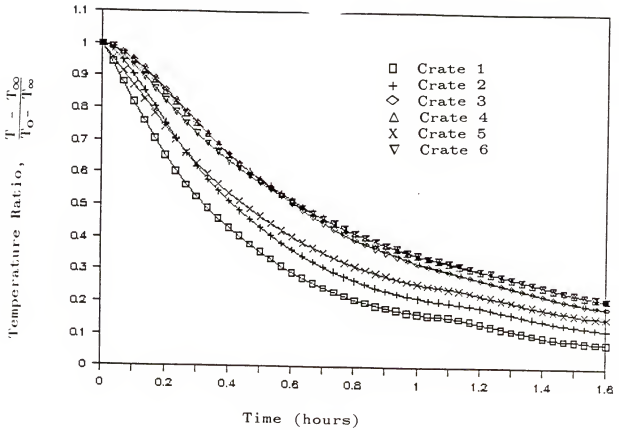


Figure 20 Experimental Cob Temperatures for Hydrocooling Six Crates of Sweet Corn at $6.8 \text{ l/(s.m}^2\text{)}$

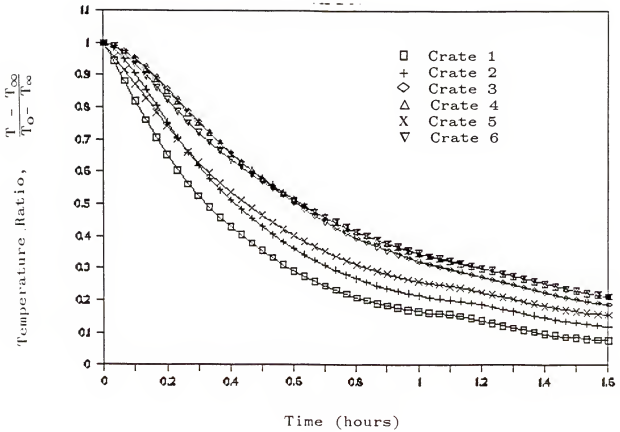


Figure 21 Experimental Cob Temperatures for Hydrocooling Six Crates of Sweet Corn at $4.8 \text{ l/(s.m}^2\text{)}$

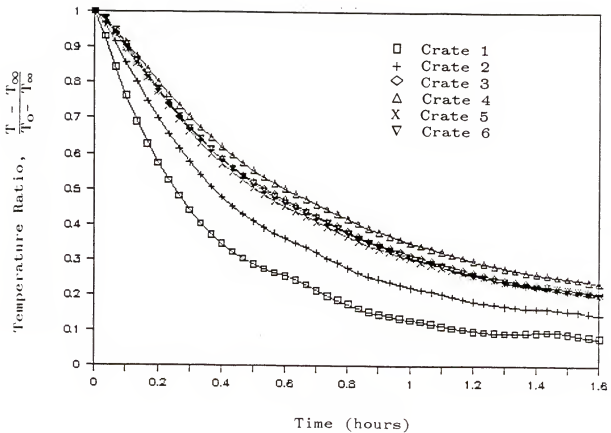


Figure 22 Experimental Cob Temperatures for Hydrocooling Six Crates of Sweet Corn at $6.8 \text{ l}/(\text{s.m}^2)$

If this were the case, one would expect the sixth crate to cool faster also. This was not observed during this project.

Figures 23 and 24 show the comparison between the rate of cooling for ears of corn with the silk towards the direction of water flow and the ears with the silk facing away from the water. These show that ears of corn with the silk towards the direction of water flow cooled down 30% faster than ears with the silk facing away from the water. Water possibly enters the ears with the silk towards the direction of water flow, bypassing the insulation provided by the husks. The heat from the center of the corn then is conducted only to the kernels and then convected away by the water.

Although the curves for the hydrocooling tests did show a distinctive bed effect, (figures 20 to 22), only a 1.1 C temperature rise was observed in the cooling water. This variation in cooling times between the crates is possibly due to poor water distribution within the crates. When the numerical model that assumes uniform water circulation within the crates was used to simulate hydrocooling, the simulation results showed that seven-eighths cooling times were similar for all the crates at all flow rates used.

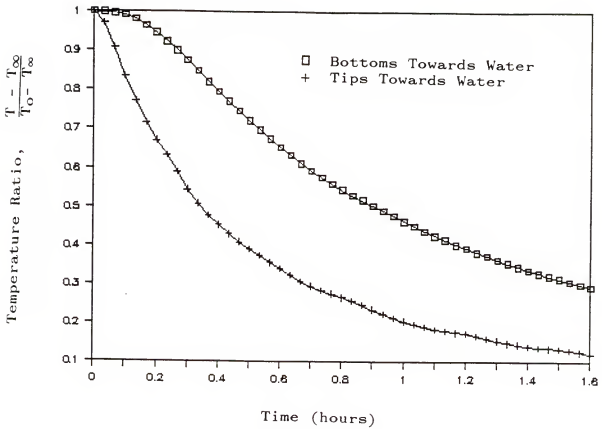


Figure 23 Experimental Cob Temperatures for Hydrocooling of Sweet Corn at $2.0 \text{ l/(s.m}^2\text{)}$ with Either End Facing the Direction of Water Flow

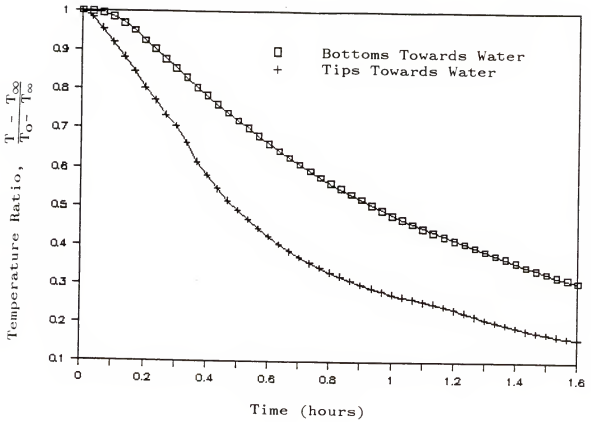


Figure 24 Experimental Cob Temperatures for Hydrocooling of Sweet Corn at $2.0 \text{ l/(s.m}^2\text{)}$ with Either End Facing the Direction of Water Flow

Convection Heat Transfer Coefficient

Empirical equations for predicting surface heat transfer coefficient for flow over cylinders are varied between researchers (Heldman and Singh, 1981; Geankoplis, 1960). To overcome the difficulty of selecting a suitable equation for this study, the convective heat transfer coefficient was determined experimentally for the first crate using the lumped heat capacity method. The data obtained was curvefitted to the equation

$$Nu = C_r Re^m Pr^n$$

by performing a linear regression on the natural logarithm of the equation. The constants C_r , m and n were determined as 0.22, 0.72 and 0.34 respectively. These values were for $1100 \leq Re \leq 3700$. The correlation coefficient was 0.98 (Fig. 25).

The value of h would be expected to vary through the bed due to change in air temperature as it moves through the bed. Baird, (1973) showed that this change is basically negligible for flow through a bed of spheres. Calculations based on a film temperature change of 15.6 C predicted only a one percent change in the value of the convection coefficient.

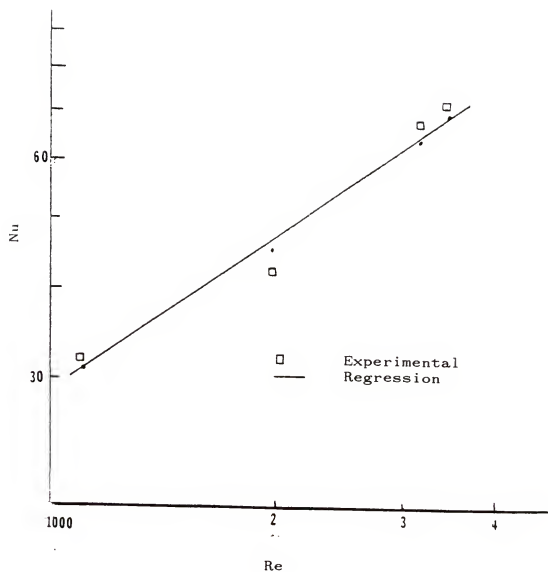


Figure 25 Nusselt-Reynolds Relationship During Forced Air Cooling of Sweet Corn

Other researchers (Bakker-Akkerma and Bicket, 1966) have generally used average values of h for the entire bed and this has produced satisfactory results in most cases.

During this study, the convection coefficients were measured at three crates during hydrocooling and forced air cooling and are shown in Tables 9 and 10. The values for the three crates were different during either cooling operation. This difference may have been introduced by the method used in the determination. The methodology used assumes a uniform temperature fluid surrounding the high conductivity material. This condition could only be satisfied at the first crate as the fluid temperature changed constantly at the other crates. The actual difference in the convection coefficient may not be as high as shown in these tables.

The convection coefficient would also give an indication of the relative rate at which the product would cool. The relative cooling rates of the first three crates in either cooling operation follow the same pattern as the convection heat transfer coefficient. There is a large difference in the values measured for hydrocooling and this tends to support the bed effect observed in the data. As mentioned earlier, the water temperature did not change by a large amount and the values measured experimentally may

Table 9
Convection Heat Transfer Coefficients Measured During
Hydrocooling Cooling

<u>Flow Rate</u>	<u>h</u>	<u>Crate Number</u>
(l/ (s.m ²))	(W/ (m ² .C))	
2.0	484.64	1
2.0	459.58	2
2.0	358.34	3
4.8	477.86	1
4.8	472.86	2
4.8	361.52	3
6.8	714.58	1
6.8	477.75	2
6.8	455.75	3

Table 10
 Convection Heat Transfer Coefficients Measured During
 Forced Air Cooling

<u>Flow Rate</u>	<u>h</u>	<u>Crate Number</u>
(m ³ / (s.kg) × 10 ⁴)	(W/ (m.K))	
5.2	32.54	1
5.2	30.83	3
13.0	47.65	1
13.0	45.31	2
13.0	35.09	3

be true indicators of the way the convection coefficient varied during these tests.

The copper cylinder used in determining the heat transfer coefficient during forced air cooling was placed at the center of the crate. Copper has a very high conductivity compared to that of corn and conduction heat transfer may take place between the corn and the cylinder as the copper cylinder would cool down faster. This would significantly lower the cooling rate of the cylinder and thus the value of the convection heat transfer coefficient determined because the log plot will have a gentler slope. It appeared that this contributed significantly to the value of h measured as higher than measured values of h produced better agreement between experimental and simulation data. By varying the value of h used in the mathematical simulation it was found that good agreement between experiment and simulation was obtained when the value of h used was fifty percent higher than that measured for the flow rate.

Pressure Drops

Pressure drops were measured across individual crates and across the whole load of six crates. By performing a regression on the equation

$$\Delta p = A v^n$$

Table 11 shows the values obtained for A and n. The values of n obtained in the regressions were very close to 2 in all the six cases tested. The data was subsequently forced into the equation

$$\Delta p = A v^2$$

The values of A obtained for this case are shown in Table 12. The correlation coefficient was 0.95. These show that the pressure drops across crates of sweet corn vary as the square of the velocity.

Pressure drops across individual crates also varied as the square of the velocity differing only in the value of the constant A (figures 26 and 27). Other researchers (Chau et al., 1978) also found that pressure drops across boxes of citrus varied as the square of the velocity. The pressure drops used in determining the correlation equation were measured in kPa/m^2 and the velocity measured in m/s . The pressure drops presented here were measured for a velocity range of 0.01 to 0.56 m/s .

The average crate pressure drops (Table 11) were used to study the variation, if any, of pressure drops across several crates of sweet corn. The variation was found to be a polynomial of the form

$$\Delta p = a + bx + cx^2 \quad (49)$$

Table 11

Pressure Drops Measured Across Crates of Sweet Corn

$$\Delta p = A v^n$$

(Δp is in kPa/m^2 , and v is in m/s)

<u>No of Crates</u>	<u>A</u>	<u>n</u>	<u>σ^2</u>
1	1.82	1.89	0.03
2	5.94	2.01	0.02
3	11.34	2.11	0.04
4	14.70	2.07	0.03
5	21.71	2.03	0.05
6	25.67	1.97	0.03

Table 12

Modified Pressure Drops Measured Across Crates of Sweet
Corn

$$\Delta p = A v^2$$

(Δp is in kPa/m^2 and v is in m/s)

<u>No of Crates</u>	<u>A</u>	<u>\underline{g}^2</u>
1	2.1	0.76
2	5.8	0.57
3	9.7	0.35
4	13.2	0.45
5	20.6	2.31
6	27.3	2.51

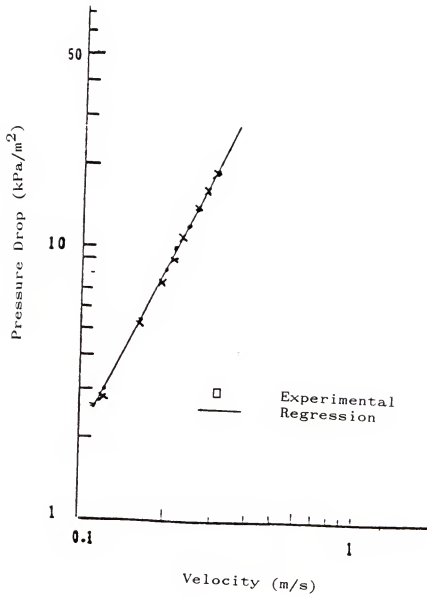


Figure 26 Pressure Drops Across Six Crates of Corn During Forced Air Cooling

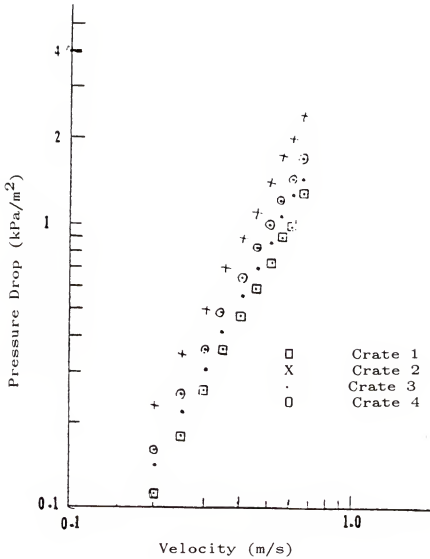


Figure 27 Pressure Drops Across Individual Crates of Sweet Corn During Forced Air Cooling

where a, b and c are constants and x is the number of crates. By performing a regression analysis on the data in Table 11 the constants were found to -2.52, 4.15 and 0.10 for a, b and c respectively. The regression coefficient was 0.96. Performing the same analysis using the values in Table 12, the regression coefficient was 0.99 and the values of the constants were 0.56, 1.34 and 0.52 for a, b and c respectively. Although the packing of the ears of corn in each crate is random, this analysis shows that there is a definite polynomial relationship between the number of crates of sweet corn and the pressure drop across them.

Forced Air Cooling

The sizes of the ears of corn used in the forced air cooling tests are shown in Table 3. The average crate weight is also shown in this table.

The first three crates during forced air cooling, in a load of six, cooled at about the same rate but a large increase in half cooling time and seven-eight cooling time was noticed beyond this (Figures 28 and 29). Forced air cooling showed that higher air flow rates produced consistently faster cooling (Figures 30 to 31). Higher flow rates did not improve the uniformity of cooling. This was consistent in all the tests.

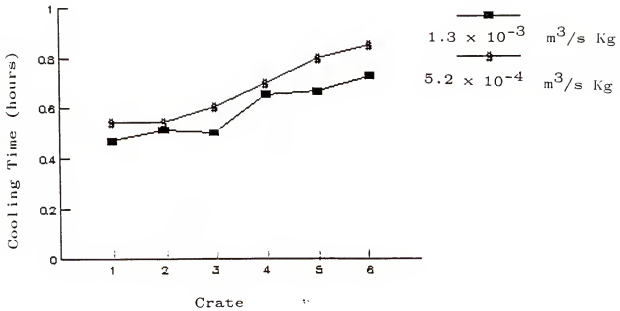


Figure 28 Half Cooling Times for Sweet Corn at Two Air Flow Rates

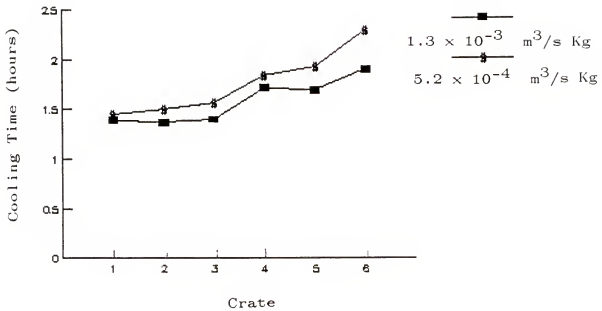


Figure 29 Seven-Eight Cooling Times for Sweet Corn at Two Air Flow Rates

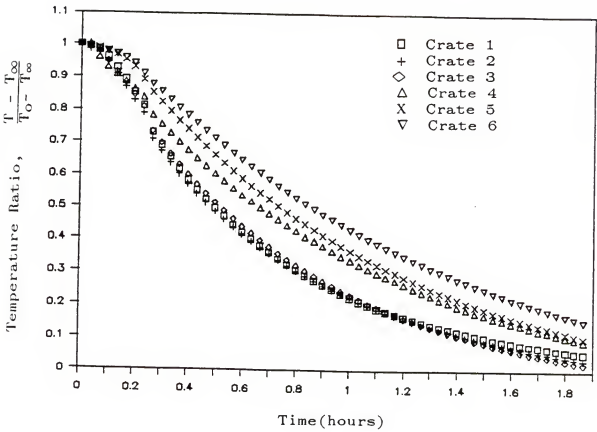


Figure 30 Experimental Cob Temperatures for Air Cooling of Six Crates of Sweet Corn at $5.2 \times 10^{-4} \text{ m}^3/(\text{s} \cdot \text{kg})$

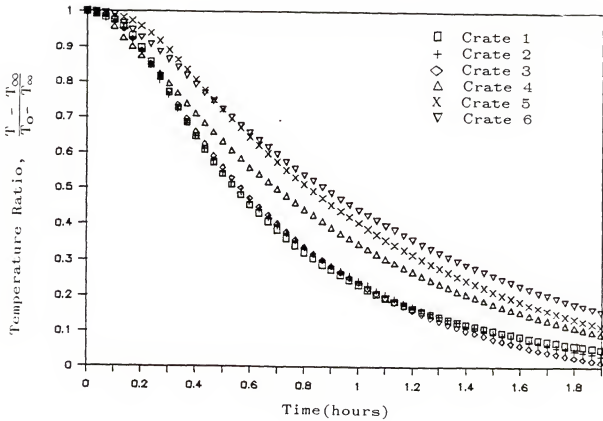


Figure 31 Experimental Cob Temperatures for Air Cooling of Six Crates of Sweet Corn at $1.3 \times 10^{-3} \text{ m}^3/(\text{s} \cdot \text{kg})$

This information, together with that obtained from the measured pressure drops across crates of sweet corn indicate that forced air cooling of pallet loads of sweet corn by forcing air through it as was done during this study, may require a large amount of energy. For example, to cool down six stacked crates of corn of an average weight of 17 kg from 26 °C to 5 °C in three hours would require $0.033 \text{ m}^3/(\text{s.kg})$ air flow rate and a 10 °C rise in air temperature. This would be forced against a pressure drop of 5.70 kPa/m^2 as calculated from the relationship given earlier. This pressure drop may be very high for most applications. Lower air flow rates would have to be used leading to longer cooling times and the quality of the cooled product may be compromised during the cooling operation.

The temperature of the exit air from each crate was measured and plotted as a function of time for all flow rates. The plots show that the exit air temperature became lower than the entering air temperature at some time during the cooling (Figures 32 to 34). This may have been caused by evaporative cooling from the free water that was left on the surface of the corn after heating. A calculation showed that 0.49 kg/hr of evaporating water was required to cause the temperature change that was observed during the test at the high flow rate of $1.3 \times 10^{-3} \text{ m}^3/(\text{s.kg})$.

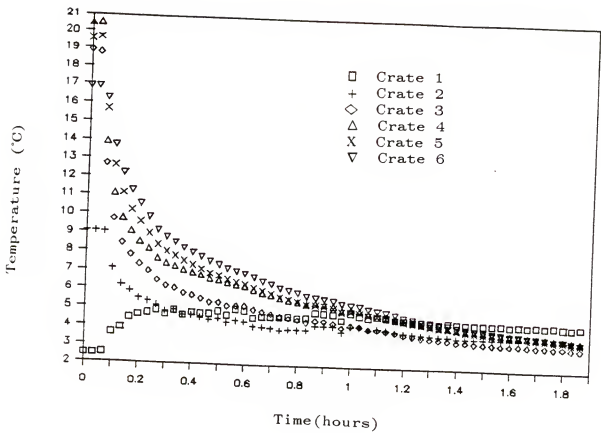


Figure 32 Experimental Air Temperatures Measured After Each Crate During Air Cooling at $5.2 \times 10^{-4} \text{ m}^3/(\text{s.kg})$

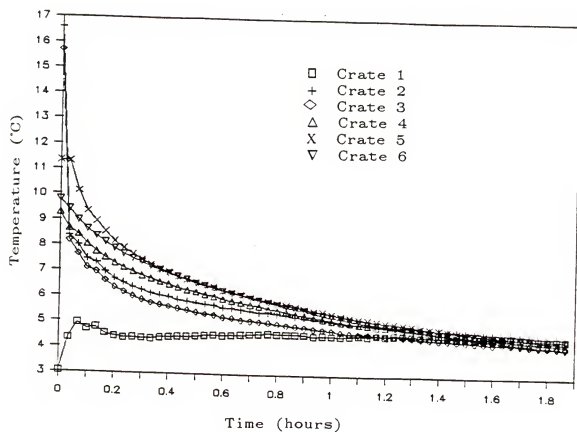


Figure 33 Experimental Air Temperatures Measured After Each Crate During Air Cooling at $1.04 \times 10^{-3} \text{ m}^3/(\text{s.kg})$

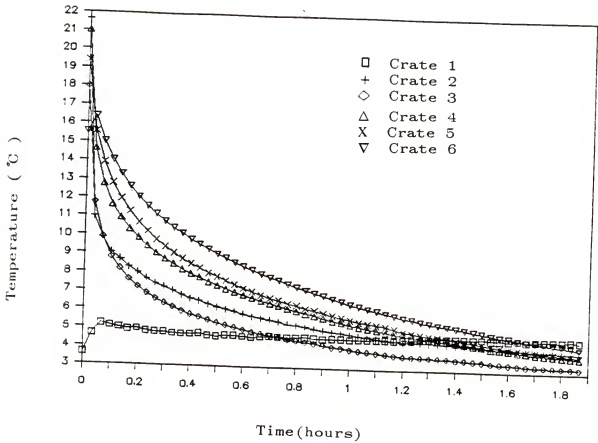


Figure 34 Experimental Air Temperatures Measured after Each Crate Drying Air Cooling at $1.3 \times 10^{-3} \text{ m}^3/(\text{s.kg})$

Air flow rates were measured at the beginning and at the end of each test. It was noticed that the flow at the end of the tests had increased by as much as fifteen percent for the high flow rates. The cooling air may have dried the husks, producing less resistance to the air flow.

Hydrocooling generally produces faster cooling because of the high heat capacity of water and the high convection heat transfer coefficient between the water and the product. During this study, forced air cooling was faster. Air flow through the crates was more uniform than water circulation during the tests. The spacers used (Fig 8) to reduce air leakage were successful and the large air flows used resulted in faster cooling. Poor water circulation through the crates reduced the efficiency of water as a cooling medium. This is apparent in the bed effects observed in the hydrocooling data. The first crate during hydrocooling did not cool faster than the first crate during forced air cooling. Previous discussion has indicated that the rate of cooling was affected by both the direction the corn silk were facing and the position of the corn in the crate. Since the crate temperature is the average of all temperatures measured in the crate, the slower cooling ears may have contributed to the overall slower cooling rate of the crate compared to forced air cooling.

Mathematical Modeling

A mathematical model was developed to simulate the heat and mass transfer for a single ear of sweet corn and for a bed of sweet corn in wire bound crates. In order to use the shape described in Figure 2, it was necessary to develop a relationship between the length of the corn and its radius.

The diameter of the ear of corn was measured as a function of its length and the data fitted to a second degree polynomial of the form

$$r = a + bl + cl^2$$

where a, b and c are constants and r and l represent the radius and length measured in millimeters. The length was measured from the base of the cob where the kernels begin up to the end of the section that contained all the three components considered in the numerical model. Values for the constants obtained for three ears of corn are 22.8, 0.07 and -9.95×10^{-4} with a correlation coefficient of 0.89.

A relationship was also developed between the radius of the whole corn and that of the kernel, and between the radius of the corn and that of the cob. The results showed the following relationship:

$$\frac{r_{\text{kernel}}}{r_{\text{corn}}} = 0.89 \pm 0.02$$

$$\frac{r_{\text{cob}}}{r_{\text{corn}}} = 0.55 \pm 0.05$$

where r_{cob} is measured from the center of the cob to the base of the kernels and r_{kernel} is measured from the base of the kernels to the husks. It was possible then to compute the radii of the components used in the model once the overall radius was determined. Grizzell and Bennett (1966) estimated that the cob was about two thirds of the radius of the whole corn.

To check the simulation model, the same properties were assigned to the cob, the kernels and the husk and the data generated from the numerical model was compared with the analytical solution (Heisler, 1947) for a cylinder with the same thermophysical properties. A better than 1 C agreement was obtained at the center of the cylinder (Fig 35).

The model was developed using the thermal properties shown in Table 6. Ten nodes were used along the radius, three nodes in both the cob and kernels and one node in the husk, together with the three interface nodes and eight nodes along the length of the ear of corn. The experimental temperatures were compared with nodes 1, 5 and 9 for the cob, kernel and husk respectively. This model showed very good agreement at all three levels of comparison (Fig 36). The data shown in Fig 36 is for an ear of corn measuring

0.05 m in diameter and 0.20 m long. The mass-average temperature obtained from the numerical model was compared with the kernel temperatures and this showed good agreement (Fig 37).

The single corn composite model simulated experimental data well and can be used to predict temperature variation in an ear of corn during cooling. The model also provided another means of comparison, the mass-average temperature. In cooling sweet corn, the current practice is to monitor cob temperatures although the kernels is the section that is of interest to the consumer. The model, besides providing kernel temperatures, has shown that the temperature of the kernels can also be approximated by calculating the mass average temperature (Fig 37).

Using the effective thermal properties for the whole ear of corn, a homogeneous model was also developed to simulate the cooling of single ears of sweet corn. Data generated by this model was compared with experimental data at three points on the ear; the cob center, the kernels and the husk.

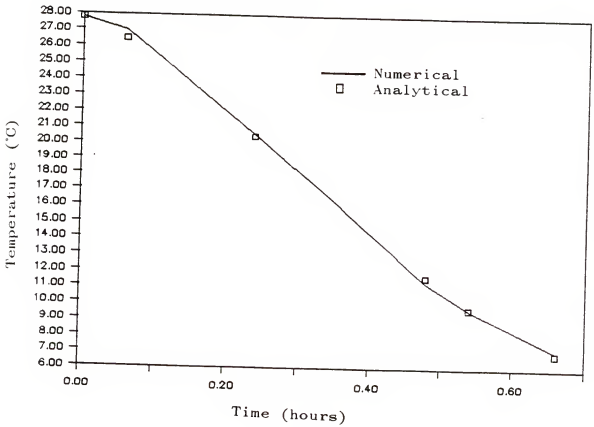


Figure 35 Comparison of the Numerical Scheme with Analytical Solution for The Center of an infinite Cylinder at h of $28 \text{ W}/(\text{m}^2 \cdot \text{K})$

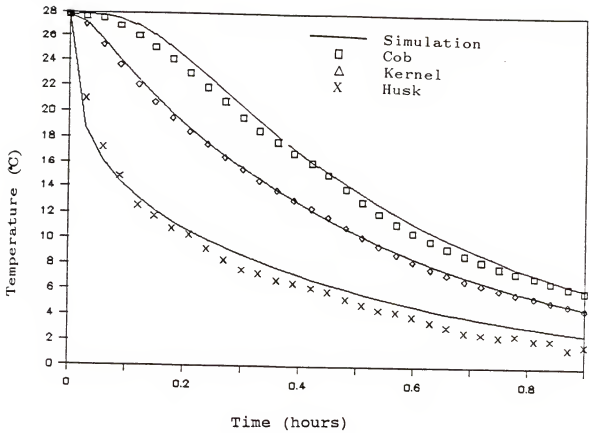


Figure 36 Simulation and Experimental Result for the Composite Model for a Single Ear of Corn at h of $85 \text{ W}/(\text{m}^2 \cdot \text{K})$

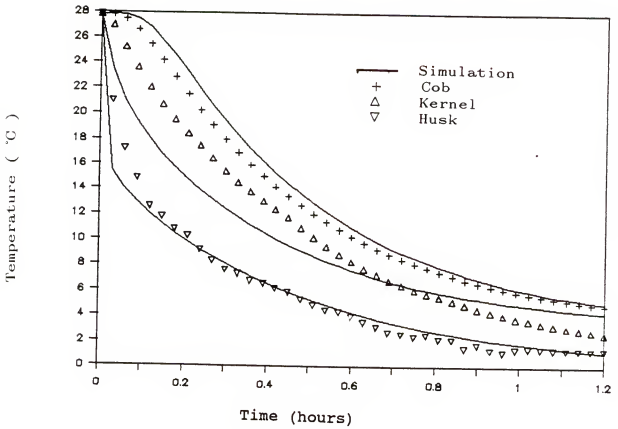


Figure 37 Comparison of the Mass-average Temperature and the Kernel Temperature at h of $85 \text{ W/(m}^2\cdot\text{K)}$

Poor agreement was obtained at the kernel and husk levels but fairly good agreement was obtained at the center of the cob (Fig 38). A homogeneous object is made from materials with the same thermal and physical properties. Comparison of the model with experimental data at any other point but the center would therefore not be valid as the discontinuities in material composition are not present for the homogeneous model.

Baird (1973), showed that treating a grapefruit as a homogeneous sphere resulted in higher surface temperatures than when the composite analysis was used. The temperature of the husk generated by this homogeneous model is higher than the observed temperatures and higher than that generated by the composite model (figures 36 and 37).

Figures (39) to (47) show the comparisons between experimental and simulation data plotted separately for clarity. Agreement for the bed model was very good for the first two layers at all air flow rates. The third layer showed good agreement also but the simulation was poorer towards the end of the cooling.

A distinct bed effect was noticed during the hydrocooling of sweet corn. Water has a high heat capacity and hydrocooling is not expected to show any significant bed effect. To verify this, the model which assumes uniform water distribution throughout the bed, was run to simulate

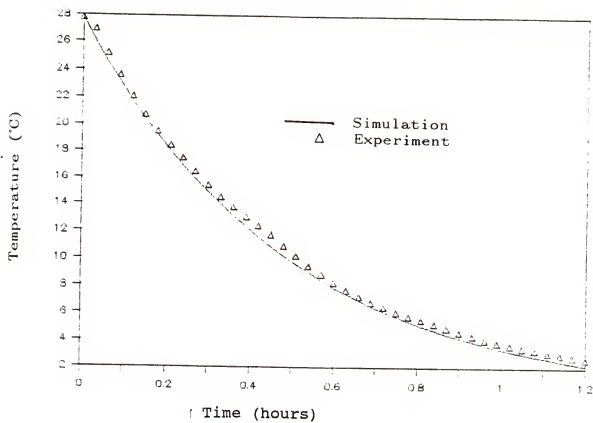


Figure 38 Simulation and Experimental Result for the Homogeneous Model for a Single Ear of Corn at h of $85 \text{ W}/(\text{m}^2.\text{K})$

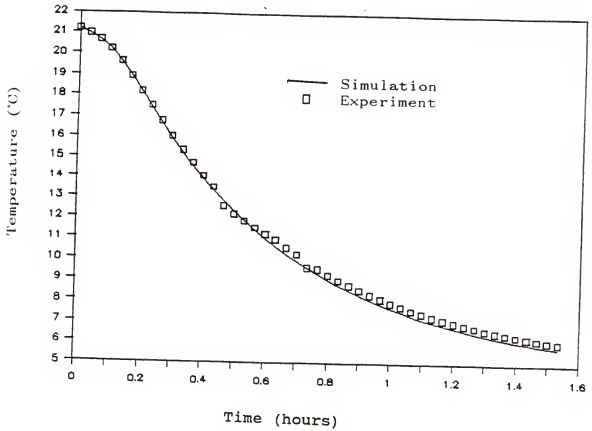


Figure 39 Simulation and Experimental Cob Temperatures for the First Crate of Sweet Corn at $5.2 \times 10^{-4} \text{ m}^3/(\text{s.kg})$

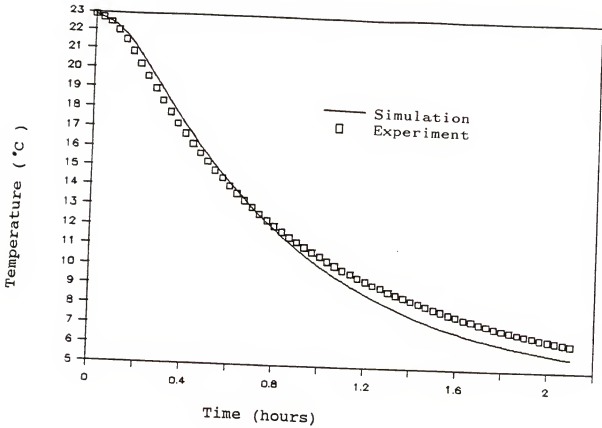


Figure 40 Simulation and Experimental Cob Temperatures for the Second Crate of Sweet Corn at $5.2 \times 10^{-4} \text{ m}^3/(\text{s.kg})$

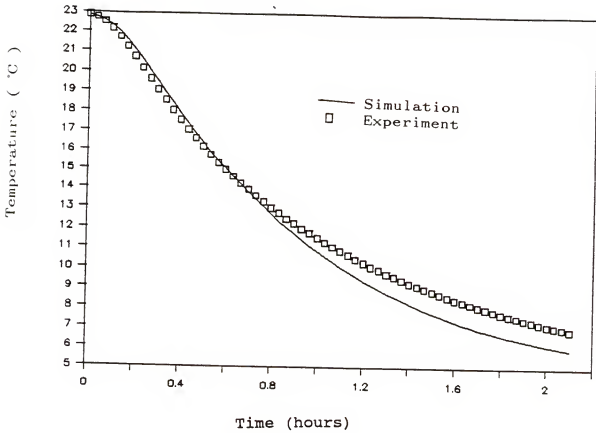


Figure 41 Simulation and Experimental Cob Temperatures for the Third Crate of Sweet Corn at $5.2 \times 10^{-4} \text{ m}^3/(\text{s.kg})$

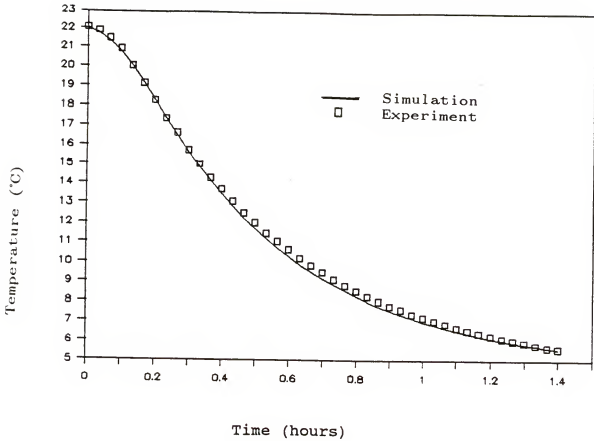


Figure 42 Simulation and Experimental Cob Temperatures for the First Crate of Sweet Corn at $1.0 \times 10^{-3} \text{ m}^3/(\text{s.kg})$

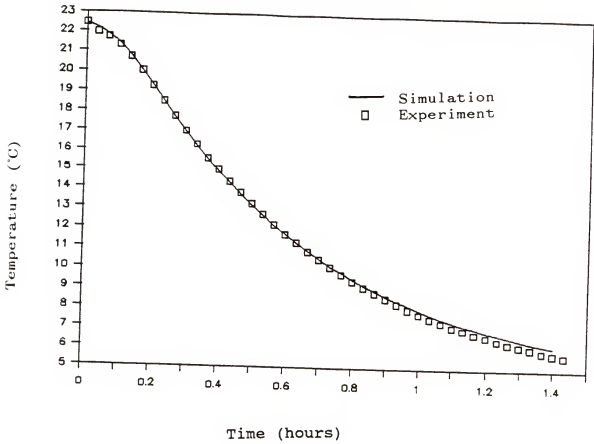


Figure 43 Simulation and Experimental Cob Temperatures for the Second Crate of Sweet Corn at $1.0 \times 10^{-3} \text{ m}^3/(\text{s.kg})$

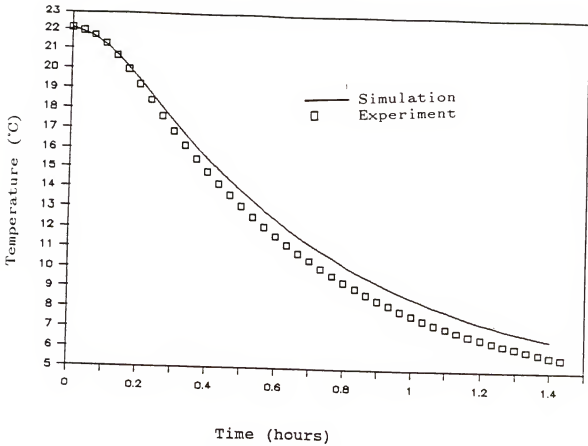


Figure 44 Simulation and Experimental Cob Temperatures for the Third Crate of Sweet Corn at $1.0 \times 10^{-3} \text{ m}^3/(\text{s.kg})$

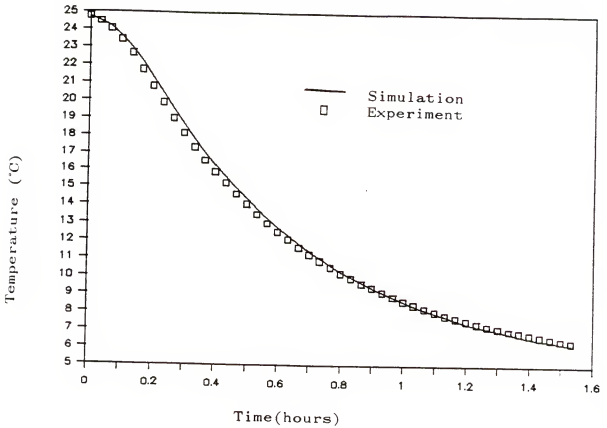


Figure 45 Simulation and Experimental Cob Temperatures for the First Crate of Sweet Corn at $1.3 \times 10^{-3} \text{ m}^3/(\text{s.kg})$

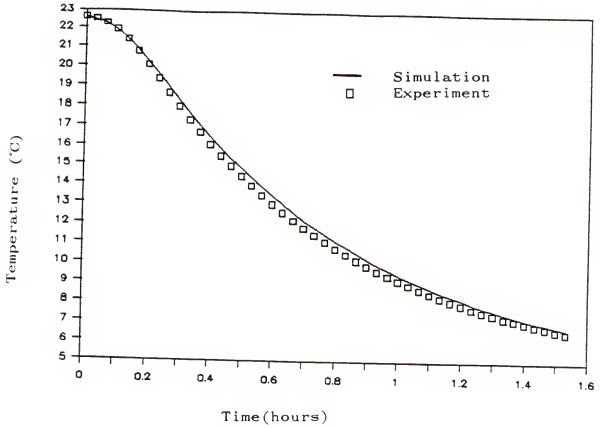


Figure 46 Simulation and Experimental Cob Temperatures for the Second Crate of Sweet Corn at $1.3 \times 10^{-3} \text{ m}^3/(\text{s.kg})$

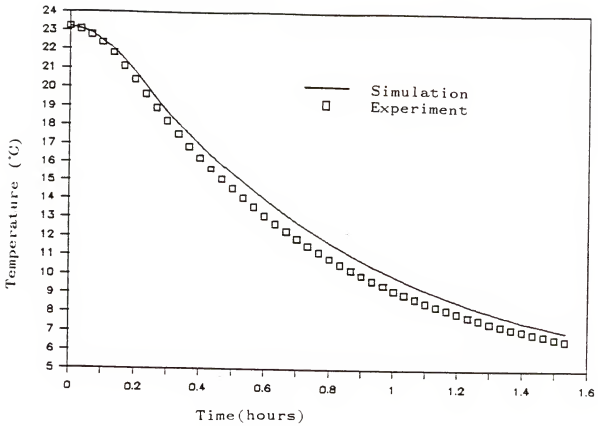


Figure 47 Simulation and Experimental Cob Temperatures for the Third Crate of Sweet Corn at $1.3 \times 10^{-3} \text{ m}^3/(\text{s.kg})$

hydrocooling and to check for the bed effect. The simulation results showed that seven-eight cooling times were similar at all flow rates. This further supports the proposition mentioned earlier, that the bed effect was caused by poor water circulation within the crates and between crates.

CONCLUSIONS

Experimental procedures were described for determining the thermophysical properties of the constituents of sweet corn. Values of the thermophysical properties were presented. These were found to be within theoretical expectations. The value for the diffusivity of the husk was the only departure from this. This departure suggests that the use of a homogeneous theory in determining the properties of the husk may be erroneous. Further research is needed to look into this problem.

Heat transfer coefficients were measured during the forced air cooling and hydrocooling of sweet corn and a Nusselt-Reynolds relationship for forced air cooling was established.

Hydrocooling revealed that higher water flow rates produced more uniform cooling of crates but did not significantly reduce the overall cooling time. This further showed that the improved cooling was due to better water circulation because large volumes of water were available. The design of the wire bound crate appeared to be the cause of poor water circulation. This research thus proposes a

redesign of the container for precooling sweet corn. A container design that allow water to enter at a faster rate than it can drain out could utilise the high efficiency of immersion cooling while maintaining the labor saving qualities of pallet handling. A container could be made from waxed fiberboard with a larger water inlet area than the exit. This would retain more water in the carton and improve the surface heat convection.

The research also showed that more cooling water was available at some points in a crate than at others causing the corn in these regions to cool faster. The difference in cooling rates at different locations in a crate was not significant during forced air cooling.

A mathematical model was developed to simulate the heat transfer during the cooling of an ear of sweet corn. The model represented well the experimental data. Comparison of the homogeneous model developed with the effective properties also showed good agreement at the center of the ear. Because this model is simpler to implement and faster, fairly accurate estimates of the cob temperatures can be obtained faster. This model will not give any accurate information on the temperature of the kernels or the husks. Some work is needed to accurately determine the effective thermal properties of corn.

A bed model was also developed to simulate the cooling of sweet corn in bulk. This model could give good

estimates of bulk temperatures but is slow because of the numerous computational steps involved. With eight nodes along the radius and eight nodes along the length of the ear of corn it takes approximately two hours to simulate 1.7 hours, on a computer with eight megahertz central processing unit speed and a numeric coprocessor, of cooling three crates of sweet corn.

APPENDIX A
EVALUATION OF h VALUE FOR THE THERMAL DIFFUSIVITY
EXPERIMENT

The thermal diffusivities were calculated using the equation

$$h = \frac{\rho C_p V m}{A}$$

where the symbols represent

h = heat transfer coefficient,

ρ = density,

C_p = specific heat capacity,

V = volume,

m = slope,

A = heat transfer area.

The area and volume are calculated from

$$\begin{aligned} A &= 2\pi r^2 + 2\pi rL \\ V &= \pi r^2 L \end{aligned}$$

where r and L are the radius and length of the cylinder respectively.

Temperature-time data was collected on copper cylinders and the average slopes of the plot of the natural

logarithm of the temperature ratio versus time for the two cylinders used are

$$m_1 = 0.180 \text{ s}^{-1}$$

$$m_2 = 0.125 \text{ s}^{-1}$$

Cylinders one and two have the following dimensions:

$$D_1 = 0.029 \text{ m}, \quad A_1 = 0.011 \text{ m}^2$$

$$L_1 = 0.106 \text{ m}, \quad V_1 = 6.59 \times 10^{-5} \text{ m}^3$$

$$D_2 = 0.038 \text{ m}, \quad A_2 = 0.021 \text{ m}^2$$

$$L_2 = 0.154 \text{ m}, \quad V_2 = 1.76 \times 10^{-4} \text{ m}^3$$

The properties for copper are

$$\rho = 8954.2 \text{ kg/m}^3$$

$$C_p = 0.383 \text{ kJ/(kg.K)}$$

The calculated convection transfer coefficients are

$$\alpha_1 = 3,698.2 \text{ W/m}^2$$

$$\alpha_2 = 3,592.8 \text{ W/m}^2$$

Convection heat transfer coefficients were also measured on brass block measuring 10.5 cm x 7.8 cm x 1.34 cm. The properties of brass are

$$\rho = 8522 \text{ kg/m}^3$$

$$C_p = 0.385 \text{ kJ/(kg.k)}$$

The slope of the cooling curve is $m_3 = 0.154$ and the calculated convection heat transfer coefficient for the block is 2570.9 w/m^2 .

APPENDIX B

EXPERIMENTAL DETERMINATION OF SAMPLE VOLUME AND DENSITY

The volume and density of the cob, kernel and husk were measured using the water displacement technique described by Mohsenin (1986). A 360 mL container was used to submerge the corn into 300 ml of water. The water displacement caused by holding the product submerged was measured using a digital balance.

The volumes were measured progressively for the whole corn, the kernels and cob, and the cob. The volume was calculated from

$$V = \frac{\text{Weight of water}}{\text{Density of water}}$$

Density and Volume for the Cob

<u>Mass</u> (kg)	<u>Volume</u> (m ³ X 10 ⁵)	<u>Density</u> (kg/m ³)
0.076	8.9	851.1
0.089	9.8	904.2
0.074	8.2	900.3
0.092	10.9	847.3
0.078	8.7	893.8
0.079	8.8	894.8
0.059	6.5	904.5

Density and Volume for the Kernel

<u>Mass</u> (kg)	<u>Volume</u> (m ³ × 10 ⁵)	<u>Density</u> (kg/m ²)
0.099	10.2	965.9
0.095	9.8	965.1
0.074	7.5	985.5
0.106	10.4	1024.1
0.083	8.9	929.5
0.056	6.1	919.8
0.070	6.9	1014.4

Density and Volume for the Husk

<u>Mass</u> (kg)	<u>Volume</u> (m ³ × 10 ⁵)	<u>Density</u> (kg/m ³)
0.041	8.2	498.8
0.053	9.4	561.6
0.071	13.9	510.7
0.041	7.0	585.56
0.070	13.5	518.7
0.062	11.6	535.9
0.053	9.9	532.9

The values for the density and the volume used in the model are the averages of these.

APPENDIX C

STEADY STATE HEAT TRANSFER RESISTANCE

For a plate of thickness, L , with thermal conductivity, k subject to uniform heat flux q_o W/m^2 at one boundary and dissipating the heat to a medium at temperature T_∞ at the other boundary, The heat flow across the plate is

$$Aq_o = \frac{T_1 - T_2}{\frac{L}{Ak} + \frac{1}{Ah}}$$

where T_1 and T_2 are the temperatures at boundary one and two respectively and A is the heat transfer area. The first term in the denominator is the resistance due to the thickness of the plate while the second term is the resistance due to convection.

For the copper plate used in the the experiment, $L = 6.7$ mm and $k = 386$ $W/(m. C)$. The measured convection coefficient was 2570.9 W/m^2 . The resistances were 1.736×10^{-5} C/W for the thickness and 3.89×10^4 C/W due to convection. The resistance due to the thickness is only 4% of that due to convection and will thus have only a small effect on the heat transfer across the plate.

APPENDIX D

TRANSPIRATION FROM FRUITS AND VEGETABLES

The rate of moisture loss from a product surface can be expressed as

$$\dot{m} = \frac{A(P_s - P_a)}{\frac{1}{K_s} + \frac{1}{K_a}}$$

where

\dot{m} = rate of moisture loss (mg/s),

A = product surface area, (m^2),

P_s = water vapor pressure of evaporating surface (kPa),

P_a = water vapor pressure of surrounding air (kPa),

K_s = skin mass transfer coefficient (mg/(s.m².kPa)),

K_a = air film mass transfer coefficient (mg/(s.m².kPa))

The water vapor pressure is a function of the absolute temperature expressed as

$$\ln(P_s) = \frac{C_8}{T} + C_9 + C_{10}T + C_{11}T^2 + C_{12}T^3 + C_{13}\ln(T).$$

where T is the absolute temperature in R and the constants are

$$C_8 = -104404$$

$$C_9 = -11.2947$$

$$C_{10} = -0.027$$

$$C_{11} = 1.290 \times 10^{-5}$$

$$C_{12} = 2.478 \times 10^{-9}$$

$$C_{13} = 6.546$$

The air film mass transfer coefficient, K_a , can be calculated from the Sherwood-Reynolds-Schmidt correlation

$$Sh = Sc^{0.3}(0.35 + 0.34Re^{0.5} + 0.15Re^{0.58});$$

where

$$Sh = \frac{K_a d}{D}, \text{ the Sherwood number (dimensionless),}$$

d = diameter of product (m),

D = diffusivity of water vapor in air (m^2/s),

$$Sc = \frac{\mu}{\rho D}, \text{ the Schmidt number (dimensionless),}$$

ρ = density of air (kg/m^3),

μ = dynamic viscosity of air ($kg/(m.s)$),

$$Re = \frac{\rho v d}{\mu}, \text{ the Reynolds number (dimensionless),}$$

v = velocity of air (m/s).

The Sherwood number yields K_a with a driving force in kg/m^3 . This is converted to vapor pressure units by use of the perfect gas laws. For this study the skin mass transfer coefficient was assumed infinite because of the water used in heating the corn before drying.

APPENDIX E

COMPUTER PROGRAM

```
{ All values used in the program are in English Units}

program cornbed;

  const

    pi      = 3.141593;

    densair = 0.0735;

    relhum  = 0.80;

    patm    = 14.696;

    cpc     = 0.807;

    cpair   = 0.241;

  type

    { To use larger arrays, changes should be made
      at these type declarations}

    vec1    = array[1..20] of real;

    vec      = array[1..8] of real;

    mat      = array[1..10,1..8] of real;

    tcorn   = array[1..20] of mat;

  var

    tcbegin,tmas,tmout,tm,dt1,stp, masscorn,cornnum,

    mflow,x,massm,tin,deltx,suma,stepa      : real;

    bedsize,j                               : integer;
```

```

pos,tempbeda,tempair           : vec1;
rad,vol,a,az,mas,temp,temp1,tempbed      : mat;
r,deltrc,deltrk,deltrh,tela,rk,rc,rh     : vec;
deltz,l,bir,biz,as,tinf,mass           : real;
m,n,i,count,nc,nk,ii,nh,layer           : integer;
k1,cp1,h,rho1,delt,alpha,del,par,t0,tel  : real;
k2,cp2,rho2,k,cp,rho,ra,time,rk1,heatco,
k3,rho3,cp3,dt,test,st,step,transco     : real;
quit,stop                          : boolean;
datafile,datafile2,datafile1           : text ;
diskfilename,diskfilename2,diskfilename1: string[15];
massavetemp,tcen,pv,p,delhr,hr          : real;
corn,corna                          : tcorn;

{$I func.inc}
{$I supbed.Inc}
{$I geobed.inc}
{$I transp.inc}
{$I heatbed.Inc}

procedure initializebed;

var

    i,ii,n1,n2    : integer;

init      : vec1;

begin

    writeln(' ENTER NUMBER OF CRATES TO SIMULATE AND
            NUMBER OF LAYERS PER CRATE');

```

```

readln(count,layer);
    bedsize      := count*layer;
for i := 1 to count do begin
    writeln('    ENTER AVERAGE TEMPERATURE OF
              CRATE['',i:1,'']');
    readln(init[i]); end;
n1 := 1;
n2 := layer;
    for i := 1 to count do begin;
        for ii := n1 to n2 do begin
            pos[ii]      := init[i];
            tempbeda[ii] := init[i]; end;
        n1 := n1 + layer;
        n2 := n2 + layer; end;
    writeln('    ENTER MEDIUM TEMPERATURE');
    readln(tin);
writeln('ENTER LENGTH OF CORN AND NUMBER OF NODES
              IN LENGTH');
readln(l,n);
deltz      := 1/(n-2);
writeln('    ENTER NUMBER OF NODES IN COB, KERNELS
              AND HUSK');
readln(nc,nk,nh);
m          := nc+nk+nh+3;
writeln('    ENTER AVERAGE WEIGHT OF EACH EAR AND

```

```

# NUMBER OF EARS IN EACH CRATE');
readln(masscorn,cornnum);
cornnum := cornnum/layer;
writeln(' ENTER TIME TO PRINT TEMPERATURES AND TO
STOP SIMULATION IN HOURS');
readln(step,stp);
stepa := step;
diskfilenametouse;
writeln(' ENTER TOTAL AIR FLOW IN CFM');
readln(mflow);
  for ii := 1 to bedsize do begin
    for i := 1 to m do begin
      for j := 1 to n do begin
        corn[ii][i,j] := tempbeda[ii];
        corna[ii][i,j] := tempbeda[ii];
        tempair[ii] := tin;
      end;
    end;
  end;
end; {initializeBED}
procedure Singmod(var test,tmas,tcen : real;
                  ttest : real;corn:mat);
VAR
  I,J : INTEGER;
begin

```

```

    solvsing(test,ttest,corn);
    output1(tmas,tcen);
end; {singmod}
procedure heatgain(var tmout : real; Tcbegin,tm,tmin,ta :
                                                             real);
var
    deltcorn, deltm,massc,coef,
    area,heatout,cratearea,
    heatlosscorn,heatgainm    : real;
begin
    coef    := 0.643;
    cratearea := 5.042;
    area    := (cratearea*count)/bedsize;
    {area = area of box exchanging heat with room}
    massc   := masscorn*cornnum ;
    deltcorn := ABS(tcbegin - tm);
    heatout  := coef*area*(ta-35)*delt;
    heatlosscorn := massc*cpc*deltcorn;
    heatgainm   := (mflow*densair*cpc*60*delt);
    deltm       := (heatlosscorn - heatout)/heatgainm;
    tmout       := tmin + deltm;
    delhr       := (suma*cornnum)/(layer*mflow*densair*60);
    hr          := hr + delhr;
    pv          := (hr*patm)/(hr+0.6219);
end; {heatgain}

```



```

begin
  initializebed;
  solve;
  dt := delt;
  time := delt;
  OUTPUT2;
  repeat
    quit := false;
    begin
      TINF := TIN;
      pressure(p,tinf);
      pv    := relhum*p;
      hr    := (0.6219*pv)/(14.56 - pv);
      for ii := 1 to bedsize do
        begin
          suma := 0.0;
          t0 := tempbeda[ii];
          for i:= 1 to m do begin
            for j := 1 to n do
              tempbed[i,j] := corn[ii][i,j]; end;
            singmod(test,tmas,tcen,tinf,tempbed);
            tempbeda[ii] := tmas;
            pos[ii]      := tcen;
          for i := 1 to m do begin
            for j := 1 to n do

```

```

        corna[ii][i,j] := temp1[i,j];
    end;
    heatgain(tmout,t0,tmas,tinf,tempair[ii]);
    tinf := tmout;
    tempair[ii] := tmout;
    WRITELN(' CENTER TEMP',tcen:10:2,'MEDIUM TEMP',
            tinf:10:2,' EXITING LEVEL ',II:5);
end; {ii}
for ii := 1 to bedsize do begin
    for i := 1 to m do begin
        for j := 1 to n do
            corn[ii][i,j] := corna[ii][i,j];
        end; {i} end; {ii}
    printout(test,time,step,stp);
    time := time + delt;
END; {REPEAT}
until quit = true;
cleanup;

end.

{Func.inc}

function power(x,b:real):real;
begin (*power*)
    power := exp(b*ln(x))
end; (*power*)

function AA(x,y : real) : real;

```

```

begin
    aa := pi*(power(x,2) - power(y,2));
end; {aa}
Function Heatgen(t : real;i,j : integer) : real;
    const
        a = 2.47E-05;
        b = 2.48;
    begin
        heatgen := a * power(t,b)*mas[i,j];
    end; { Heatgen }
Function Convection(flow,d:real):real;
    const
        meu = 1.25E-5;
        rho = 0.0735;
        k    = 0.0153;
        pr   = 0.71;
    var
        re,vel,tempo : real;
    begin
        vel := flow/(1.54*60);
        d   := 2.0*d;
        re  := (rho*vel*d)/meu;
        tempo := 0.22*(power(re,0.72)*power(pr,0.34));
        convection := (k*tempo)/d;
    end;

```

```

Function Latent(t:real):real;
  var
    tempo : real;
  begin
    tempo := t + 459.69;
    Latent := 1075.8965 - 0.56983*(tempo - 4961.69);
  end;

Function Radial(x:real):real;
  var
    temp,x1 : real;
  begin
    x1      := x*304.8;
    temp    := power(x1,2);
    radial  := 0.00328*(22.85 + 0.075*x1 - 9.95e-4*temp);
  end; {radial}

  {Supbed.inc}
procedure check;
  begin
    writeln;
    GotoXy(1,25); writeln(' PRESS ANY KEY TO CONTINUE');
    repeat until keypressed;
  end; {check}

procedure output;
  const

```

```

    lay    = 3;
var
    i,j : integer;
    delbed : real;
begin
    delbed := deltx*bedsize;
    write('ENTER FILENAME TO WRITE PROPERTIES TO    ');
    readln(diskfilename2);
    assign(datafile2,diskfilename2);
    rewrite(datafile2);
    writeln(datafile2);
    writeln(datafile2);
    writeln(datafile2);
    writeln(datafile2,'                PROPERTIES OF COB');
    writeln(datafile2);
    writeln(datafile2,'DENSITY                ',rho1:6:2);
    writeln(datafile2,'CONDUCTIVITY                ',K1:6:3);
    writeln(datafile2,' HEAT CAPACITY                ',cp1:6:3);
    writeln(datafile2,' NODES IN COB                ',NC:6);
    writeln(datafile2);
    writeln(datafile2);
    writeln(datafile2,'    PROPERTIES OF KERNEL                ');
    writeln(datafile2);
    writeln(datafile2,'DENSITY                ',rho2:6:2);
    writeln(datafile2,'CONDUCTIVITY                ',K2:6:3);

```

```

writeln(datafile2,' HEAT CAPACITY      ',cp2:6:3);
writeln(datafile2,' NODES IN KERNEL    ',NK:6);
writeln(datafile2);
writeln(datafile2);
writeln(datafile2,'   PROPERTIES OF HUSK      ');
writeln(datafile2);
writeln(datafile2,'DENSITY                ',rho3:6:2);
writeln(datafile2,'CONDUCTIVITY          ',K3:6:3);
writeln(datafile2,' HEAT CAPACITY      ',cp3:6:3);
writeln(datafile2,' NODES IN HUSK        ',NH:6);
writeln(datafile2);
writeln(datafile2);
writeln(datafile2,'   OTHER   PROPERTIES      ');
writeln(datafile2);
writeln(datafile2,'HEAT TRANS COEFFICIENT ',h:6:2);
writeln(datafile2,'MEDIUM TEMP          ',tin:6:2);
writeln(datafile2,'SIM.  TIME (HOURS) ',time:6:2);
writeln(datafile2,'TIME STEP (HOURS)    ',delt:6:3);
writeln(datafile2,' NODES IN LENGTH     ',n:3);
writeln(datafile2,' NODES IN RADIUS      ',m:3);
writeln(datafile2,'LENGTH OF CORN (FEET) ',l:6:2);
writeln(datafile2,' EARS PER LAYER      ',CORNNUM:6:2);
writeln(datafile2,' LAYERS PER CRATE     ',LAY:6);
writeln(datafile2,'CRATES SIMULATED     ',COUNT:6);
writeln(datafile2,'MEDIUM FLOW RATE     ',MFLOW:6:2);

```

```

        writeln(datafile2);
        writeln(datafile2);
    end;    {output}
procedure TimeAdjust;
begin
    time := time + delt;
    end;    { timeAdjust}
procedure MassAve(var massavetemp:real);
var
    i,j,i1,i2 : integer;
    sum1,sum2 : real;
begin
    sum1 := 0.0;
    sum2 := 0.0;
    for i := 1 to m do begin
        for j := 1 to n do begin
            sum1 := sum1 + mas[i,j]*temp1[i,j];
            SUM2 := SUM2 + mas[i,j];
        end;
    end;
    massavetemp := sum1/sum2;
end;
Procedure DiskFilenametoUse;
begin
    GoToXY(10,25);ClrEol;

```

```

        Write('ENTER FILENAME TO WRITE DATA TO ');
        Readln(Diskfilename);
        Assign(datafile,diskfilename);
        Rewrite(Datafile);

    end; {diskfilenametouse}
Procedure Cleanup;
begin
    close(datafile);
    output;
    close(datafile2);
end; {closeup}
procedure output1(var tmas,t : real);
begin
    massave(massavetemp);
    tmas:= massavetemp;
    t    := temp1[1,2];
end;
procedure output2;
var
    i : integer;
begin
    write(datafile,time : 10:2);
    for i := 1 to bedsize do
        write(datafile,pos[i]:10:2);
    for i := 1 to bedsize do

```



```

        write(datafile,tempbeda[i] : 10 :2);
        writeln(datafile);writeln('TIME ELAPSED',time:7:3);
    end; {output2}
procedure printout(var test : real;t,step,st : real);
var
    h2 : real;
begin
    test := dt + delt;
    if (abs(t - stepa)) <= 0.001 then
        begin
            output2;
            stepa := stepa + step;
        end
    else
        begin
            if (abs(t - st)) <= 0.01 then
                quit := true
            else
                quit := false;
            end; end;
end;
procedure printouta(var test : real;dt,st : real);
begin
    test := dt + delt;
    if (abs(dt - st)) <= 0.001 then
        stop := true

```

```

        else
            stop := false;
        end;
    procedure split;
    begin
        k1 := 0.221;
        k2 := 0.263;
        k3 := 0.164;
        rho1 := 55.90;
        rho2 := 60.14;
        rho3 := 33.39;
        cp1 := 0.817;
        cp2 := 0.850;
        cp3 := 0.807;
    end;{split}

{Geobed.inc}

Procedure Radiustep(var rstepc,rstepk,rsteph,
                    rc1,rk1,rh1,length:real;
                    nc,nk,nh : integer);

var
    r      : real;
begin
    r      := radial(length);
    rc1    := 0.55*r;

```

```

rk1  := 0.89*r;
rh1  := r;
rstepc := rc1/nc;
rstepk := (rk1-rc1)/(nk+1);
rsteph := (r - rk1)/(nh+0.5);
end; {radiustep}
Procedure CalcRadius(drc,drk,drh,r:vec;
                    nc,nk,nh,m,n:integer);
var
i,i1,i2,i3,i4,j   : integer;
ral                : mat;
begin
i1      := nc + 2;
i2      := nc + nk + 1;
i3      := i2 + 1;
for i := 2 to nc+1 do begin
  for j:= 1 to n do begin
    ral[i,j] := 0.0;
    ral[i,j] := ral[i-1,j] + deltrc[j];
  end; end;
for i := i1 to i3 do begin
  for j:= 1 to n do begin
    ral[i,j] := ral[i-1,j] + deltrk[j];
  end; end;
for i := i3+1 to m-1 do begin

```

```

    for j:= 1 to n do begin
        ral[i,j] := ral[i-1,j] + deltrh[j];
    end; end;

    for j := 1 to n do
        ral[m,j] := ral[m-1,j] + (deltrh[j]/2.0);
    for j := 1 to n do
        rad[m,j] := ral[m,j];
    for i := m-1 downto 1 do begin
        for j := 1 to n do
            rad[i,j] := ral[i+1,j] - ((ral[i+1,j]-ral[i,j])/2.0); end;
        end;{CalcRadius}
Procedure RadCalc(var deltrc,deltrk,deltrh:vec;
                    deltz:real;nc,nk,nh,m,n:integer);
var
    drc,drk,drh,rc1,rk1,rh1,length      : real;
    j                                     : integer;
Begin
    length := 0.0001;

    Radiustep(drc,drk,drh,rc1,rk1,rh1,length,nc,nk,nh);
    deltrc[1] := drc;
    deltrk[1] := drk;
    deltrh[1] := drh;
    rc[1]      := rc1;
    rk[1]      := rk1;
    rh[1]      := rh1;

```

```

length      := length + deltz/2.0;
Radiustep(drc,drk,drh,rc1,rk1,rh1,length,nc,nk,nh);
deltrc[2]   := drc;
deltrk[2]   := drk;
deltrh[2]   := drh;
rc[2]       := rc1;
rk[2]       := rk1;
rh[2]       := rh1;
for j := 3 to n-1 do begin
    length := length + deltz;
    Radiustep(drc,drk,drh,rc1,rk1,rh1,length,nc,nk,nh);
    deltrc[j] := drc;
    deltrk[j] := drk;
    deltrh[j] := drh;
    rc[j]     := rc1;
    rk[j]     := rk1;
    rh[j]     := rh1;
end; {j}

length := length + deltz/2.0;
Radiustep(drc,drk,drh,rc1,rk1,rh1,length,nc,nk,nh);
deltrc[n] := drc;
deltrk[n] := drk;
deltrh[n] := drh;
rc[n]     := rc1;
rk[n]     := rk1;

```

```

        rh[n]      := rh1;

        calcRadius(deltrc,deltrk,deltrh,rh,nc,nk,nh,m,n);
end;{radcal}

Procedure AreaVol(var az,rad:mat;deltz:real;m,n:integer);
var
    i,j  : integer;
begin
    for i := 2 to m do begin
        for j := 1 to n do begin
            az[i,j] := pi*(power(rad[i,j],2)-power(rad[i-1,j],2));
            az[m-1,j] := pi*(power(rad[m,j],2)-power(rad[m-2,j],2));
            vol[i,j] := az[i,j]*deltz;
            az[1,j] := pi*power(rad[1,j],2);
            vol[1,j] := az[1,j]*deltz;
            vol[m,j] := 0.0;
        end; {j}
        vol[I,1] := 0.0;
        vol[i,n] := 0.0;
    end; {i}
    vol[1,1] := 0.0;
    vol[1,n] := 0.0;
    end; {areavol}

Procedure Areai(var a:mat;rad:mat;deltz:real;m,n:integer);
var
    i,j  : integer;

```

```
begin
```

```
  for i := 1 to m do begin
```

```
    for j := 2 to n-1 do begin
```

```
      a[i,j] := 2.0*pi*deltz*rad[i,j];
```

```
    end; {j}
```

```
      a[i,1] := pi*deltz*rad[i,1];
```

```
      a[i,n] := pi*deltz*rad[i,n];
```

```
    end;{i}
```

```
  end;{areai}
```

```
Procedure Masses(var mas:mat;vol:mat;rho1,rho2,rho3:real;
                  rc,rk:vec;nc,nk,nh:integer);
```

```
var
```

```
  temp1,temp2,temp11,temp22,
```

```
  aa1,aa2                                :   vec;
```

```
  i,j,i1,i2,i3,i4                        :   integer;
```

```
begin
```

```
  i1   := nc + 2;
```

```
  i2   := i1 + nk - 1;
```

```
  i3   := i2 + 2;
```

```
  for j := 1 to n do
```

```
    begin
```

```
      temp1[j] := rc[j]-(deltrc[j]/2.0);
```

```
      temp2[j] := rk[j]-(deltrk[j]/2.0);
```

```
      temp11[j] := rc[j]+(deltrk[j]/2.0);
```

```
      temp22[j] := rk[j]+(deltrh[j]/2.0);
```

```

aa1[j] := (aa(rc[j],temp1[j])*rho1 +
aa(temp11[j],rc[j])*rho2)/
(aa(rc[j],temp1[j])+aa(temp11[j],rc[j]));
aa2[j] := (aa(rk[j],temp2[j])*rho2 +
aa(temp22[j],rk[j])*rho3)/
(aa(rk[j],temp2[j])+aa(temp22[j],rk[j]));
end;{j}
for i := 1 to nc do begin
  for j:= 1 to n do begin
    mas[i,j] := vol[i,j]*rho1;
  end;{j} end;{i}
for j:=1 to n do
  mas[nc+1,j] := vol[nc+1,j]*aa1[j];
for i := i1 to i2 do begin
  for j:= 1 to n do
    mas[i,j] := vol[i,j]*rho2; end;
  for j:= 1 to n do
    mas[i2+1,j] := vol[i2+1,j]*aa2[j];
    for i := i3 to m do begin
      for j := 1 to n do
        mas[i,j] := vol[i,j]*rho3; end;
    end; {masses}
procedure Radius(var deltrc,deltrk,deltrh:vec;
  l,rho1,rho2,rho3:real;m,n:integer);
begin

```



```

Radcalc(deltrc,deltrk,deltrh,deltz,nc,nk,nh,m,n);
areai(a,rad,deltz,m,n);
areavol(az,rad,deltz,m,n);
masses(mas,vol,rho1,rho2,rho3,rc,rk,nc,nk,nh);
end;

procedure swap;

var
    i,j    :   integer;
begin
    for i := 1 to m do
        begin
            for j := 1 to n do
                begin
                    temp1[i,j] := temp[i,j];
                end; {j}
            end; {i}
        end; {swap}
    end;

procedure TimeStep(var deltime : real;i,j : integer;
                   deltr,alfa : real);

var
    param : real;
begin
    param := ((a[i,j] + a[i-1,j])/deltr +
              (2*az[i,j]/deltz));
    deltime := vol[i,j]/(alfa*param);

```

```

end; {TimeStep}

procedure TimeStepInt(var deltime : real; i, j : integer;
                      k1, k2, k3, del1, del2, al : real);

var
    param : real;
begin
    param := (((a[i, j]*k2)/del2) + ((k1*a[i-1, j])/del1) +
              ((2*k3*az[i, j])/deltz));

    deltime := al/(param);
end; {TimeStepInt}

procedure Interfacer(var pat, kz : vec; k1, k2 : real;
                     RHO1, RHO2, CP1, CP2 : real;
                     deltr1, deltr2, r : vec);

var
    I, j : integer;
    r1, r2, ra1, ra2,
    v1, v2, deltr : vec;
begin
    for j := 1 to n do begin
        r2[j] := r[j];
        r1[j] := r[j] - deltr1[j]/2;
        ra1[j] := r[j];
        ra2[j] := r[j] + deltr2[j]/2;
        v1[j] := aa(r2[j], r1[j])*deltz;
        v2[j] := aa(ra2[j], ra1[j])*deltz;
    end;
end;

```

```

    pat[j] := rho1*cp1*v1[j] + rho2*cp2*v2[j];
    kz[j] := (aa(r2[j],r1[j])*k1 +
    aa(ra2[j],ra1[j])*k2)/aa(ra2[j],ra1[j]);
    deltr[j] := (deltr1[j] + deltr2[j])/2;
end;{j}
end;

procedure timestepcheck(var deltime : real);
var
    alfa1,alfa2,alfa3,param,tempo : real;
    param1                          : mat;
    deltima,pat,kz                  : vec;
    i1,i2,i3                        : integer;
begin
    split;
    i1 := nc + 2;
    i2 := nc + nk + 1;
    i3 := i2 + 2;
    alfa1 := k1/(rho1*cp1);
    alfa2 := k2/(rho2*cp2);
    alfa3 := k3/(rho3*cp3);
    for i := 2 to nc do begin
        for j := 2 to n-1 do begin
            timestep(param,i,j,deltrc[j],alfa1);
            param1[i,j] := param;
        end;end;
end;end;

```

```

interfacer(pat,kz,k1,k2,rho1,rho2,cp1,cp2,deltrc,deltrk,rc);
    i := nc + 1;
    for j := 2 to n-1 do begin
timestepint(param,i,j,k1,k2,kz[j],deltrc[j],
                deltrk[j],pat[j]);
        param1[i,j] := param;
    end;
    for i := i1 to i2 do begin
        for j := 2 to n-1 do begin
            timestep(param,i,j,deltrk[j],alfa2);
            param1[i,j] := param;
        end;end;
interfacer(pat,kz,k2,k3,rho2,rho3,cp2,cp3,deltrk,deltrh,rk);
    i := i2 + 1;
    for j := 2 to n-1 do begin
timestepint(param,i,j,k2,k1,kz[j],
                deltrk[j],deltrh[j],pat[j]);
        param1[i,j] := param;
    end;
    for i := i3 to m-1 do begin
        for j := 2 to n-1 do begin
            timestep(param,i,j,deltrh[j],alfa3);
            param1[i,j] := param;
        end;end;
        tempo := param1[m-1,n-1];

```

```

    for i := 2 to m-1 do begin
        for j := 2 to n-1 do begin
            if(tempo - param1[i,j]) <= 0.0 then
                tempo := tempo
            else
                tempo := param1[i,j];
            end; end;
        delt := tempo;
    end;

{Transp.inc}

procedure parameters(var kair:real;d,t,flow:real);
    const
        diff = 2.75E-4;
        meu  = 1.25E-5;
        dens = 0.0735;
        kon  = 0.0153;
    var
        vel,re,sh,sc,diam    : real;
begin
    diam := 2.0*d;
    vel  := flow/(1.5*60);
    re   := (dens*vel*diam)/meu;
    sc   := meu/(dens*diff);
    sh   := power(sc,0.3)*(0.35 + 0.34*power(re,0.5) +

```

```

0.15*power(re,0.58));

kair := ((18*144*sh*diff)/(d*1543.32*t))*3600;

end;

procedure pressure(var p : real;t : real);

  const

    c8= -10440.4;
    c9= -11.2946669;
    c10 = -0.02700133;
    c11 = 0.1289706E-4;
    c12 = -0.2478068E-8;
    c13 = 6.5459673;
    x = 2.0;
    y = 3.0;
    z = 4.0;
    pi= 3.14159;

  var

    aa1,aa,bb,
    tem    : real;

  begin

    aa := c11*power(t,x) + c12*power(t,y) ;
    tem:= aa + (c8/t) +c9 + c10*t + c13*ln(t);
    p := exp(tem);

  end;

procedure transpiration(var tema : real;

  tstart,tinf,flow,radiuss,rho,

```

```

        ta,length,area : real);

const

    ks  = 5.0E20;

    esp= 0.9;

var

    q, mdot,kas,ktest,
    tskin,tem1,tem2,ka,
    l,t,t1
                                : real;
    quit
                                : boolean;

begin

    t  := tstart + 459.69;
    t1 := tinf + 459.69;
    parameters(kas,radiuss,t,flow);
    ktest := 1/kas + 1/ks;
    ka     := 1/ktest;
    pressure(p,t);
    mdot := abs(ka*(-p + pv));
    suma := suma + (mdot*area);

    tema := mdot;

end;

{Heatbed.inc}

procedure gennode(var tel:real; rho1,cp1,k1,tinf:real;
                  deltr:vec;t:mat;i,j:integer);

var

```

```

    alpha: real;
begin
    alpha := k1/(rho1*cp1);
    tel    := (alpha*delt/vol[i,j])*((a[i-1,j]/
                                deltr[j])*temp1[i-1,j] -
                                ((a[i-1,j]/deltr[j]) + (a[i,j]/deltr[j]) +
                                (az[i,j-1]/deltz)
                                + (az[i,j]/deltz) - (vol[i,j]/
                                (alpha*delt)))*temp1[i,j] +
                                (a[i,j]/deltr[j])*temp1[i+1,j]
                                + (az[i,j-1]/deltz)*temp1[i,j-1] +
                                (az[i,j]/deltz)*temp1[i,j+1])
            + heatgen(temp1[i,j],i,j);
end;

procedure bottom(var tel : real; i : integer ;
                 k,rho,cp,tinf,deltr : real);
var
    tel3,biz,mdot,qtr      : real;
begin
    biz := h*deltz/k;
    transpiration(mdot,temp1[i,1],tinf,mflow,rad[i,1],
                 rho,tinf,l,az[i,1]);
    qtr := (deltr*latent(temp1[i,1])*az[i,1]*mdot)/k;
    tel  := (Az[i,1]*tinf + (2.0*az[i,2]/biz)*
    temp1[i,2] - qtr)/

```



```

      (az[i,1] + (2.0*az[i,2]/biz));
end;

procedure side(var tela : real; j : integer ;
               k,rho,cp,h,tinf : real);

var
    tell,bir,mdot,qtr      : real;
begin
    bir := h*deltrh[j]/k;
transpiration(mdot,temp1[m,j],tinf,mflow,rad[m,j],
               rho,tinf,l,a[m,j]);
    qtr := (deltrh[j]*latent(temp1[m,j])
            *a[m,j]*mdot)/k;
    tela := ((2.0*a[m-1,j]/bir)*temp1[m-1,j] +
            a[m,j]*tinf - qtr)/
            ((2.0*a[m-1,j]/bir) + a[m,j]);
end;

procedure top(var tel : real; i: integer ;
               k,rho,cp,tinf,deltr : real);

var
    tell,biz,mdot,qtr      : real;
begin
    biz := h*deltz/k;
transpiration(mdot,temp1[i,n],tinf,mflow,rad[i,n],
               rho,tinf,l,az[i,n]);
    qtr := (deltr*latent(temp1[i,n])*az[i,n]*mdot)/k;

```

```

tel := ( (2.0*az[i,n-1]/biz)*temp1[i,n-1] +
az[i,n]*tinf - qtr)/
(( 2.0*az[i,n-1]/biz) + az[i,n]);
end;

procedure topendsur(k,rho,cp,tinf : real);
var
mdot,qtr,bir      : real;
begin
bir := h*deltrh[n]/k;
transpiration(mdot,temp1[m,n],tinf,mflow,rad[m,n],
rho,tinf,l,a[m,n]);
qtr := (deltrh[n]*latent(temp1[m,n])*a[m,n]*mdot)/k;
temp[m,n] := ((2.0*a[m-1,n]/bir)*temp1[m-1,n] +
tinf*a[m,n] - qtr)/
((2.0*a[m-1,n]/bir) + a[m,n]);
end;

procedure centre(var tel : real;j:integer; k,rho,cp: real);
var
del,PAR,ALPHA      : real;
LEN,LEN1,LEN2      : REAL;
begin
alpha := k/(rho*cp);
par := alpha*delt/vol[1,j];
tel := par*((a[1,j]/deltrc[1])*temp1[2,j] -
((a[1,j]/deltrc[1])

```

```

+ (az[1,j-1]/deltz) + (az[1,j]/deltz) -
(1/par))*temp1[1,j] +
(az[1,j-1]/deltz)*temp1[1,j-1] +
(az[1,j]/deltz)*temp1[1,j+1])
+ heatgen(temp1[1,j],1,j);

end;

procedure topendcen(k,rho,cp,tinf : real);
var
    mdot,qtr,biz : real;
begin
    biz := h*deltz/k1;
transpiration(mdot,temp1[1,n],tinf,mflow,rad[1,n],
rho,tinf,l,az[1,n]);
    qtr := (deltrc[n]*latent(temp1[1,n])*az[1,n]*mdot)/k1;
temp[1,n] := ((2.0*az[1,n-1]/biz)*temp1[1,n-1]
+ az[1,n]*tinf - qtr)
/((2.0*az[1,n-1]/biz) + az[1,n]);
end;

procedure bottomcen(k,rho,cp,tinf : real);
var
    mdot,qtr,biz : real;
begin
    biz := h*deltz/k;
transpiration(mdot,temp1[1,1],tinf,mflow,rad[1,1],
rho,tinf,l,az[1,1]);

```

```

qtr := (deltrc[1]*latent(temp1[1,1])*az[1,1]*mdot)/k1;
temp[1,1] := (az[1,1]*tinf + (2*az[1,2]/biz)*temp1[1,2] -
qtr)/(az[1,1] + (2.0*az[1,2]/biz));
    end;    {bottomcen}

procedure bottomsides(k,rho,cp,tinf : real);
    var
        mdot,qtr,bir : real;
    begin
        bir := h*deltrh[1]/k;
transpiration(mdot,temp1[m,1],tinf,mflow,rad[m,1],
rho,tinf,l,a[m,1]);
qtr := (deltrh[1]*latent(temp1[m,1])*a[m,1]*mdot)/k;
temp[m,1] := ((2.0*a[m-1,1]/bir)*temp1[m-1,1]
+ a[m,1]*tinf -qtr)/
((2.0*a[m-1,1]/bir) + a[m,1] );
    end;    {bottomsides}

procedure Interface(var t : vec ; temp1 : mat;
                    k1,k2,tinf : real;
                    RH01,RH02,CP1,CP2 : real;
                    deltr1,deltr2,r : vec;
                    n,mi : integer);
    var
        RH030,CP30 : REAL;
        I,j : integer;
        r1,r2,ra1,ra2,RA3,RA4,RA5,

```

```

    v1,v2,pat,kz,deltr    :   vec;
begin
    RH030    := (RH01 + RH02)/2.0;
    CP30     := (CP1 + CP2)/2.0;
    for j    := 1 to n do begin
        RA3[J] := R[J];
        RA4[J] := R[J];
        r2[j]  := r[j];
        r1[j]  := r[j] - deltr1[j]/2;
        ra1[j] := r[j];
        ra2[j] := r[j] + deltr2[j]/2;
        v1[j]  := aa(r2[j],r1[j])*deltz;
        v2[j]  := aa(ra2[j],ra1[j])*deltz;
        pat[j] := rho1*cp1*v1[j] + rho2*cp2*v2[j];
        kz[j]  := (aa(r2[j],r1[j])*k1 +
        aa(ra2[j],ra1[j])*k2)/aa(ra2[j],ra1[j]);
        deltr[j] := (deltr1[j] + deltr2[j])/2;
    end;{j}

    bottom(tel,mi,kz[1],rho30,cp30,tinf,deltr[1]);
    t[1] := tel;
    for j := 2 to n-1 do
        begin
            t[j] := (delt/pat[j])*((k1*a[mi-1,j]/
            deltr1[j])*temp1[mi-1,j] -
            ((k1*a[mi-1,j]/deltr1[j]) +

```

```

      (k2*a[mi,j]/deltr2[j]) +
      ((kz[j]/deltz)*(az[mi,j-1] + az[mi,j]) -
      (pat[j]/delt)))*temp1[mi,j] +
      (k2*a[mi,j]/deltr2[j])*temp1[mi+1,j]
      + ((kz[j]/deltz)*(az[mi,j-1]*temp1[mi,j-1] +
      az[mi,j]*temp1[mi,j+1])))
      + heatgen(temp1[mi,j],mi,j);
end; {j}

top(tel,mi,kz[n],rho30,cp30,tinf,deltr[n]);
t[n] := tel;
{TimeStepInt(mi,n,k1,k2,kz[n],deltr1[n],deltr2[n],pat[1]);}

end;

procedure Block(i : integer; k,rho,cp,tinf : real;
                deltr:vec;N:INTEGER);

var
    j                : integer;
    alpha,TEL        : real;
begin
    alpha := k/(rho*cp);
    bottomcen(k,rho,cp,tinf);

    for j := 2 to n-1 do
        begin
            {TimeStep(i,j,deltr,alpha);}

            centre(tel,j,k,rho,cp);

            temp[i,j] := tel ;

```

```

        end; {j}
    topendcen(k,rho,cp,tinf);
    end; {Block}
procedure Block1(i: integer; k,rho,cp,tinf : real;
                deltr:vec;n:integer);
var
    j,na          : integer;
    alpha         : real;
begin
    alpha := k/(rho*cp);
    bottom(tel,I,k,rho,cp,tinf,deltr[1]);
    temp[i,1] := tel;
    for j := 2 to n-1 do
        begin
            {TimeStep(na,j,deltr,alpha);}
            gennode(tel,rho,cp,k,tinf,deltr,temp1,I,j);
            temp[i,j] := tel;
        end; {j}
    top(tel,i,k,rho,cp,tinf,deltr[n]);
    temp[i,n] := tel;
end; {Block1}
procedure Crossover(i : integer; k1,k2,cp1,rho1,CP2,RHO2,
                tinf : real;deltri,deltr2,ra : vec;
                n:integer );
var

```

```

j      : integer;

begin

interface(tela,temp1,k1,k2,tinf,RH01,RH02,CP1,CP2,
deltr1,deltr2,ra,n,i);

      for j := 1 to n do BEGIN
            temp[i,j] := tela[j]; END;

end; {Crossover}

procedure Block2(i : integer; k,rho,cp,tinf : real;deltr :
vec;n:integer);

var

j, na : integer;

alpha : real;

begin

alpha := k/(rho*cp);

for na := i to m-1 do begin

bottom(tel,na,k,rho,cp,tinf,deltr[1]);

temp[na,1] := tel;

for j := 2 to n-1 do

begin

{TimeStep(na,j,deltr,alpha);}

gennode(tel,rho,cp,k,tinf,deltr,temp1,na,j);

temp[na,j] := tel;

end; {j}

top(tel,na,k,rho,cp,tinf,deltr[n]);

temp[na,n] := tel;

```



```

end; {na}

bottomside(k,rho,cp,tinf);

for j := 2 to n-1 do
begin
    {TimeStep(m,j,deltr,alpha);}
    side(tel,j,k,rho,cp,h,tinf);
    temp[m,j] := tel;
end; {j}

Topendsur(k,rho,cp,tinf);

end; { Block2}

procedure solve;
begin
    split;
    radius(deltrc,deltrk,deltrh,l,rho1,rho2,rho3,m,n);
    timestepcheck(delt);
    h := convection(mflow,rad[1,1]);
end; {solve}

procedure Solvsing(var test : real;tinf : real;t : mat);
var
    i,J,NA,i1,i2,i3      : integer;
begin
    i1 := nc + 2;
    i2 := nc + nk + 1;
    i3 := i2 + 2;

    for i := 1 to m do begin

```

```

    for j := 1 to n do
        temp1[i,j] := t[i,j]; end;
    I := 1;
    block(I,k1,rho1,cp1,tinf,deltrc,n);
    for I := 2 to nc do
        block1(I,k1,rho1,cp1,tinf,deltrc,n);
        NA := I + 1;
    Crossover(NA,k1,k2,cp1,rho1,CP2,RH02,tinf,
        deltrc,deltrk,rc,n);
        for i := i1 to i2 do
            block1(i,k2,rho2,cp2,tinf,deltrk,n);
            i := i + 1;
        Crossover(i,k2,k3,cp2,rho2,CP3,RH03,tinf,
        deltrk,deltrh,rk,n);
            block2(I3,k3,rho3,cp3,tinf,deltrh,n);
        swap;
    end; {solvsing}

```

SAMPLE INPUT DATA FOR COMPUTER PROGRAM

PROPERTIES OF COB

DENSITY	55.90
CONDUCTIVITY	0.221
SPECIFIC HEAT CAPACITY	0.817
NUMBER OF NODES IN COB	2

PROPERTIES OF KERNEL

DENSITY	60.14
CONDUCTIVITY	0.263
SPECIFIC HEAT CAPACITY	0.850
NUMBER OF NODES IN KERNEL	2

PROPERTIES OF HUSK

DENSITY	33.39
CONDUCTIVITY	0.164
SPECIFIC HEAT CAPACITY	0.807
NUMBER OF NODES IN HUSK	1

OTHER PROPERTIES

HEAT TRANSFER COEFFICIENT	7.84
MEDIUM TEMPERATURE	40.00
SIMULATION TIME (HOURS)	1.03
TIME STEP (HOURS)	0.002
NUMBER OF NODES IN LENGTH	8
NUMBER OF NODES IN RADIUS	8
LENGTH OF CORN (FEET)	0.39

AVERAGE MASS OF CORN (LB)	0.56
NUMBER OF EARS PER LAYER	18.00
NUMBER OF LAYERS PER CRATE	3
NUMBER OF CRATES SIMULATED	3
MEDIUM FLOW RATE	100.00

LIST OF REFERENCES

- Ames, W. F. 1977. Numerical Methods for Partial Differential Equations. Academic Press, Inc., New York.
- Appleman, C. O. 1918. Respiration and Catalase Activity in Sweet Corn. Amer. J. Bot. 5:207-209.
- Appleman, C. O. and Arthur, J. M. 1919. Carbohydrate Metabolism in Green Sweet corn. J. Agric. Res. 17:137-152.
- Arthey, V. D. 1975. Quality of Horticultural Products. John Wiley and Sons, Inc., New York.
- Awbery, J.H. 1927. The Flow of Heat in a Body Generating Heat. Phil. Mag. 4(7):629-639.
- Baird, C.D. 1973. Heat Transfer in Beds of Citrus fruits During Forced Convection Cooling. Ph D. Dissertation, University of Florida, Gainesville.
- Baird, C. D. and Gaffney, J. J. 1976. A Numerical Procedure for Calculating Heat Transfer in Bulk Loads of Fruits and Vegetables. ASHRAE Trans. 82(2):525-540.
- Baird, C. D. , Gaffney, J. J. and Kinard, D. T. 1975. Research Facility for Forced-Air Precooling of fruits and Vegetables. Trans of ASAE 18(2):376-379.
- Bakker-Arkema, F. W. 1970. Cooling of a Bed of Potatoes (or Apples, Tomatoes, Sugar-Beets, Onions): A Simplified Model. Proceedings of the Institute for Simulation of Cooling and Drying Beds of Agricultural Products. Agricultural Engineering Department, Michigan State University, East Lansing, Michigan.
- Bakker-Arkema, F. W. and Bickert, W. G. 1966. A Deep Bed Computational Cooling Procedure for Biological products. Trans of ASAE 9:834-836.

- Barker, J. J. 1965. Heat Transfer in Packed beds. Ind. Eng. Chem. 57(4):43.
- Beck, J. V. 1966. Transient Determination of Thermal Properties. Nuclear Engineering and Design 3:373.
- Bellagha, S. and Chau K. V. 1985. Heat and Mass Transfer During the Cooling of Tomatoes Individually and in Bulk. ASAE Paper #85-6002. St Joseph, Michigan.
- Bennett, A. H. 1963a. Thermal Characteristics of Peaches as Related to Hydrocooling. USDA-AMS Tech. Bull. #1292, 36pp. U.S.D.A., Washington, D.C.
- Bennett, A. H. 1963b. Research and Observation in the Practice of Precooling of Fruits and Vegetables. ASAE Paper #63-319. St Joseph, Michigan.
- Bennett, A. H. 1964. Precooling Fruits and Vegetables. Trans of ASAE 7(3):265-270. St Joseph, Michigan.
- Bennett, A. H., Chace, W. G. and Cubbedge, R. H. 1962. Estimating Thermal Conductivity of Fruit and Vegetable Components - the Fitch Method. ASHRAE J. 4(9):80-85.
- Bennett, A. H., Chace, W. G. and Cubbedge, R. H. 1964. Thermal Conductivity of Valencia Oranges and Marsh Grapefruit. ASHRAE Trans 70:256-259.
- Bennett, A. H. and Henry, F. E. 1978. Effect of Repeated Cooling and Heating on Cooling Rate of Pallet Loads of Sweet Corn Packed in Corrugated Shipping Containers. Proc. Fla. State Hort. Soc. 91:330-333.
- Bennett, A. H., Henry, F. E. and Adam J. C. 1976. Precooling Pallet Loads of Sweet Corn Packed in Wirebound Crates. USDA - ARS - S - 99 U.S.D.A., Washington, D.C.
- Bird, R. B., Stewart, W. E. and Lightfoot, E. N. 1966. Transport Phenomena. John Wiley and Sons, Inc., New York.
- Bhowmik, S.R. and Hayakawa, K. I. 1979. A New Method for Determining the Apparent Thermal Diffusivity of Thermally Conductive Food. J. of Food Sci. 44:469-474.
- Carey, E. E., Rhodes, A. M. and Dickerson, D. B. 1982. Post Harvest Levels of Sugars and Sorbitol in Sugary Enhancer (su, se) and Sugary (sh,se) Maize. Hort. Sci. 17(2):241-242.

- Carnahan, B., Luther, H. A. and Wilkes O. J. 1969. Applied Numerical Methods. John Wiley and Sons, Inc. New York.
- Carslaw, H. S. and Jaeger, J. C. 1959. Conduction of Heat in Solids. Oxford University Press, London.
- Charm, S. 1963. A Method for Experimentally Evaluating Heat Transfer Coefficients in Freezers and Thermal Conductivity of Frozen Foods. Food Technology. 17:93-96
- Charm S. 1978. Fundamentals of Food Engineering. Avi Publishing Co., Westport, Connecticut.
- Chau, K. V. and Gaffney, J. J. 1985. A Mathematical Model for the Transpiration from Fruits and Vegetables. ASAE Paper #85-6005. St Joseph, Michigan.
- Chau, K. V. Gaffney, J.J. Baird, C.D. and Church G.A. 1985. Resistance to Air Flow of Oranges in Bulk and in Cartons. Trans of ASAE 28(6):2083-2088.
- Chau, K. V. and Gaffney, J. J. and Bellagha S. 1984. Simulation of Heat and Mass Transfer in Products with Internal Heat Generation and Transpiration. ASAE paper #84-6513. St Joseph, Michigan.
- Choi, Y. 1985. Food Thermal Property Prediction as Affected by Temperature and Composition. Ph. D. Dissertation, Purdue University, West Lafayette, Indiana.
- Churchill, S. W. and Bernstein M. 1977. A Correlation for Forced Convection from Gases and Liquids to a Circular Cylinder in Cross Flow. J. Heat Transfer 99:300-306.
- Churchill, S. W. and Chu H. H. S. 1975. Correlating Equations for Laminar and Turbulent Free Convection from a Horizontal Cylinder. Int. J. Heat Mass Transfer 18:1049.
- Clary B. L. and Nelson G. L. and Smith, R. E. 1968. Heat Transfer from Hams During Freezing by Low Temperature Air. Trans of ASAE 11(4):496-499.
- Cowell, N.D., Evans, H.L., Hicks, E.W. and Miller, J.D. 1959. Conduction Errors in Thermocouples Used for Heat Penetration in Foods which Heat by Conduction. Food Technology. 8(8):425-429.
- Dickerson, R. W. 1965. An Apparatus for the Measurement of Thermal Diffusivity of Foods. Food Technology

19(5):198-204.

- Dickerson, R. W. and Read Jr. R. B. 1968. Calculation and Measurement of Heat Transfer in Foods. Food Technology 22:1533-1535,1545,1547-1549.
- Eckert, E.R.G. and Drake, R.M. Jr 1972. Analysis of Heat and Mass Transfer. McGraw-Hill Book Company, New York.
- Evensen, K. B. and Boyer, C.D. 1986. Carbohydrate Composition and Sensory Quality of Fresh and Stored Sweet Corn. J. Amer. Soc. Hort. Sci. 111(5):734-738.
- Florida Agricultural Statistics 1986. Vegetable Summary. Florida Crop and Livestock Reporting Service, Orlando, Florida.
- Furnas, C.C. 1930. Heat Transfer from a Gas Stream to a Bed of Broken Solids. Trans. Amer. Ins. Chem. Engrs. 24:142-186.
- Garwood, D.L., McArdle, F.J., Vandershire, S.F. and Shannon, J.C. 1976. Postharvest Carbohydrate Transformations and Processesd Quality of High Sugar Maize Genotype. J. Amer. Soc. Hort. Sci. 101:400-404.
- Geankoplis, C.J 1972. Mass Transfer Phenomena. Holt, Rhinehart and Winston, New York.
- Green, W.P., Hukill, W.V. and Rose, D.H. 1941. Calorimetric Measurement of the Heat of Respiration of Fruits and Vegetables. USDA Tech. Bull. # 771. U.S.D.A., Washington, D.C.
- Grizzell, W.G. and Bennett, A.H. 1966. Hydrocooling Stacked Crates of Celery and Sweet Corn. USDA-ARS, 52-12. U.S.D.A., Washington, D.C.
- Guillou, R. 1958. Some Engineering Aspects of Cooling Fruits and Vegetables. Trans ASAE 1(1):38-39,42.
- Guillou, R. 1960. Coolers for Fruits and Vegetables. Univ. Calif. Agric. Exp. Sta. Bull. #773
- Gaffney, J.J., Baird, C.D. and Chau, K.V. 1985. Influence of Airflow Rate, Respiration, Evaporative Cooling, and Other Factors Affecting Weight Loss Calculations for Fruits and Vegetables. ASHRAE Trans. 91(1):690-707.
- Gaffney, J.J., Baird, C.D. and Eshleman, W.D. 1980. Review and Analysis of the Transient Method for Determining Thermal Diffusivity of Fruits and Vegetables. ASHRAE

- Trans. 86(2):261-280.
- Haile, D.G. and Sorenson, J.W 1968. Effect of Respiration . Heat of Sorghum Grain on Design Conditioned-Air Storage System. Trans ASAE 11(3):335-338.
- Hardenburg, R.E., Watada, A.E and Wang, C.Y. 1986. The Commercial Storage of Fruits, Vegetables, and Florist and Nursery Stocks. U.S.D.A. Agriculture Handbook 66. U.S.D.A., Washington, D.C.
- Harper, J. C. 1976. Elements of Food Engineering. AVI Publishing co., Westport, Connecticut.
- Hayakawa, K. and Bakal, A 1973. New Computational Procedure for Determining the Apparent Thermal Diffusivity of a Solid Body Approximated with an Infinite Slab. J. of Food Sci. 38:623-629.
- Hayes, C. F. 1984. Thermal Diffusivity of Papaya Fruit. J. of Food Sci. 49:1219-1221.
- Heisler, M. P. 1947. Temperature Charts for Induction and Constant Temperature Heating. Trans ASME 69:227-236.
- Heldman, D.R. and Singh, P.R. 1981. Food Process Engineering. AVI Publishing Company, Inc. Westport, Connecticut.
- Henry, F.E., Bennett, A.H. and Segall, R.H. 1976. 'Hydraircooling' Vegetables Products in Unit Loads. Trans. ASAE 16(4):731-733,739.
- Henry, F. E., Bennett, A.H. and Segall, R. H. 1976. Hydraircooling: A New Concept for Precooling Pallet Loads of Vegetables. Ashrae Trans. 82(2):541-547.
- Hougen, O.A. and Marshall, W.R. Jr. 1947. Adsorption from a Fluid Stream Flowing Through a Stationary Granular Bed. Chem. Eng. Prog. 43:197-208.
- Kader, A.A. 1985. Postharvest Biology and Technology: an Overview. In: Post Harvest Technology of Horticultural Crops. Coop. Ext. U of Calif. Special pub #3311
- Kazarian, E. A. and Hall, C. W. 1965. Thermal Properties of Grain. Trans ASAE 8(1):33-48.
- Lentz, C. P. 1961. Thermal Conductivity of Meats, Fats, Gelatin Gels and Ice. Food Tech. 15:245.
- Luikov, A. N. 1968. Analytical Heat Diffusion Theory.

Acedemic Press, New York.

McAdams, W.N. 1954. Heat Transmission McGraw-Hill, New York.

Mitchell, F.G., Guillou, R. and Parsons, R. A. 1972. Commercial Cooling of Fruits and Vegetables. Cal. Agric. Exp. Stn. Ext. Service Manual #43.

Mohsenin, N.N. 1980. Thermal Properties of Foods and Agricultural Materials. Gordon and Breach. New York.

Mohsenin, N.N. 1986. Physical Properties of Plant and Animal Materials: Structure, Physical Characteristics, and Mechanical Properties. Gordon and Breach. New York.

Murakami, E.G., Choi, Y. and Okos, M.R. 1985. An Interactive Computer Program for Predicting Thermal Properties. ASAE paper #85-6511. St Joseph Michigan.

Ozizik, M. N. 1980. Heat Conduction. John Wiley and Sons, New York.

Perry, J.H. 1984. Perry's Chemical Engineers' Handbook. McGraw-Hill, New York.

Perry, R.L and Perkins, R.M. 1968. Hydrocooling Sweet Corn. ASAE Paper #68-880. St Joseph, Michigan.

Pflug, I.J. and Blaisdale, J.L. 1963. Method of Analysis of Precooling Data. ASHRAE J. 5(11):33-40.

Pflug, I.J. and Blaisdale, J.L. and Kopelman, J. 1965. Developing Temperature-Time Curves for Objects that can be Approximated by a Sphere, Infinite Plate or Infinite Cylinder. ASHRAE Trans. 71:248-258.

Reidel, L. 1969. Measurement of Thermal Diffusivity of Foodstuffs rich in Water. Kalttechnik-Klimtisierung 21(11):315-316.

Reidy, G.A. and Rippen, A.L. 1971. Methods for Determining Thermal Conductivity in Foods. Trans ASAE 14(2):248-253.

Romero, R.A. 1987. Transpiration from fruits and Vegetables in Storage. Ph. D. Dissertation, University of Florida, Gainesville, Florida.

Romero, R.A. and Chau, K.V. 1987. A Mathematical Simulation of the Transpiration from Fruits and Vegetables in

- Bulk Storage. ASAE paper #87-6007. St Joseph, Michigan.
- Ryall, A.L. and Pentzer, W.T. 1982. Handling, Transportation and Storage of Fruits and Vegetables. AVI Pub. Co., Westport, Connecticut.
- Sastry, S. K. 1984. Convection Heat Transfer Coefficients for Canned Mushrooms Processed in Still Retorts. ASAE Paper #84-6517. St Joseph, Michigan.
- Scholz, E.W., Johnson, H.B. and Buford, W.R. 1963. Heat Evolution Rate of Some Texas-Grown Fruits and Vegetables. Rio Grande Valley Hort. Soc. J. 17:170-175.
- Seibel, J.E. 1892. Specific Heat of Various Products. Ice and Refrigeration 2:256.
- Showalter, R.K. 1955. Quality of Florida Sweet Corn as Affected by Marketing Practices. Fl. State Hort. Soc. Proc. 182-185.
- Showalter, R.K. 1957. Effect of Wetting and Top Icing Upon the Quality of Vacuum-Cooled and Hydrocooled Sweet Corn. Proc. of the Fl. State Hort. Soc. 70(10):214-219.
- Showalter, R.K. 1963. Shank and Husk Trimming Effects on Sweet Corn. Proc. Fla. State Hort. Soc. 76:308-312.
- Showalter, R.K. 1967. Sweet Corn Shelf Life as Affected by Trimming and Packaging. Proc. Amer. Soc. Hort. Sci. 91:881-884.
- Shuman, T.E.W. 1929. Heat Transfer : A Liquid Flowing Through a Porous Prism. J. of Franklin Institute, 208:405-416.
- Sims, W.L., Kasmire, R.F. and Lorenz O.A. 1971. Quality Sweet Corn Production. Calif. Agric. Expt. Sta. Ext. Serv. Cir. 557. 22pp.
- Smith, R.E. and Bennett, A.H. 1965. Mass Average Temperature of Fruits and Vegetables During Transient Cooling. Trans. ASAE 8(2):249-253.
- Snyder G. 1986. Mathematical Model for Temperature Distribution for Thermally Processed Shrimp. M Sc. Thesis, University of Florida, Gainesville.
- Spalding, D.H., Davis, L.P. and Reeder, E.F. 1978. Quality of Sweet Corn Stored in Controlled Atmosphere or Under

- Low Pressure. J. Amer. Soc. Hort. Sci. 103(5):592-595.
- Staph, H.E. 1949. Specific Heat of Foodstuffs. Refrig. Engineering 57(8):767-771.
- Stewart, J.K. and Barger, W.R. 1960. Effects of Cooling Method and Top Icing on the Quality of Peas and Sweet Corn. Proc. Amer. Soc. Hort. Sci. 75:470-475.
- Stewart, J.K. and Couey H.M. 1963. Hydrocooling Vegetables: A Practical Guide to Predicting Final Temperature and Cooling Times. USDA Market Res. Rept. 637. 32pp. U.S.D.A Washington, D.C.
- Uno, J. and Hayakawa, K. 1980. A Method for Estimating Thermal Diffusivity of Heat Conduction Food in A Cylindrical Can. J. of Food Sci. 45:692-695.
- U.S.D.A., 1973. USDA Standards for Food and Farm Products. Agriculture Handbook #341. U.S.D.A., Washington, D.C.
- U.S.D.A., 1982. Agricultural Statistics. U.S.D.A. Washington, D.C.
- Winter, J.D., Nyland, R.E. and Legun, A.F. 1951. Refrigeration is Key to Corn Quality. Refrig. Eng. 59:398-406.
- Winter, J.D., Nyland, R.E. and Legun, A.F. 1954. Fresh Sweet Corn in the Midwest. Minn. Agric. Exp. Stn. Bull. #427. 28pp.
- Winter, J.D., Nyland, R.E. and Legun, A.F. 1965. Relation of Sugar Content to Flavor of Sweet Corn after Harvest. Proc. Am. Soc. Hort. Sci. 65:393-395.

BIOGRAPHICAL SKETCH

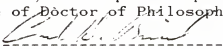
Joseph Edwin Berinyuy was born in Cameroon and attended elementary and high school there. He completed his Bachelor of Science (Hons) degree in physics at the University of Ibadan in Nigeria in 1978. He then taught high school physics for three years before going to Silsoe College, England where he obtained a Master of Science degree in agricultural engineering.

Joseph will be returning to a teaching and research position in Cameroon on the completion of his doctoral work and degree in August, 1988.

I certify that I have read this study and that in my opinion it conforms to acceptable standards of scholarly presentation and is fully adequate, in scope and quality, as a dissertation for the degree of Doctor of Philosophy.

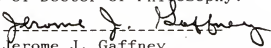
Khe V. Chau, Chairman
Associate Professor of
Agricultural Engineering

I certify that I have read this study and that in my opinion it conforms to acceptable standards of scholarly presentation and is fully adequate, in scope and quality, as a dissertation for the degree of Doctor of Philosophy.



Carl D. Baird
Professor of
Agricultural Engineering

I certify that I have read this study and that in my opinion it conforms to acceptable standards of scholarly presentation and is fully adequate, in scope and quality, as a dissertation for the degree of Doctor of Philosophy.



Jerome J. Gaffney
Associate Professor of
Agricultural Engineering

I certify that I have read this study and that in my opinion it conforms to acceptable standards of scholarly presentation and is fully adequate, in scope and quality, as a dissertation for the degree of Doctor of Philosophy.

Jeffrey K. Brecht
Assistant Professor of
Horticultural Sciences

I certify that I have read this study and that in my opinion it conforms to acceptable standards of scholarly presentation and is fully adequate, in scope and quality, as a dissertation for the degree of Doctor of Philosophy.

Chung K. Hsieh

Chung K. Hsieh
Professor of
Mechanical Engineering

This dissertation was submitted to the Graduate Faculty of the College of Engineering and to the Graduate School and was accepted as partial fulfillment of the requirement for the degree of Doctor of Philosophy.

August 1988

Hubert A. Bevis

Dean, College of Engineering

Dean, Graduate School